CHAPTER IV

SHISHIJIMICINS A-C, NEW MEMBERS OF ENEDIYNE GLYCOSIDES THAT INDUCE COLLAPSE OF THE NUCLEUS FROM THE MARINE TUNICATE *DIDEMNUM PROLIFERUM*

1. Introduction

The lipophilic extract of the tunicate *Didemnum proliferum* Kott (**Fig. IV-1**), collected off Shishijima Island, the Amakusa Islands, June 1999, induced extremely unusual morphological transformation. When the cells were exposed to the lipophilic extract at 10 μg/mL, their nuclei were first dotted with granules, then gradually lost their shapes, and finally disappeared in the course of cell death (**Fig. IV-2**). The extract also exhibited remarkable antimicrobial activity against three fungi (*Candida* albicans, *Mortierella ramanniana,* and *Penicillium chrysogenum*) and four bacteria (*Bacillus subtilis, Escherichia coli, Pseudomonas aeruginosa,* and *Staphylococcus aureus*), indicating that the active principles may act on the universal physiological system existing from prokaryotes to multicellular organisms. Isolation and structure elucidation of active constituents was attempted.

Fig.V-1. *Didemnum proliferum* collected off Shishijima Island.

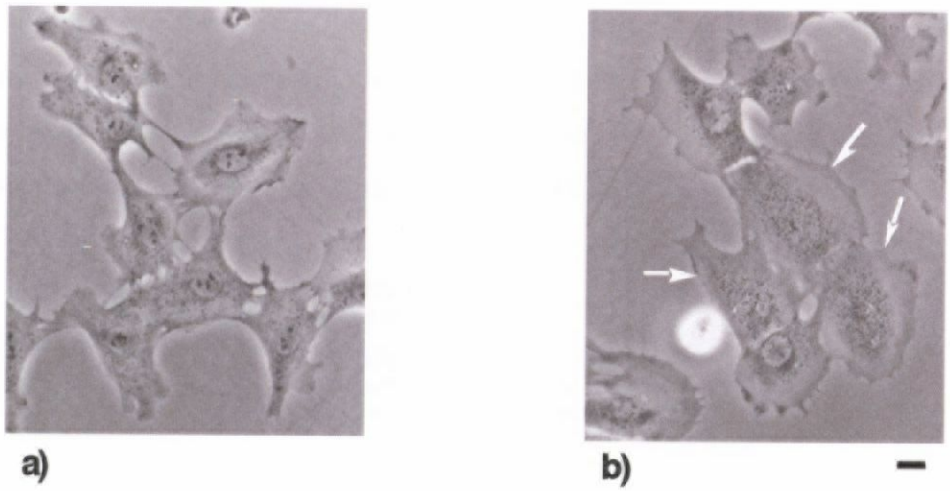

Fig. IV-2. Morphological changes of 3Y1 cells caused by the lipophilic extract of *Didemnum proliferum*. a) Untreated cells. b) Cells treated with 10 μg/mL of the extract for 12 hours. The arrows indicate cells with nucleus collapse. Bar represents 20 μm.

2. Results and Discussion

2-1. Isolation

The most laborious part of this work was to collect the animal. The tunicate is 1 mm thick and grows sporadically on various substrates such as oyster shells. The colonies differ in size, but in most cases they do not cover an area of larger than 1 cm^2. Moreover, they are easy to break when peeled from substrates. These properties of the animal made its collection difficult and required a total of five dives to collect 190 g of the animals.

Isolation of shishijimicins (**4-1~4-3**) was guided by antifungal activity against *Penicillium crysogenum*, which was the most sensitive and gave clearer results in shorter time than the cell-morphology based assay. Of course, the two bioactivities were confirmed to be parallel in the first isolation trial from the ethanolic solution of the specimen bottle containing 75 g of the animal.

The alcoholic extract of the sample was successively partitioned between CH_2Cl_2 and 60% MeOH and then between 90% MeOH and *n*-hexane. The aqueous MeOH layer was subjected to CPC using a solvent mixture EtOAc/*n*-heptane/MeOH/H_2O.

The antifungal fractions were combined and purified by ODS-HPLC with acidic aqueous MeCN to afford shishijimicins A-C (**4-1**~**4-3**), along with namenamicin (**4-4**),[82] an enediyne glycoside derived from the tunicate *Polysyncraton lithostrotum*. All compounds were obtained as TFA salts (**Scheme IV-1**).

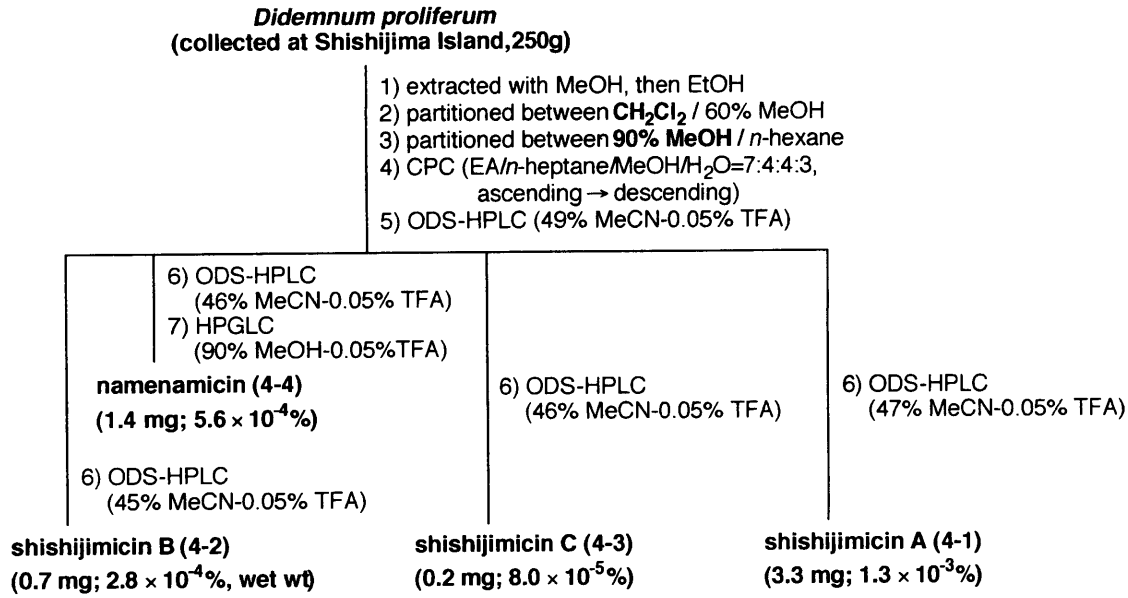

Scheme IV-1. Isolation Procedure of Shishijmicins (4-1~4-3).

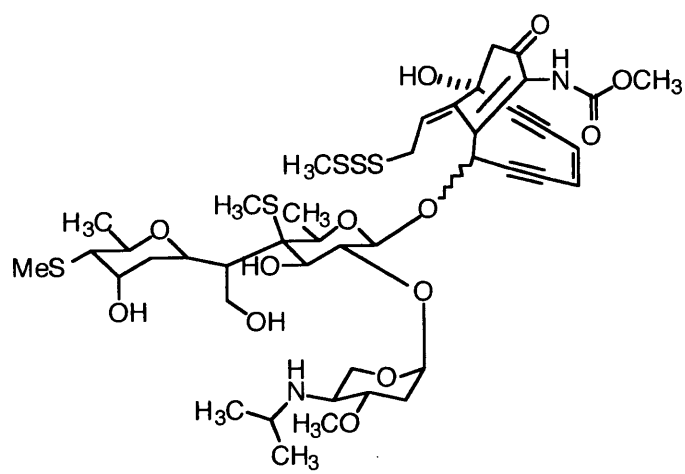

namenamicin (4-4)

2-2. Structure Elucidation

2-2-1. Shishijimicin A

HRFABMS indicated that shishijimicin A (**4-1**) had aS molecular formula of $C_{46}H_{52}N_4O_{12}S_4$ (found *m/z* 1003.2372, calcd *m/z* 1003.2362 $[M+Na]^+$), revealing a highly unsaturated nature of this compound. The ^1H (**Figs. IV-11 and IV-17**) and ^{13}C NMR (**Figs. IV-12 and -18**) spectra were well-resolved, but it was necessary to measure the spectra in two solvents for a detailed structure analysis. Generally, spectra obtained in DMSO-d_6 were more informative in terms of crosspeaks from exchangeable protons. On the otherhand, those in CD_3OD gave sharper proton signals. Analysis of ^{13}C and HMQC data (**Fig. IV-14**) led to the following structural units; two ketones, three olefinic protons, four aromatic methine, two of which were significantly downfield shifted to δ 8.41 and 8.33, two acetal methines, seven oxymethine, one of which was abnormally downfield shifted to δ 6.22, an oxymethylene, two *S*-Me, an carbamoyl Me, three aliphatic Me, an *S*-methylene, a methylene adjacent to a ketone, two *N*-methines, 6 exchangeable protons, and 18 quarternary carbons.

1) Amino sugar (Sugar B)

The pentose unit was deduced from COSY and HMBC data (**Figs. IV-13 and IV-15**) as well as by *J* values measured in CD_3OD in a straightforward manner. COSY correlations of H1''/$H_2$2'', $H_2$2''/H3'', H3''/H4'', and H4''/$H_2$5'' as well as HMBC correlations from OMe6'' (δ 3.36) to C3''(δ 75.0) and from one of $H_2$5'' (δ 3.96) to the anomeric carbon C1'' (δ 100.0) led to the construction of the planar structure. The equatorial orientation of H3'' and H4'' were apparent from coupling constants of H3'' (ddd, *J*=4.5, 9.5, 9.5 Hz), while a small *J* value (brt, 2.9 Hz) of H1'' proved its α-anomeric substitution.

The ^{13}C chemical shift of C4'' (56.4) was consistent with its nitrogen-bearing nature. However, it was not clear which functionality, isopropylamine (δ 1.28 d *J*=6.5 Hz/20.3, 1.31 d *J*=6.5 Hz/19.0, 3.46m/50.3) or methylcarbamoyl (δ 3.74/53.7; 157.8), was attached to C4''. Although no further HMBC correlation was observed for this portion, the HOHAHA spectrum (**Fig. IV-19**) measured in DMSO-d_6 at 300 K supported to place the isopropylammonium moiety at C4'' (**Fig. IV-3**). Correlations were observed

from two ammonio protons at δ 8.22 and 8.53 to all of the isopropyl protons and to sugar protons, H3'', H4'', and $H_2$5'', and thus a 2,4-dideoxy-3-*O*-methyl-4-(*N*-isopropylamino)-α-xylopyranside unit was completed. A NOESY ((**Fig. IV-22**) crosspeak between 6''OMe and 9''CH_3 supported this assignment.

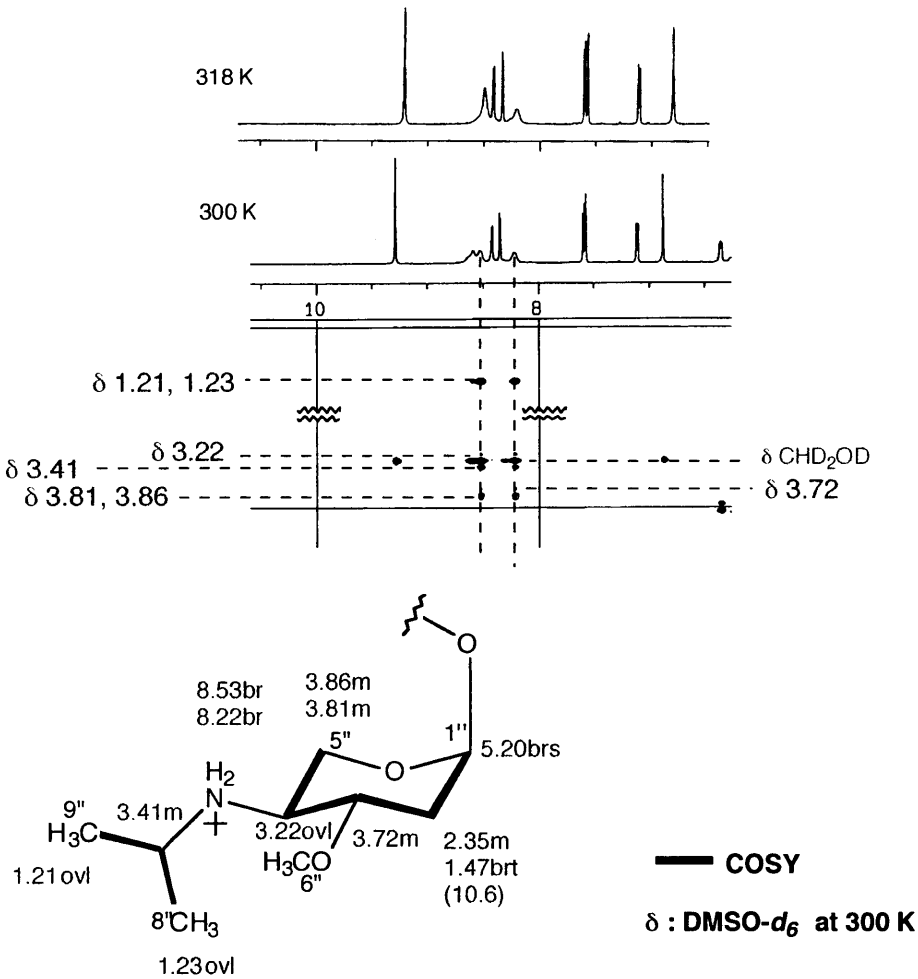

Fig. IV-3. Magnified figure of the HOHAHA spectrum of shishijimicin A (4-1) in DMSO-d_6 at 300 K.

2) β-Carboline unit (Fig. IV-4)

The five aromatic proton signals [δ 7.12 (H14'), 7.57 (H12'), 7.60 (H15'), 8.33 (H11'), and 8.41 (H10')] together with two exchangeable signals [δ 9.21s (O*H*13') and 11.66s (N*H*16')] were characteristic of 6-hydroxy-9*H*-β-carboline.[83,84] In fact, the first three signals and one of the exchangeable protons (δ 9.21s) were constructed into 3,4-disubstitued phenol by a $^3J_{HH}$ coupling pattern and HMBC crosspeaks (**Figs. IV-4 and IV-21**). The last pair of aromatic protons (H10' and H11') was assignable to protons

on position 3 and 4 of β-carboline by their δ and *J* values, while the remaining exchangeable proton (N*H*16') had correlations to C11'a, C11'b and C15'b, placing itself at 9*H* position. The upfield-shifting of C8' (δ 135.1) together with the UV data [217 nm (ε 110000), 306 (43000), and 407 nm (7700)], showing bathochromic shift from typical values for 6-hydroxy-β-carboline,[83,84] indicated the extention of the conjugated system from C8'. However, the nature of the substituent on C8' was not clarified due to the lack of further HMBC cross peaks.

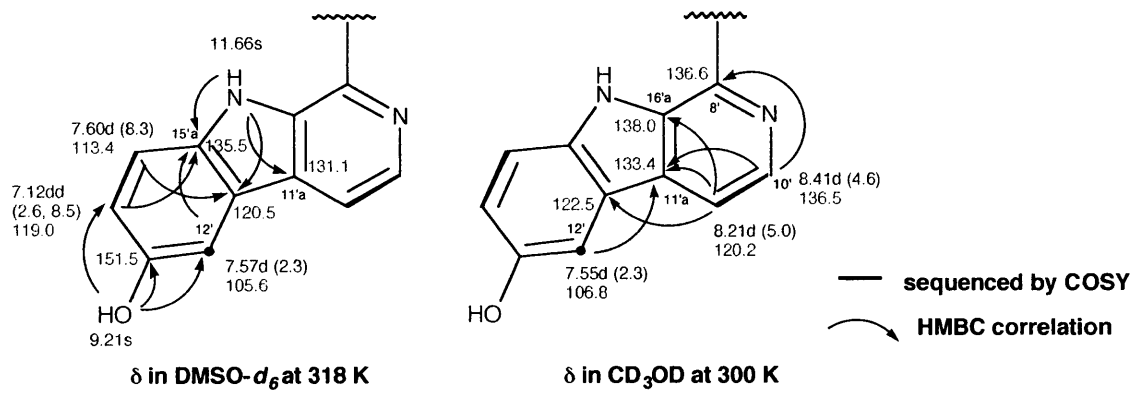

Fig. IV-4. Key HMBC correlations observed in β-carboline moiety.

3) SMe sugar (Sugar A)

The other sugar was composed of three oxymethines (CH2': δ 4.35 dd *J*=7.7, 8.9 Hz/79.7, CH3': 5.74 d *J*=8.8 Hz/80.0, CH5': 5.49 q *J*=6.4 Hz/74.4), one each of quartenary sp^3 carbon (C4': δ 74.7), ketone (C7': δ 197.9), anomeric methine (CH1': δ 4.95 d*J*=7.7 Hz/103.0), thiomethyl (SMe4': δ 2.46s/15.2), and C-methyl ($CH_3$6': δ 1.18 d *J*=6.5 Hz/17.2). The COSY experiment revealed the connectivities of C1'-C2'-C3' and of C5'-C6'. Unusual COSY crosspeaks, SMe-4'/H3' and SMe-4'/H5' were consistent with an SMe-bearing quartenary carbon flanked by C3' and C5', which was supported by the HMBC correlations from H3', SMe4', and H6' to δ 74.7 (C4'). A correlaion from H3' to δ C7' (δ197.9) linked a ketone to C4'. Finally, a correlation H5'/C1' completed a pyranoside structure.

The relative stereochemistry of this sugar was determined on the basis of *J* values and NOESY (in DMSO-d_6 at 318 K) correlations. Large *J* values between H1' and H2' (7.7 Hz) and between H2' and H3' (~8.8 Hz) established their axial orientations.

NOESY crosspeaks from H5' to both H1' and H3', placed Me6' at the equatorial position. No NOESY correlation from 4'SMe to the protons on this sugar unit and H2' was observed. Meanwhile, NOESY cross peaks from H3' and H5' to H10' of the β-carboline unit was noticed, which connected the β-carboline unit and sugar A through a ketone (C7'). So as to place H10' and H3'/H5' in the distances detected by NOESY, C7' must be equatorially oriented. Thus, the unprecedented 4,6-dideoxy-4-(β-carboline-1-carbonyl)-4-thiomethyl-β-glucopyranoside unit was established. HMBC correlation H1''/C2' and H2'/C1'' constructed an α-glycosidic linkage between C2' of Sugar A and the amino sugar.

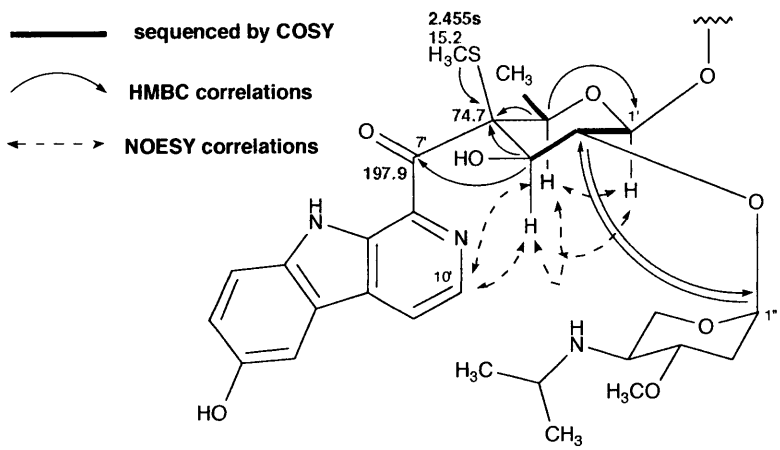

Fig. IV-5. Key HMBC (in CD_3OD at 300 K) and NOESY (in DMSO-d_6 at 318 K) correlations observed in the arylcarbohydrate moiety of shishijimicin A (4-1).

4) Enediyne Aglycon

NMR signals ascribable to the aglycon of shishijimicin A (**4-1**) contained a ketone, disubstituted *cis*- and trisubstituted olefins, an oxymethine (CH8: δ 6.22 brs/69.0), a methylene adjacent to ketone ($CH_2$12: δ 2.71 and 3.02), an S-methylene ($CH_2$15: δ 4.06 and 3.96 m/39.3), a methylcarbamate ($CH_3$18: 3.58brs/52.0), an thiomethyl ($CH_3$16: 2.56s/22.4), eight quartenary carbons (δ 146.2, 137.0, 131.8, 101.8, 98.1, 87.7, 82.4, and 71.3), and a hydroxyl group. These structural pieces together with remaining 64 mass unit corresponding to two sulfur atoms was reminiscent of calicheamicinone.[85] A substructure 4-(2-sulfanyl-ethylidene)-cyclohex-2-enone was supported by HMBC correlations: H6/C9, C10, C13; $H_2$15/C13, C14; H14/C1, C9; $H_2$12/C1, C10, C11, C13;

and 1-OH/C1, C12 (**Fig. IV-6**). Olefinic protons H4 and H5 showed HMBC crosspeaks to four quaternary carbons, 82.4 (C3), 87.7 (C6), 98.1 (C7), and 101.8 (C2), which also correlated with H8, 1-OH, and $H_2$12, disclosed 3-ene-1,5-diyne structure beween C1 and C8 (**Fig. IV-6**). Thus, a unique bicyclo[7.3.1]trideca-1(12),5-diene-3,7-diyne system was constructed. The characteristic long-range coupling beween H5 and H8 (J=1.7 Hz) was observed in both ^{1}H and COSY spectra measured in CD_3OD (**Table IV-2**).

The HMBC correlation from the anomeric proton of the thiomethyl sugar (H1') to C8 supported a glycosidic linkage between them. The chemical shift value of 16SCH_3 (δ 2.56s/22.4) was diagnostic of a methyl trisulfide and it should be connected to the SC$H_2$15 (cf. methyl disulfide: δ 2.37/19.6 in $CDCl_3$,[86] methyl tetrasulfide: δ 2.62 in CD_3OD[6]). Therefore, the methyl carbamate group must be placed on C10 (δ 131.8).

The NOESY spectrum did not give any stereochemical relationships between the aglycon and the sugars. The geometry of the exocyclic olefin of the aglycon was assigned as 13E on the basis of a NOE crosspeak between OH1 and H14. Thus, the relative structure of shishijimicin A(**4-1**) was established. NMR data were summarized in **Table IV-2** and **IV-3**.

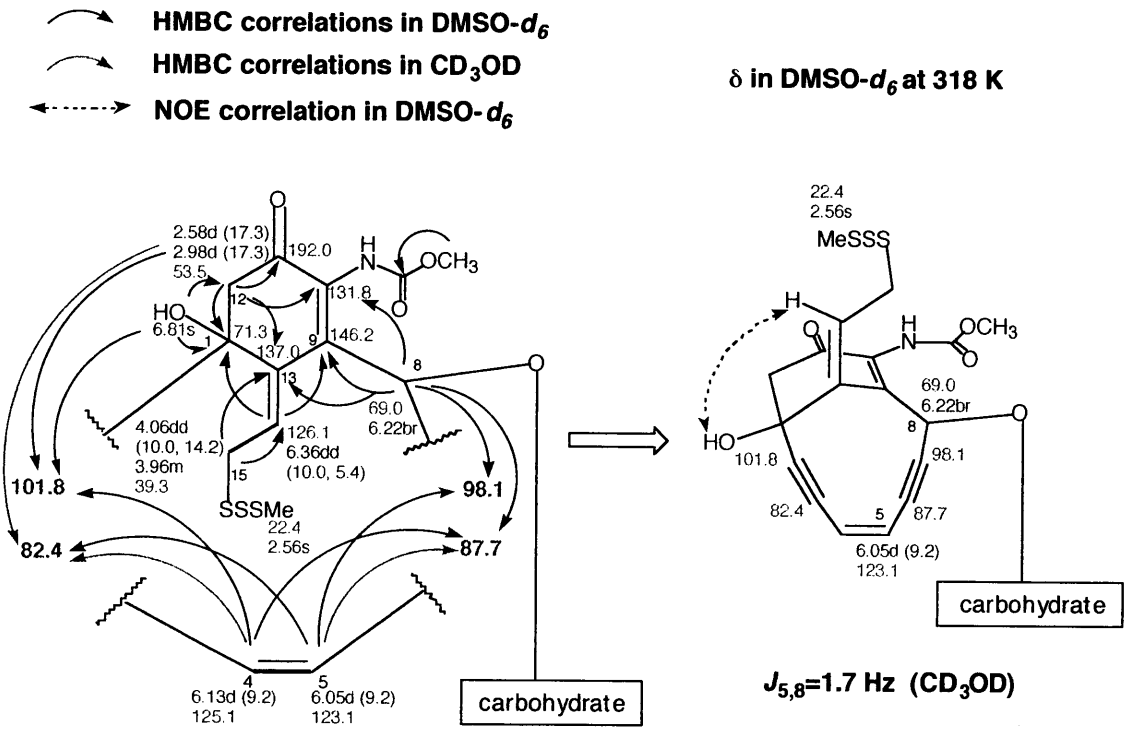

Fig. IV-6. Key HMBC and NOESY correlations observed in the calicheamicinone moiety of shishijimicin A (4-1).

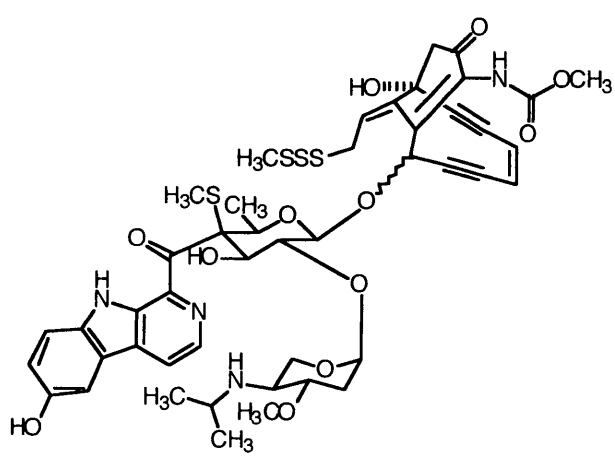

shishijimicin A (4-1)

2-2-2. Shishijimicin B

The HRFAB mass spectrum (**Fig. IV-31**) of shishijimicin B (**4-2**) established a molecular formula of $C_{45}H_{50}N_4O_{12}S_3$, which was smaller than that of shishijimicin A (**4-**

1) by a unit of CH_2S. Apparently, this difference was thought to be due to the replacement of the thiomethyl group by a hydrogen atom; in fact, the signal for 4'-SMe disappeared and a methine proton (H4': δ 4.56 dd *J*=9.8, 11.0 Hz) appeared, accompanying shifting of several signals in the ^{1}H NMR spectrum (**Fig. IV-23**). Interpretation of HOHAHA data (**Fig. V-25**) revealed the contiguous sequence from H1' to H_36', and further analysis of the HMQC (**Fig. V-26**) and HMBC (**Fig. V-27**) spectra comfirmed that shishijimicin B (**4-2**) is 4'-desthiomethylshishijimicin A. H4' was remarkably downfield shifted (δ 4.56), which may be the result of the anisotropic deshielding effect caused by the adjacent ketone (C7'). The H-H coupling constants around the pyranose ring indicated that the substituents on C3' and C4' are equatorially oriented.

The ^{1}H NMR signals of the amino sugar portions were broad or overlapped by other signals and only interpretable were the broad triplet (*J*=2.9 Hz) of the anomeric and broad doublet (*J*=12.7 Hz) of one of the protons (δ 2.48) at C2'', suggesting the anomeric H1'' to be equatorially oriented. The 1D HOHAHA difference experiment on irradiation of the same H2' showed its geminal counterpart (δ 1.60) as a broad triplet with a large *J* value (12.2 Hz, **Fig. IV-7**), thereby securing the axial nature of H3. The 1,3-diaxial relationship of H2'' and H4'' was supported by a NOE correlation between them in the ROESY spectrum (mixing time:120 ms, **Fig. IV-28**). Further evidence for this stereochemical assignment was *J* values of all the protons except for H3' obtained from the ^{1}H and TQFCOSY spectra (**Figs. IV-29 and IV-30**) measured in a mixture of $CD_3OD/CDCl_3$/pyridine-d_5 (100:100:0.5), where shishijimicin B (**4-2**) gave rather sharper signals. Diagnostic was the splitting pattern of H4' (td, *J*=9.2 and 4.6 Hz), which clearly showed axial orientation of H3' and H4' (**Fig. IV-8**). The remaining signals were almost identical with those of shishijimicin A (**4-1**). NMR data of shishijimicin B (**4-2**) are summarized in **Table IV-4**.

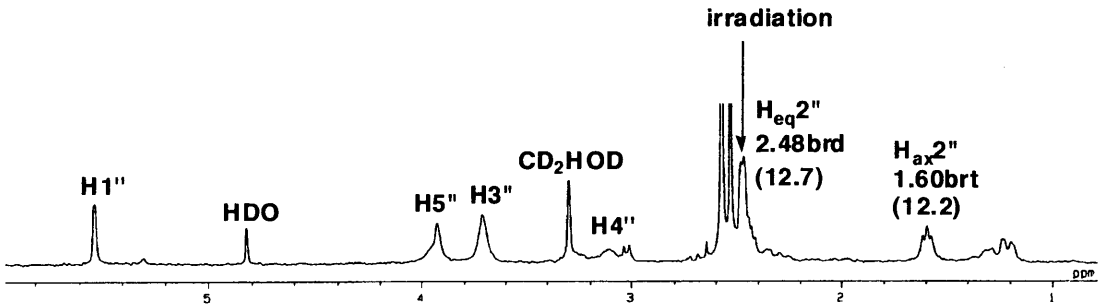

Fig. IV-7. 1D HOHAHA difference spectrum of shishijimicin B (4-2).

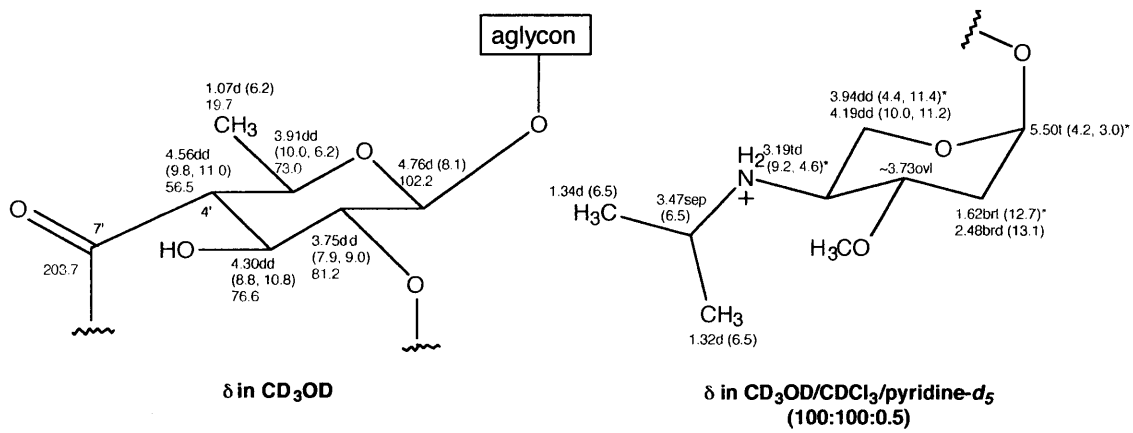

Fig. IV-8. Structure of the two sugar moieties in shishijimicin B (4-2). *Determined by PSTQFCOSY.

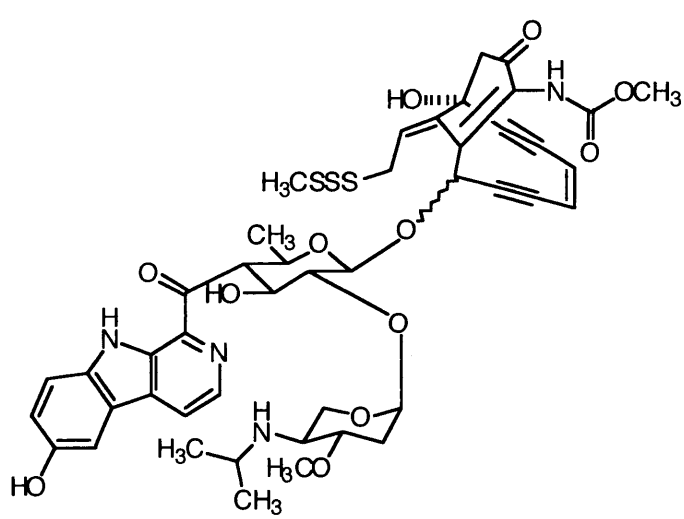

shishijimicin B (4-2)

2-2-3. Shishijimicin C

The HRFAB mass spectrum (**Fig. IV-36**) of shishijimicin C (**4-3**) established the molecular formula of $C_{45}H_{50}N_4O_{12}S_4$ (found m/z 967.2397, calcd m/z 967.2386 $[M+H]^+$), which was smaller than shishijimicin A (**4-1**) by a CH_2 unit. The ^1H NMR spectrum (**Fig. IV-32**) was almost identical with that of shishijimicin A (**4-1**), but a limited amount of the sample (0.2 mg) hampered detailed comparison of the spectra especially on the high field region (δ 0.8~3.2 Hz). Analysis of the HOHAHA spectrum (**Fig. IV-33**) revealed the presence of an ethylamino group (δ 1.23 and 2.96 in CD_3OD) in place of the isopropylamino group. Therefore, shishijimicin C (**4-3**) turned out to be an ethylamino analogue of shishijimicin A (**4-1**). Except for this difference NMR data were superimposable to those of shishijimicin A (**4-1**) as compared by COSY data in CD_3OD or in $CD_3OD/CDCl_3$/pyridine-d_5 (100:100:0.5) (**Fig. IV-35**). NMR data of shishijimicin C (**4-3**) are shown in **Table IV-4**.

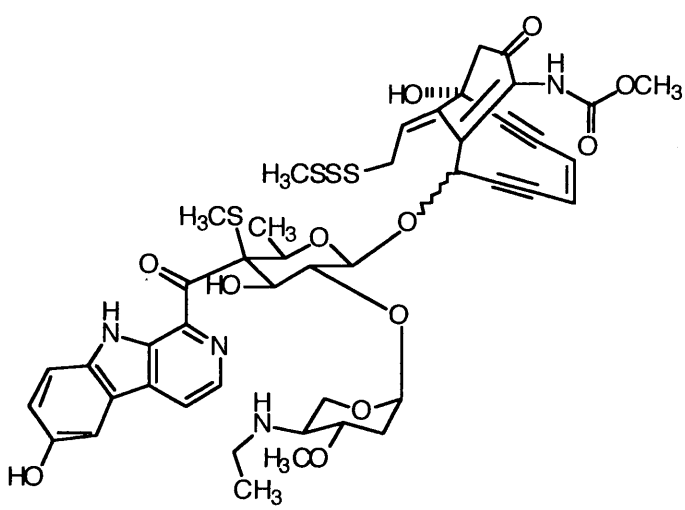

shishijimicin C (4-3)

2-2-4. Absolute Configration of Calicheamicinone in Shishijimicins (4-1~4-3)

The absolute stereochemistry of shishijimicins (**4-1~4-3**) remains to be determined. It is reported that calicheamicin γ_1^I (**4-5**) showed a characteristic CD curve with the first negative (311 nm) and second positive (272 nm) Cotton effects, attributable to the twisted interaction of the electric transition moments of dienone and enediyne

chromophores.[85] The CD spectra of shishijimicins (**4-1~4-3**) gave similar characersitic (325~321 nm, Δε -4.4~-8.5; 272~268 nm, Δε 5.6~7.1, **Fig. IV-37~-39**), suggesting the same absolute stereochemistry (**Fig. IV-9**).

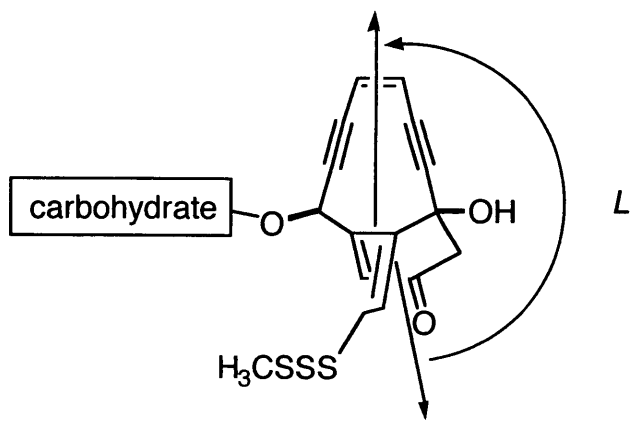

Fig. IV-9. Chirality of enediyne/dienone chromophore. The arrows denote direction of electric transition moments.

2-3. Biological Activity

The effects of shishijimicin B (**4-1**) on 3Y1 cells was dependent on the concentration. At 200 μM, many black granules were first emerged in the perinuclear region after 5-hour exposure (**Fig. IV-10 b)**). Characteristically, some of the granules localized on the nuclear surface. The damaged nuclei disappeared in 50 % of the cells in 24 hours and the site where the nucleus had occupied became microscopically indistinguishable to the perinuclear region (**Fig. IV-10 c)**). About 80 % of the cells died within 48 hours and the rest within 5 days. The course of events described above progressed faster in higher concentrations.

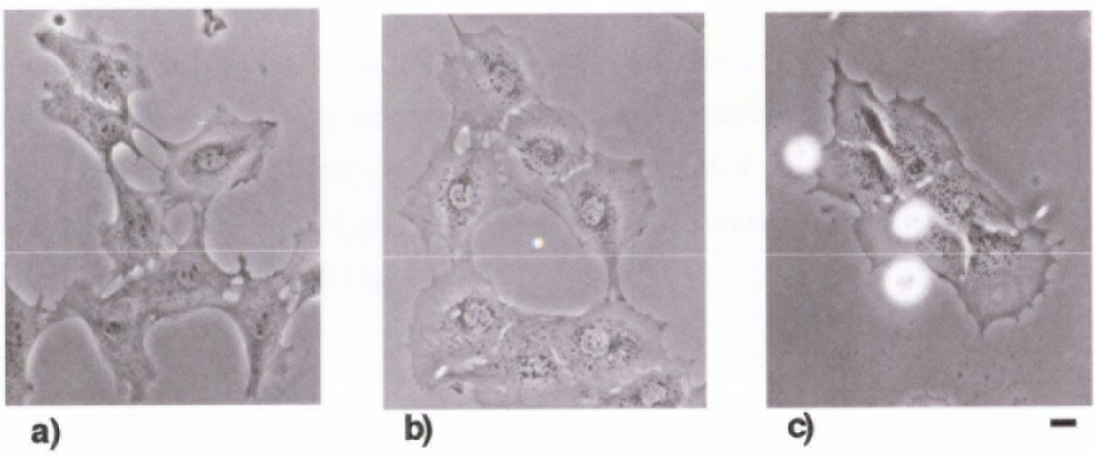

Fig. IV-10. Morphological change of 3Y1 cells caused by 200 μM of shishijimicin B (4-2). a) Control. b) Cells treated for 5 hours. c) Cells treated for 24 hours. Bar represents 20 μm.

The cytotoxicity of shishijimicins against three cell lines was summarized in **Table IV-1**. They were slightly more potent than namenamicin (**4-4**).

Table IV-1. Cytotoxicity of Enediyne glycosides Isolated from *Didemnum proliferum* against 3Y1, HeLa, and P388 Cells (IC_{50}: pM)

	4-1	**4-2**	**4-3**	**4-4**	adriamycin[a]
3Y1	2.0	3.1	4.8	13	13000
HeLa	1.8	3.3	6.3	34	17000
P388	0.47	2.0	1.7	3.3	52000

[a]Positive cytotoxicity control.

Shishijimicins A-C (**4-1**~**4-3**) are structurally related to calicheamicins (**4-5**),[85,88,89] esperamicins (**4-6**),[90,91] and namenamicin (**4-4**),[82] the first two of which are metabolites from terrestrial actinomycetes, while the last one was isolated from the marine ascidian *Polysyncraton lithostrotum*. These compounds possess a 13-(2-methyltrisulfanyl-ethylidene)-bicyclo[7.3.1]trideca-1(12),5-diene-3,7-diyne motif in common and compose a group of enediyne antitumor antibiotics with other families of enediynes

including dynemicin A,[92,93] N1999A1,[94] and chromoprotein antibiotics such as neocarzinostatin,[95,96] kedarcidin,[97,98] C-1027, and maduropeptin.[99] Among these, calicheamicin γ_1^I has been the most intensively studied by a broad array of scientists in the fields of organic synthesis, biosythesis, physical chemistry, molecular biology, and clinical medicine, leading to the recent success of antibody-directed calicheamicin cancer therapies. Currently, phase II studies are carried out for treatments of acute myeloid leukemia[100] and epithelial ovarian cancer[101] whereas a phase I study for a treatment of non-small cell lung cancer.[102]

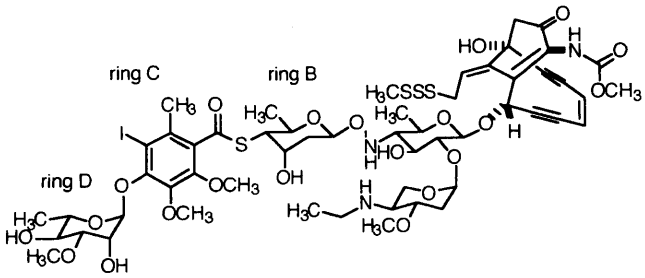

calicheamicin γ_1^I (4-5)

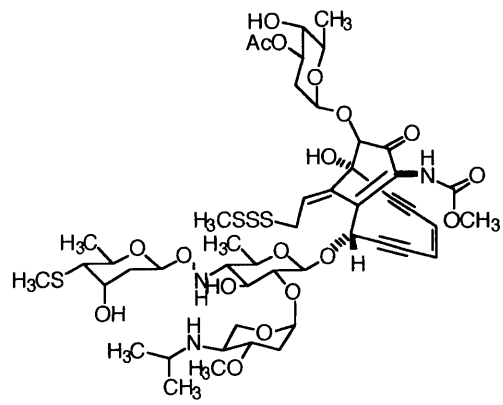

esperamicin A_1 (4-6)

The antitumor activity of enediynes is ascribed to their ability to cleave cellular DNA.[103,104] Triggered by a certain series of reactions, they are converted to diradical spieces in the course of Bergman cyclization[105-108] which proceed to abstract hydrogen atoms from the sugar-phosphate backbone of both DNA strands, and as a consequence, strand scission occurs along with formation of aldehyde which is generated by reaction of resulting carbon-centered radicals with molecular oxygen. It is obvious that shishijimicins exert their biological action through the same mode of action.

Calicheamicin γ_1^I cleaves duplex DNA with a high degree of specificity at several tetranucleotide sequences.[109,110] It was demonstrated that sugars A and B are sufficient to align the drug for double-stranded cleavage, but the entire aryl tetrasaccharide is required for specificity.[110] Further studies using DNA hairpin duplex containing one of the preferred sequences (T-C-C-T)·(A-G-G-A) in its center has inferred that iodine and sulfur atoms of the thiobenzoate ring C interact with exocyclic amino protons of the 5' and 3'-guanine bases, respectively, and contribute greatly to sequence recognition.[111]

Shishijimicins possess the 6-hydroxy-9*H*-β-carboline carbonyl functions at C4' of sugar A in place of the aryldisaccharide BCD rings, and this could result in a large alteration of sequence recognition pattern. It is of great interest to examine how the preference for DNA tracts is changed by this substitution. Analysis of shishijimicin-DNA interaction in detail will provide further insights into the molecular recognition mechanism of the carbohydrate moiety of calicheamicin γ_1^I.

3. Experimental Section

3-1. General Mehtods

Instruments used in this chapter were the same as in CHAPTERs II and III.

3-2. Animal Material

The orange thin tunicate *Didemnum proliferum* Kott was identified by Prof. Teruaki Nisikawa, the Nagoya University of Museum, Nagoya University. The animal was collected by hand-using scuba at a depth of 20 m off Shishijima Island, the Amakusa Islands, 960 km southwest of Tokyo, Japan (32° 17' N, 130°12' E). The colonies were immediately frozen and then transported to Tokyo.

3-3. Extraction and Isolation

The animal (250 g) was extracted with MeOH (500 mL) and EtOH (total 3.5 L). The combined extracts were concentrated and successively partitioned between 60% MeOH (700 mL) and CH_2Cl_2 (700 mL × 3) and between 90% MeOH (400 mL) and *n*-hexane (400 mL × 3). The aqueous MeOH solubles (347.3 mg) were filtered and then fractionated by CPC (= centrifugal partition chromatography, rotation: 1400 rpm, solvent: EtOAc/*n*-heptane/MeOH/H_2O (7:4:4:3), flow rate: 3 mL/min, normal elution=ascending mode) to afford 40 fractions (15 mL each) by normal elution and 20 fractions by reversed elution. About 1.1 μL portion of each fraction was used for bioautography against *Penicillium chrysogenum*. The fractions eluting between 255-

495 mL and 615-645 mL which exhibited remarkable growth inhibitory activity were combined and separated by reversed-phase HPLC (CAPCELL PAK C18 UG80 ϕ20 × 250 mm, SHISEIDO; 49% aqueous MeCN containing 0.05% TFA) to give four broad cytotoxic peaks. Further purification of the first, third, and fourth peaks on reversed-phase HPLC (CAPCELL PAK C18 MG ϕ20 or ϕ10 × 250 mm, SHISEIDO; aqueous MeCN containing 0.05% TFA) afforded shishijimicins B (**2**, 0.7 mg; 2.8×10^{-4}% wet wt), C (**3**, 0.2 mg; 8.0×10^{-5}% wet wt), and A (**1**, 3.3 mg; 1.3×10^{-3}% wet wt) as yellow solids, respectively. The second peak mainly contained colorless material, which proved known namenamicin[82] (1.4 mg; 5.6×10^{-4}% wet wt) after the final purification on Asahipak GS-320 (ϕ78 × 500 mm, ASAHI CHEMICAL INDUSTRY; 90% MeOH containing 0.05% TFA).

Shishijimicin A (1): a yellow solid; $[\alpha]^{28}_{D}$ -66° (c 0.16, MeOH); UV (MeOH) λ_{max} 217 nm (ε 110000), 271 (30000), 306 (43000), 337 (sh, 18000), 407 nm (7700); CD λ_{ext} 229 nm (Δε 0.0), 239 (-3.1), 254 (0.0), 269 (5.7), 287 (0.0), 322 (-8.5); HRFABMS m/z 1003.2372 $(M+Na)^+$ (calcd for $C_{46}H_{52}N_4O_{12}S_4Na$, Δ+1.0 mmu); ^1H and ^{13}C NMR data, see **Table IV-2 and -3**.

Shishijimicin B (2): a yellow solid; $[\alpha]^{25}_{D}$ -63° (c 0.05, MeOH); UV (MeOH) λ_{max} 219 nm (ε 34000), 256 (19000), 306 (13000), 328 (sh, 6800), 408 nm (2400); CD λext 233 nm (Δε 0.0), 238 (-1.1), 249 (0.0), 272 (7.1), 292 (0.0), 325 (-5.0); HRFABMS m/z 935.2623 $(M+H)^+$ (calcd for $C_{45}H_{50}N_4O_{12}S_3$, Δ-4.3 mmu); ^1H NMR [$CD_3OD/CDCl_3$/pyridine-d_5 (100:100:0.5)] δ 8.46 (1H, d, *J*=5.0 Hz, H-10'), 8.16 (1H, d, *J* =5.0 Hz, H-11'), 7.54 (1H, d, *J* =1.9 Hz, H-12'), 7.50 (1H, d, *J* =8.5 Hz, H 15'), 7.15 (1H, dd, *J* =2.3, 8.5 Hz, H-14'), 6.52 (1H, dd, *J* =5.2, 10.2 Hz, H-14), 6.20 (1H, bs, H-8), 5.94 (1H, d, *J* =9.2 Hz, H-4), 5.85 (1H, dd, *J* =9.2, 1.5 Hz, H-5), 5.50 (1H, dd, *J* =3.0, 4.2 Hz, H-1"), 4.74 (1H, d, *J* =7.7 Hz, H-1'), 4.48 (1H, t, *J* =10.4 Hz, H-4'), 4.25 (1H, dd, *J* =9.2, 10.8 Hz, H-3'), 4.19 (1H, dd, *J* =10.0, 11.2, H-5"b), 4.09 (1H, dd, *J* =14.4, 10.2 Hz, H-15b), 3.94 (1H, dd, *J* =4.4, 11.4, H-5"a), 3.91 (1H, dd, *J* =9.8, 6.4 Hz, H-5'), 3.88 (1H, dd, *J* =5.2, 14.4 Hz H-15a), 3.38 (3H, s, CH_3-6"), ~3.73 (overlapped, H-2'), ~3.73 (overlapped, H-3"), 3.73 (3H, bs, CH_3-18), 3.47 (1H, sep, *J* =6.5 Hz, H 7"), 3.19 (1H, td, *J* =9.2, 4.6 Hz, H-4"), 3.06 (1H, d, *J* =17.3 Hz, H-12b), 2.74 (1H, d, *J* =16.9 Hz, H 12a), 2.55 (3H, s, CH_3-16), 2.48 (1H, bd, *J* =13.1 Hz, H_{eq}-2"), 1.62 (1H, bt, *J* =12.7 Hz, H_{ax}-2"), 1.34 (3H, d, *J* =6.5 Hz, CH_3-8"), 1.32 (3H, d, *J* =6.5 Hz, CH_3-9"), 1.06 (3H, d, *J*

=5.8 Hz, CH_3-6'). ^1H and ^{13}C NMR data in CD_3OD, see **Table IV-4**.

Shishijimicin C (3): a yellow solid; $[\alpha]^{26}_D$ -31° (c 0.017, MeOH); UV (MeOH) λ_{max} 218 nm (ε 54000), 255 (sh, 24000), 306 (20000), 328 (sh, 11000), 408 nm (3300); CD λ_{ext} 235 nm (Δε 0.0), 238 (-1.2), 251 (0.0), 272 (6.8), 293 (0.0), 321 (-4.4); HRFABMS m/z 967.2397 $(M+H)^+$ (calcd for $C_{45}H_{51}N_4O_{12}S_4$, Δ+1.1 mmu); ^1H NMR data, see **Table IV-5**.

3-4. Cell-morphology-based Assay

The assay procedure was the same as that described in CHAPTER I.

3-4. Cytotoxicity Tests

Cytotoxicity tests against of 3Y1, HeLa, and P388 cells were done following the procedure described in CHAPTER II.

Table IV-2. NMR Data of Shishijimicin A (4-1) in CD_3OD at 300 K

position	^{13}C	^{1}H, m, J (Hz)	HMBC ($^{1}H \rightarrow ^{13}C$)[a]
aglycon			
1	73.1		
2	102.1		
3	83.8		
4	126.1	6.02 d 9.2	2, 3, 6
5	124.0	5.96 dd 9.4, 1.7	3, 6, 7
6	89.2		
7	98.7		
8	70.8	6.35 bs	6, 7, 9, 13
9	149.3		
10	132.6		
11	194.2		
12	54.7	2.71 d 16.9 (Ha)	1, 2, 3, 11, 13
		3.02 d 16.9 (Hb)	1, 2, 10, 11, 13
13	138.5		
14	128.6	6.51 dd 5.0, 10.0	1, 9
15	41.2	3.97 dd 14.2, 5.0 (Ha)	13, 14
		4.18 dd 14.4, 10.2 (Hb)	13, 14
16	23.0	2.56 s	
17	157.8		
18	53.7	3.74 bs	17
Sugar A			
1'	103.0	4.95 d 7.7	8
2'	79.7	4.35 dd 7.7, 8.9	1', 3', 1''
3'	80.0	5 74 d 8.8	1', 2', 4', 7'
4'	74.7		
4'-SMe	15.2	2.46 s	4'
5'	74.4	5.49 q 6.4	1', 3', 6'
6'	17.2	1.18 d 6.5	4', 5'
7'	197.9		
8'	136.6		
10'	136.5	8.41 d 4.6	8', 11', 11'a
11'	120.2	8.21 d 5.0	10', 11'b, 16'a
11'a	133.4		
11'b	122.5		
12'	106.8	7.55 d 2.3	11'a, 14', 15'a,
13'	153.1		
14'	120.2	7.14 dd 2.5, 8.7	12', 13', 15'a
15'	114.1	7.54 d 9.6	11'b, 12', 13'
15'a	137.5		
16'a	138.0		
Sugar B			
1''	100.0	5.53 bt 2.9	3'', 5''
2''	34.7	1.57 m (Ha)	3''

		2.47 m (Hb)	1'', 4''
3''	75.0	3.78 ddd 4.5, 9.5, 9.5	
4''	56.4	3.25 m	
5''	59.9	3.96 dd 4.6, 11.5 (Ha)	1'', 3''
		4.09 bt 10.4 (Hb)	3''
6''	56.1	3.36 s	3''
7''	50.3	3.46 m	
8''	19.0	1.31 d 6.5	7'', 9''
9''	20.3	1.28 d 6.5	7'', 8''

Table IV-3. ^{1}H and ^{13}C NMR Data of Shishijimicin A (4-1) in DMSO at 318 K

position	^{13}C	^{1}H, m, *J* (Hz)	HMBC ($^{1}H \rightarrow ^{13}C$)[a]	NOESY[b]
aglycon				
1	71.3	6.81 s (O*H*)	1, 2, 12	12, 14
2	101.8			
3	82.4			
4	125.1	6.13 d 9.2	2, 6	
5	123.1	6.05 d 9.2	3, 7	
6	87.7			
7	98.1			
8	69.0	6.22 bs	6, 7, 9, 10, 13	1', 2', 5''b
9	146.2			
10	131.8	8.49 brovl (N*H*)[c,d]		
11	192.0			
12	53.5	2.58 d 17.3 (Ha)	1, 2, 11	1, 12b
		2.98 d 17.3 (Hb)	1, 2, 10, 11, 13	1, 12a
13	137.0			
14	126.1	6.36 dd 5.4, 10.0	1, 9	1OH, 15a, 15b
15	39.3	3.96 m	13	14
		4.06 dd 14.2, 10.0	13, 14	14
16	22.4	2.56 s		
17	154.9			
18	52.0	3.58 bs	17	
Sugar A				
1'	101.4	4.86 d 7.3	8	8, 3', 5'
2'	80.2	4.18 bt 7.3	1', 3', 1''	8, 3', 1''
3'	77.5	5.69 bt 6.7		1', 2', 3'OH, 5', 10', 1''
3'OH		5.77 d 6.2	3', 4'	2', 3', 1''
4'	73.0			
4'-SMe	14.2	2.46 s	4'	
5'	71.8	5.51 q 6.2	1', 3', 6'	1', 6', 10'
6'	16.4	1.06 d 6.5	4', 5'	5'
7'	195.6			
8'	135.1			
10'	135.3	8.41 d 5.0	11'a	3', 5', 11'
11'	119.1	8.33 d 4.6	11'b, 16'a	10', 12'
11'a	131.1			
11'b	120.5			
12'	105.6	7.57 d 2.3	11'a, 14', 15'a	11', 13'OH
13'	151.5	9.21 s (O*H*)	12', 13', 14'	12', 14'
14'	119.0	7.12 dd 2.6, 8.5	12'	13'OH, 15'
15'	113.4	7.60 d 8.3	11'b, 13'	14', 15'aNH
15'a	135.5	11.66 s (15'aN*H*)	11a', 11'b, 15a'	15'
16'a	135.7			
Sugar B				
1''	98.9	5.20 bs		2', 3', 3'OH

2''	32.9	1.49 brt (10.2) (2''a)		1'', 2''b, 4''
		2.33m (2''b)		1'', 2''a, 3'', 6''
3''	72.9	3.73 m		2''a, 6''
4''	53.3	3.22 ovl		2''
4''NH_2^+		8.21 br		
		8.49 brovl[c,e]		
5''	57.8	3.82 m		
		3.87 m		
6''	55.2	3.22 s	3''	2''b, 3'', 9''
7''	48.3	3.42 m		
8''	18.1	1.23s		
9''	19.0	1.23s		

[a]Data obtained with mixing time 60 and 100 ms.

[b]Data obtained with mixing time 400 ms.

[c]Broad and overlapped.

[d]δ 8.59 at 300 K.

[e]δ 8.53 at 300 K.

Table IV-4. ^{1}H and ^{13}C NMR Data of Shishijimicin B (4-2) in CD_3OD

position	^{13}C	^{1}H, m, J (Hz)	HMBC ($^{1}H \rightarrow ^{13}C$)[a]	ROESY[b]
aglycon				
1	72.9			
2	102.2			
3	83.9			
4	126.2	6.02 d 9.2	2, 3, 6	
5	123.9	5.94 dd 9.6, 1.5	3, 7	
6	89.4			
7	98.1			
8	72.1	6.23 bs	7	1', 3'', 5''
9	ND			
10	132.7			
11	194.3			
12	54.7	2.71 d 17.3 (Ha)	1, 2, 11	12b
		3.02 d 16.9 (Hb)	1, 2, 10, 11, 13	12a
13	138.5			
14	128.8	6.53 dd 5.0 10.0		15a
15	41.0	3.95 ovl (Ha)		14
		4.14 dd 14.6, 10.4 (Hb)	13	
16	22.9	2.58 s		
17	157.8			
18	53.6	3.72 bs	17	
Sugar A				
1'	102.2	4.76 d 8.1	8	8
2'	81.2	3.75 dd 7.9, 9.0	1', 3', 1''	1''
3'	76.6	4.30 dd 8.8, 10.8	2'	
4'	56.5	4.56 dd 9.8, 11.0	3', 5', 7'	6'
5'	73.0	3.91 dd 6.2, 10.0		6'
6'	19.7	1.07 d 6.2	4', 5'	4', 5'
7'	203.7			
8'	137.4			
10'	138.3	8.48 d 5.0	8', 11', 11'a	11'
11'	120.5	8.22 d 5.0	11'b, 16'a	10', 12'
11'a	133.6			
11'b	122.4			
12'	107.0	7.56 d 1.9	14', 15'a	11'
13'	153.1			
14'	120.1	7.13 dd 2.3, 8.8	12', 13'	15'
15'	114.1	7.54 d 8.5	11'b, 13'	14'
15'a	137.6		11a', 11'b, 15a'	
16'a	137.3			
Sugar B				
1''	99.9	5.53 bt 2.9		2', 2''a, 2''b
2''	34.8	1.60 brt 12.2 (Ha)[d]		1'', 2''b, 3'' (weak), 4'', 6''
		2.48 brd 12.7 (Hb)		1'', 2''a, 3'' (strong), 6''

3''	75.8	3.73 m		8, 2''a (weak), 2''b, (strong), 6''
4''	56.6	3.15		2''a
5''	60.8	3.93 (2H) ovl		
6''	56.3	3.40 s	3''	2''a, 2''b, 3''
7''	49.5	3.31		
8''	19.8	1.25 d 5.8	7'', 9''	
9''	21.4	1.21 d 6.5	7'', 8''	

[a]Data obtained with mixing time 60 ms.

[b]Data obtained with mixing time 120 ms.

[c]Broad and overlapped.

[d]Assigned from a 1D HOHAHA difference spectrum by irradiating H2''b.

Table IV-5. ^{1}H NMR Data of Shishijimicin C (4-3) at 300 K[a]

solvent	CD_3OD	$CD_3OD/CDCl_3/C_5D_5N$
position	^{1}H, m, *J* (Hz)	^{1}H, m, *J* (Hz)
aglycon		
4	6.02 d 9.6	5.94 d 9.6
5	5.95 dd 1.5, 9.6	5.86 dd 9.6, 1.5
8	6.33 bs	6.22 bs
12	2.71 d 16.9 (Ha)	2.75 d 17.3 (Ha)
	3.01 d 17.3 (Hb)	3.02 d 16.9 (Hb)
14	6.51 dd 5.4, 10.0	6.50 dd 5.0, 10.4
15	3.95 dd 14.6, 5.2 (Ha)	3.865 dd 14.4, 4.8 (Ha)
	4.18 dd 14.6, 10.4 (Hb)	4.11 dd 14.4, 10.2 (Hb)
16	2.57 s	2.53 s
18	3.71 bs	3.71 bs
Sugar A		
1'	4.94 d 8.1	4.83 d 7.7
2'	4.35 dd 7.7, 8.5	~4.6 overlapped by HDO
3'	5 74 d 8.9	5 17 d 8.5
4'-SMe	2.45 s	2.22 s
5'	5.47 q 6.2	5.08 q 6.2
6'	1.18 d 6.2	1.27ovl[b]
10'	8.41 d 5.0	8.40 d 5.0
11'	8.21 d 5.0	8.15 d 5.0
12'	7.55 d 1.9	~7.52 overlapped by $CDCl_3$
14'	7.14 dd 2.5, 8.7	7.15 dd 2.3, 8.5
15'	7.54 d 8.9	7.48 d 8.8
Sugar B		
1''	5.52 bt 3.5	5.56 dd 3.1, 3.5
2''	1.54 t 13.3 (Ha)	1.62 brt 13.1 (Ha)
	2.40 dt 3.4, 13.2 (Hb)	2.39 td 3.6, 12.3 (Hb)
3''	3.72 ovl	3.868 td 8.7, 4.4
4''	3.03	3.11 td 8.8, 4.4
5''	3.94 (Ha)	3.97 dd 4.2, 11.5 (Ha)
	4.05 (Hb)	4.15 t 10.9 (Hb)
6''	3.37 s	3.35 s
7''	2.96 br	3.09 m
8''	1.23 t 7.1	1.28s t 7.3

[a]Data assigned from ^{1}H, PHOHAHA, and PTQFCOSY spectra.

[b]Overlapped by a large contaminant peak.

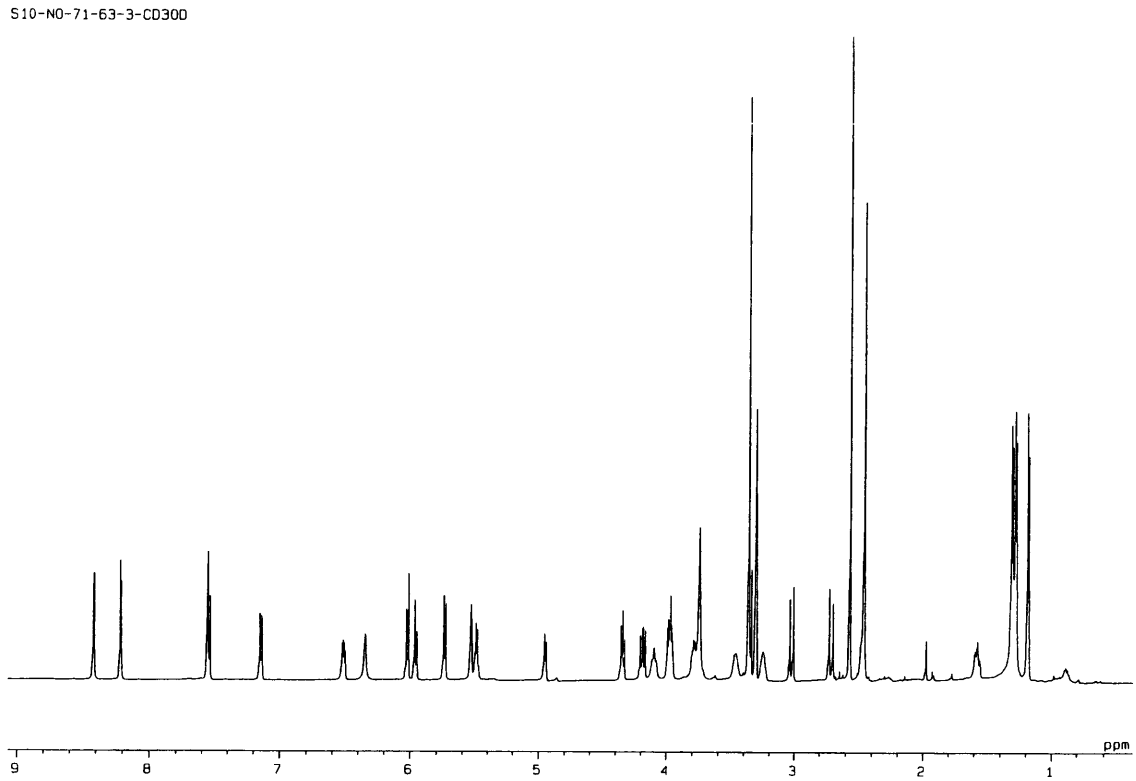

Fig. IV-11. ^{1}H NMR spectrum of shishijimicin A (4-1) in CD_3OD at 300 K.

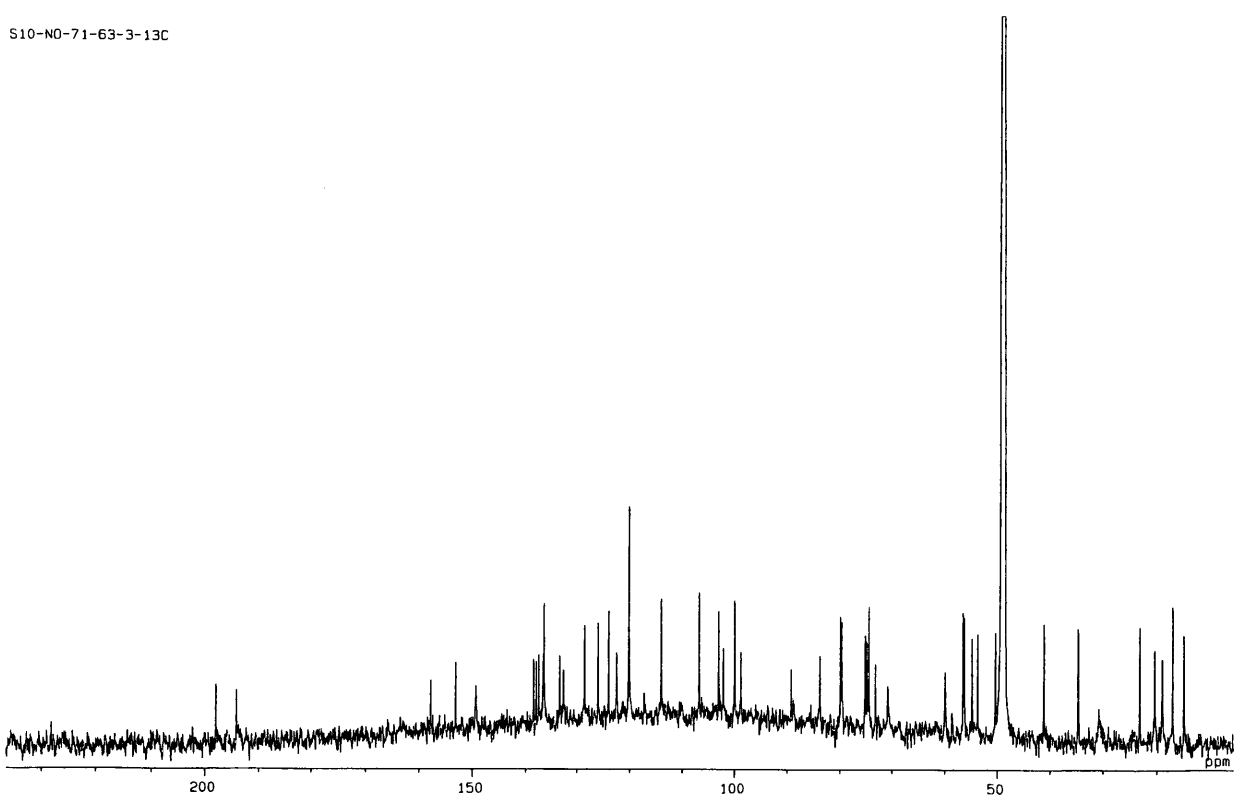

Fig. IV-12. ^{13}C NMR spectrum of shishijimicin A (4-1) in CD_3OD at 300 K.

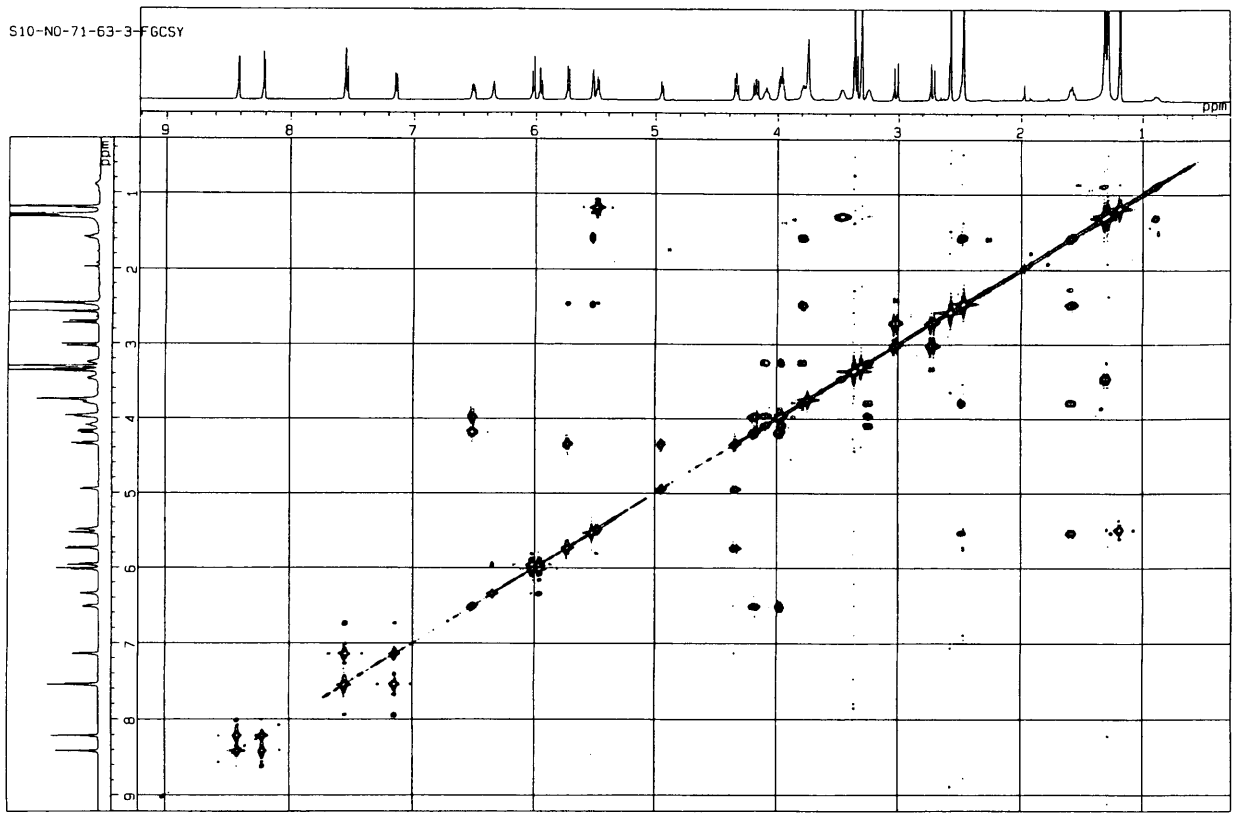

Fig. IV-13. FGCOSY45 spectrum of shishijimicin A (4-1) in CD_3OD at 300 K.

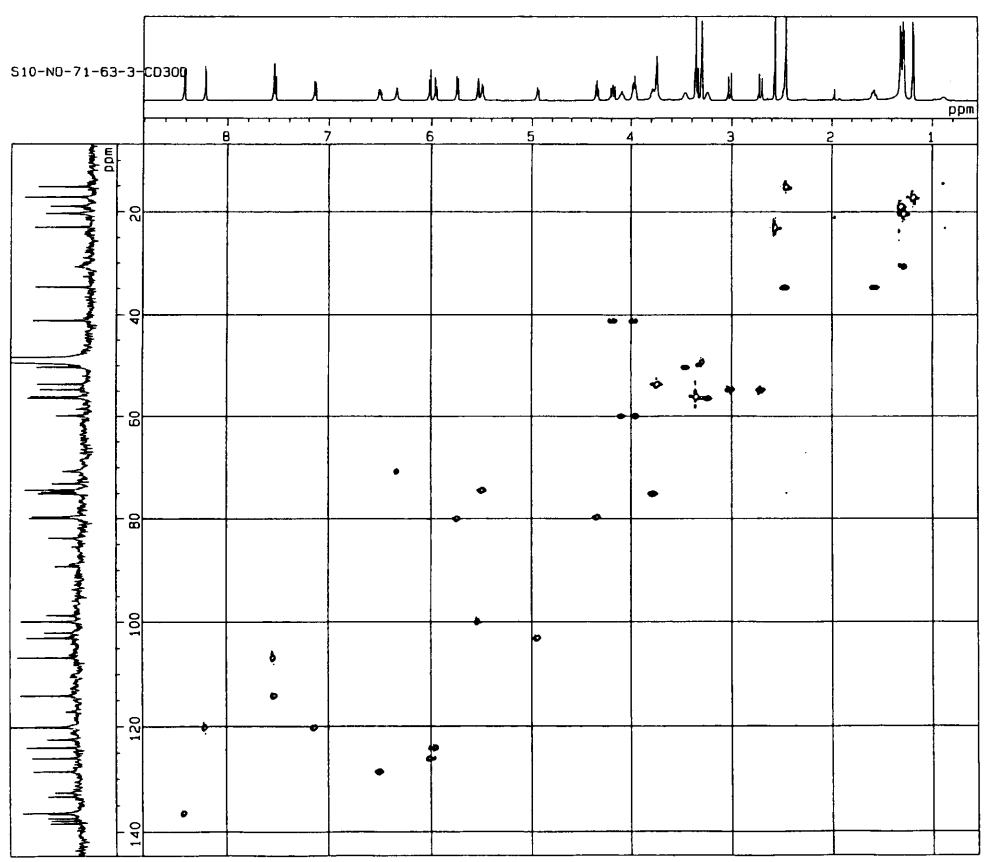

Fig. IV-14. PSFGHMQC spectrum of shishijimicin A (4-1) in CD_3OD at 300 K.

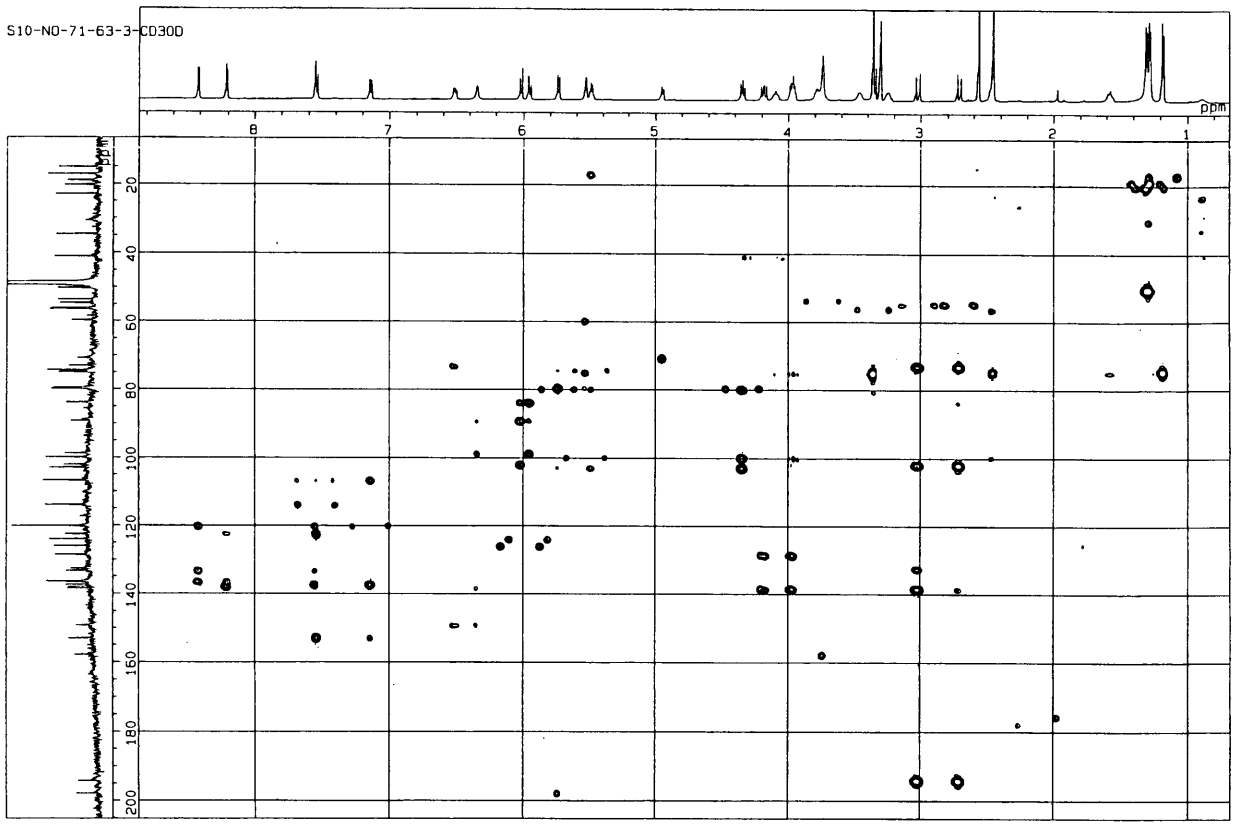

Fig. IV-15. FGHMBC spectrum of shishijimicin A (4-1) in CD_3OD at 300 K.

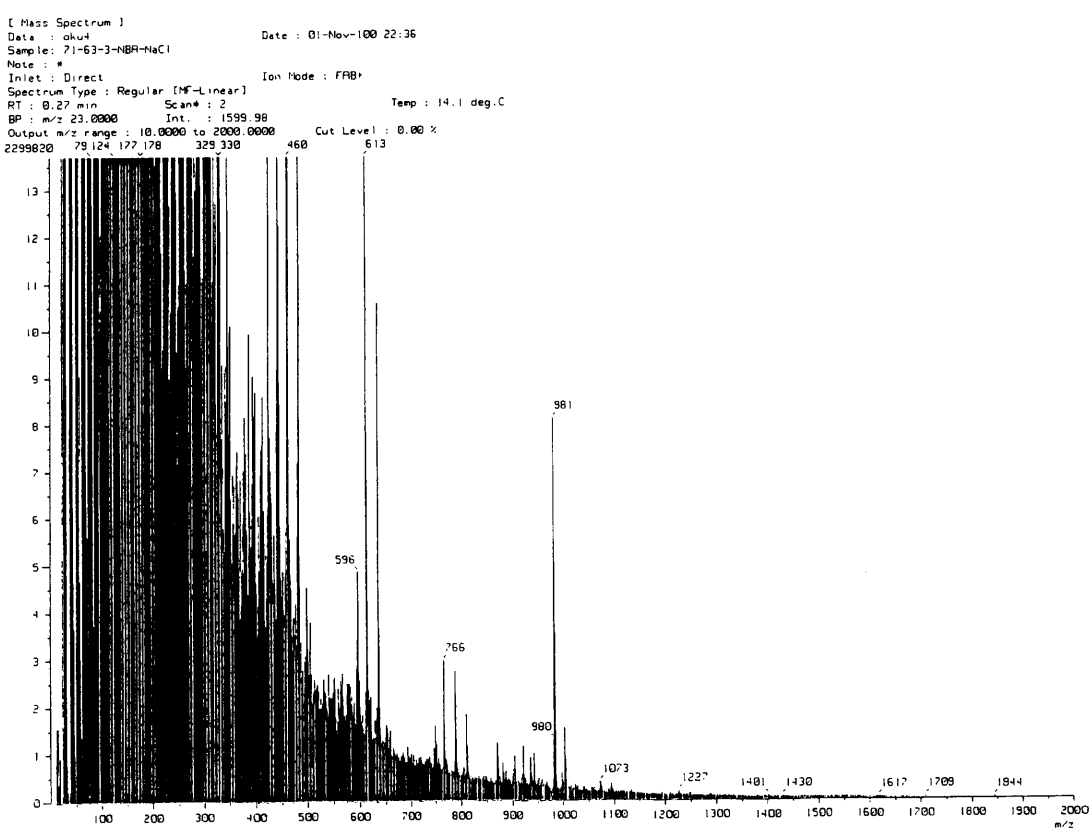

Fig. IV-16. LRFABMS (NBA matrix) spectrum of shishijimicin A (4-1).

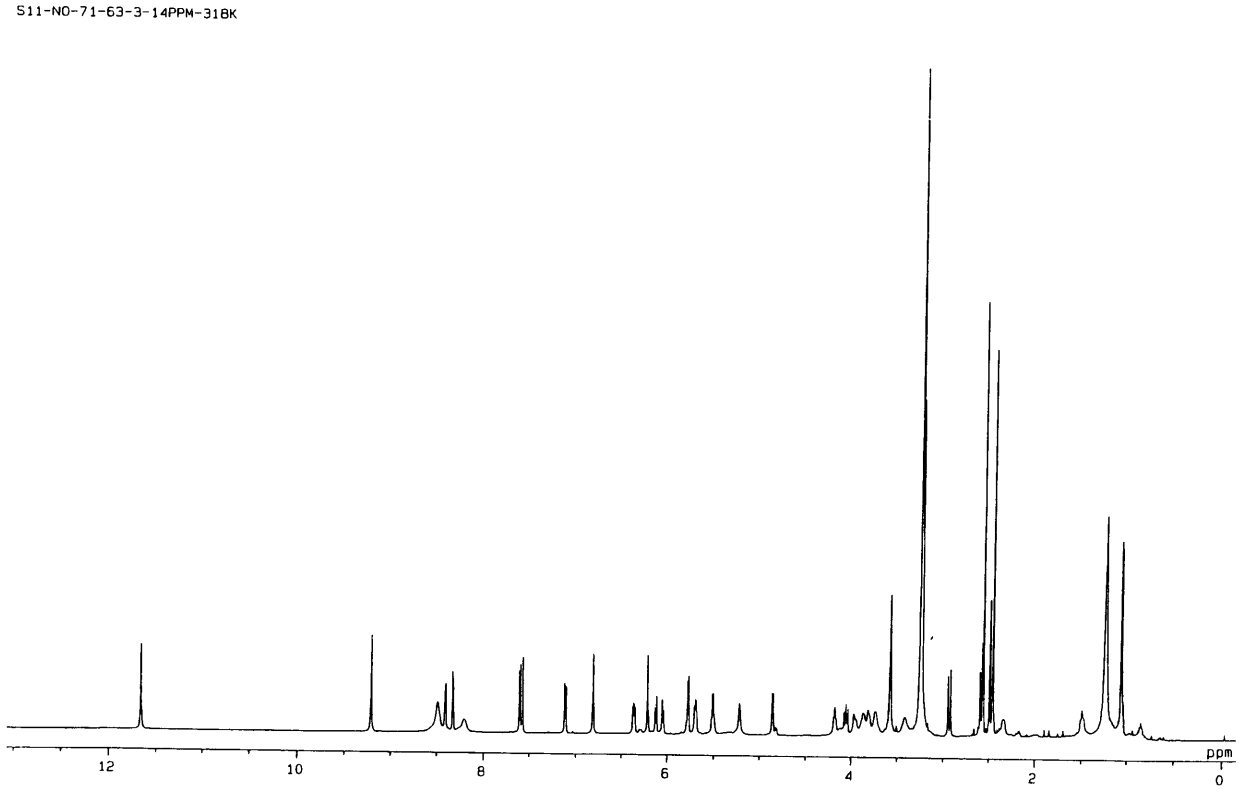

Fig. IV-17. ^{1}H NMR spectrum of shishijimicin A (4-1) in DMSO-d_6 at 318 K.

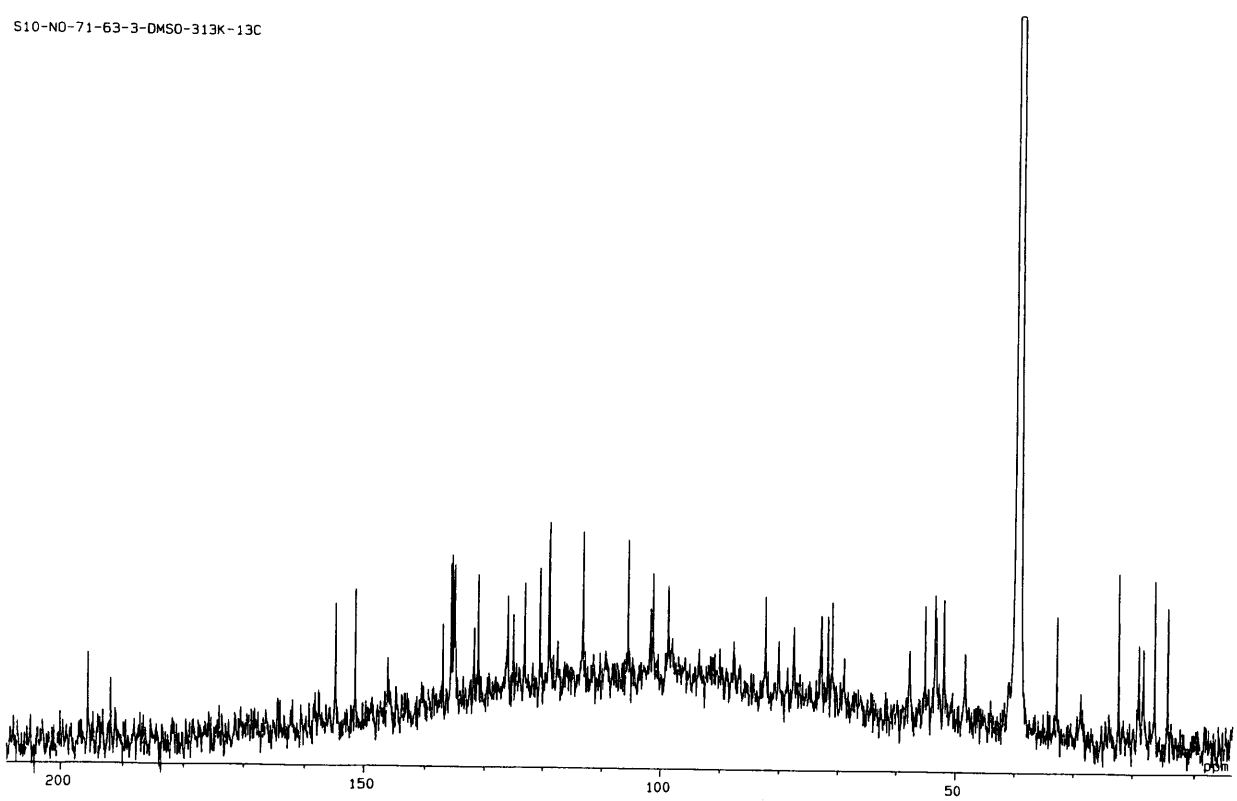

Fig. IV-18. ^{13}C NMR spectrum of shishijimicin A (4-1) in DMSO-d_6 at 318 K.

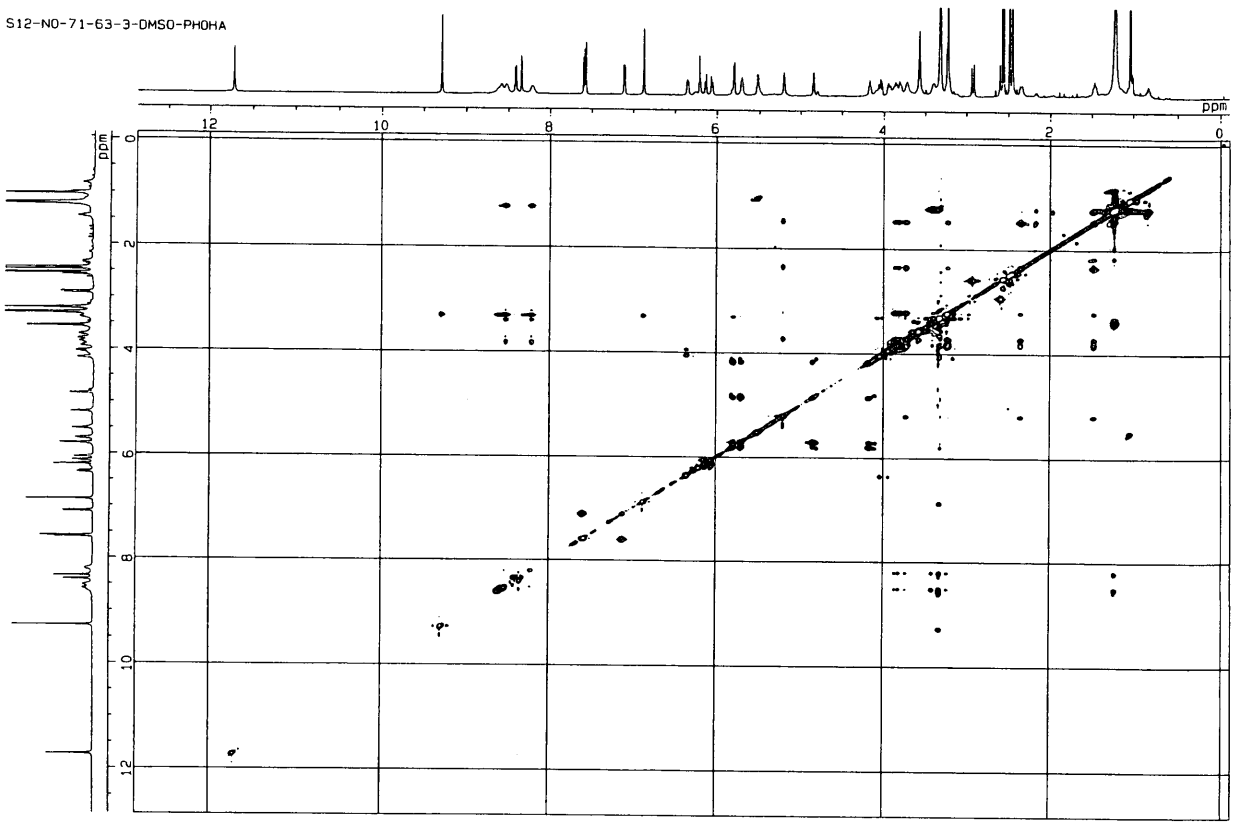

Fig. IV-19. PSHOHAHA spectrum of shishijimicin A (4-1) in DMSO-d_6 at 300 K.

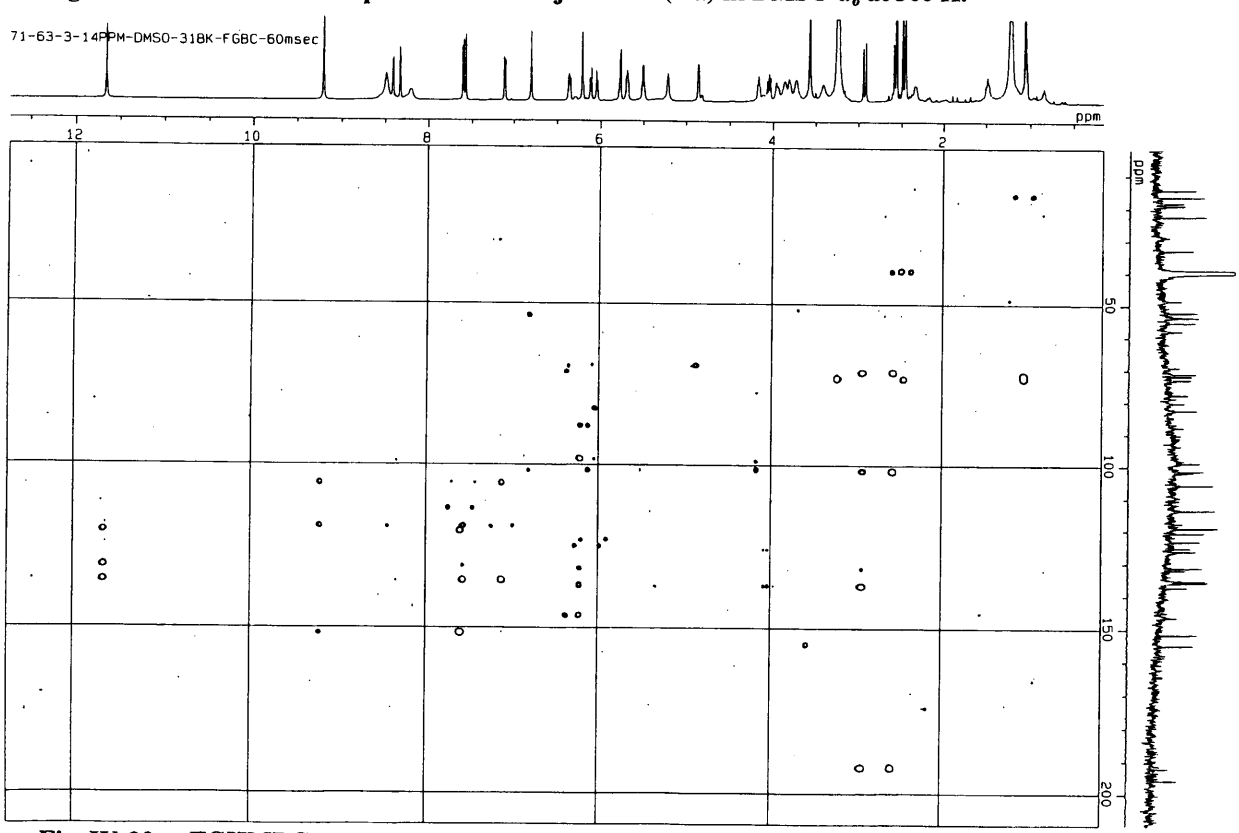

Fig. IV-20. FGHMBC spectrum of shishijimicin A (4-1) in DMSO-d_6 at 318 K.

Mixing time: 60 ms

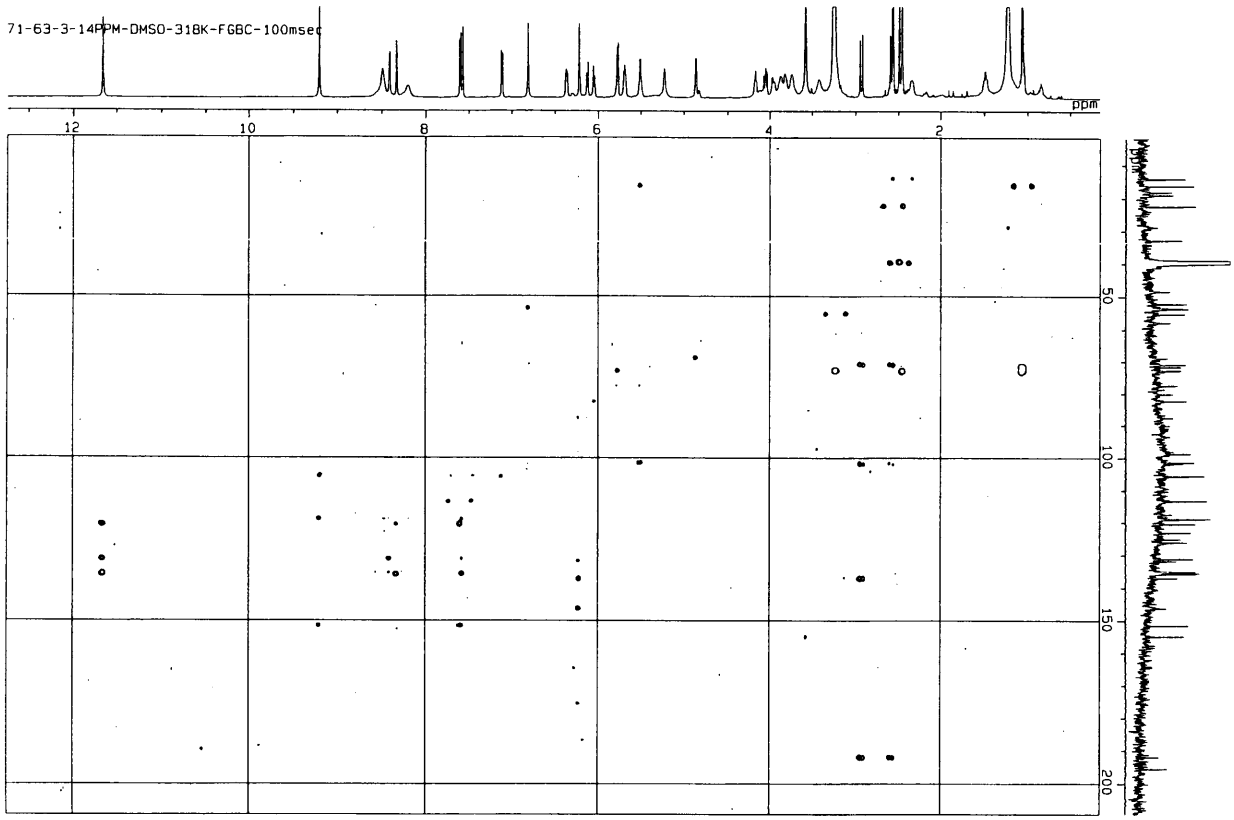

Fig. IV-21. FGHMBC spectrum of shishijimicin A (4-1) in DMSO-d_6 at 318 K.

Mixing time: 100 ms.

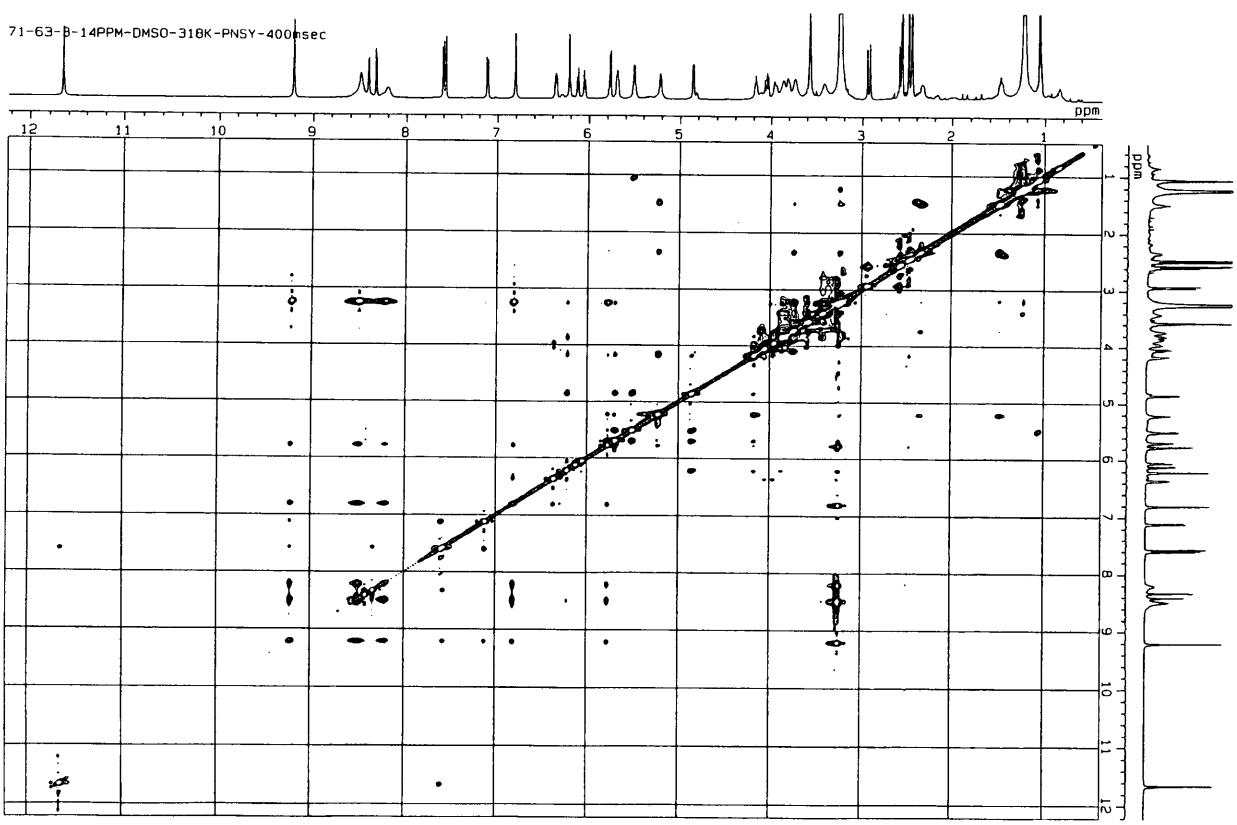

Fig. IV-22. PSNOESY spectrum of shishijimicin A (4-1) in DMSO-d_6 at 318 K.

Mixing time: 400 ms.

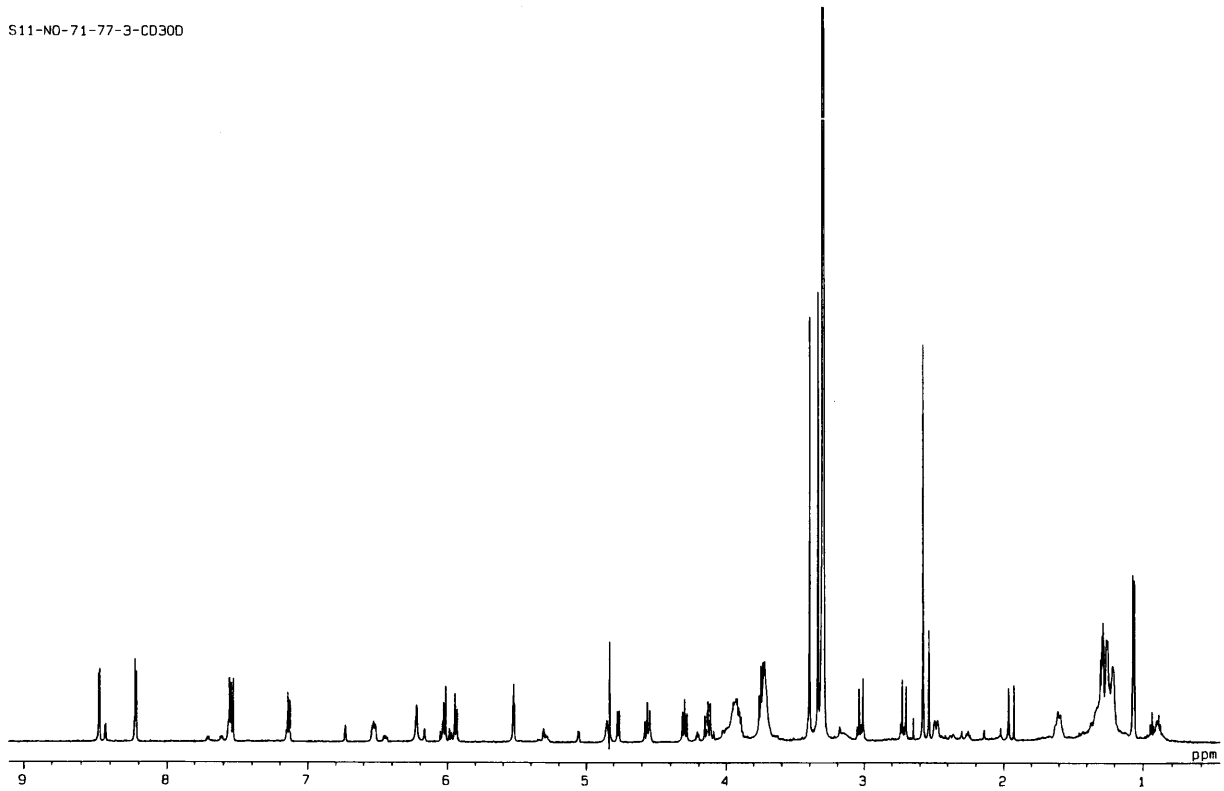

Fig. IV-23. ^{1}H NMR spectrum of shishijimicin B (4-2) in CD_3OD at 300 K.

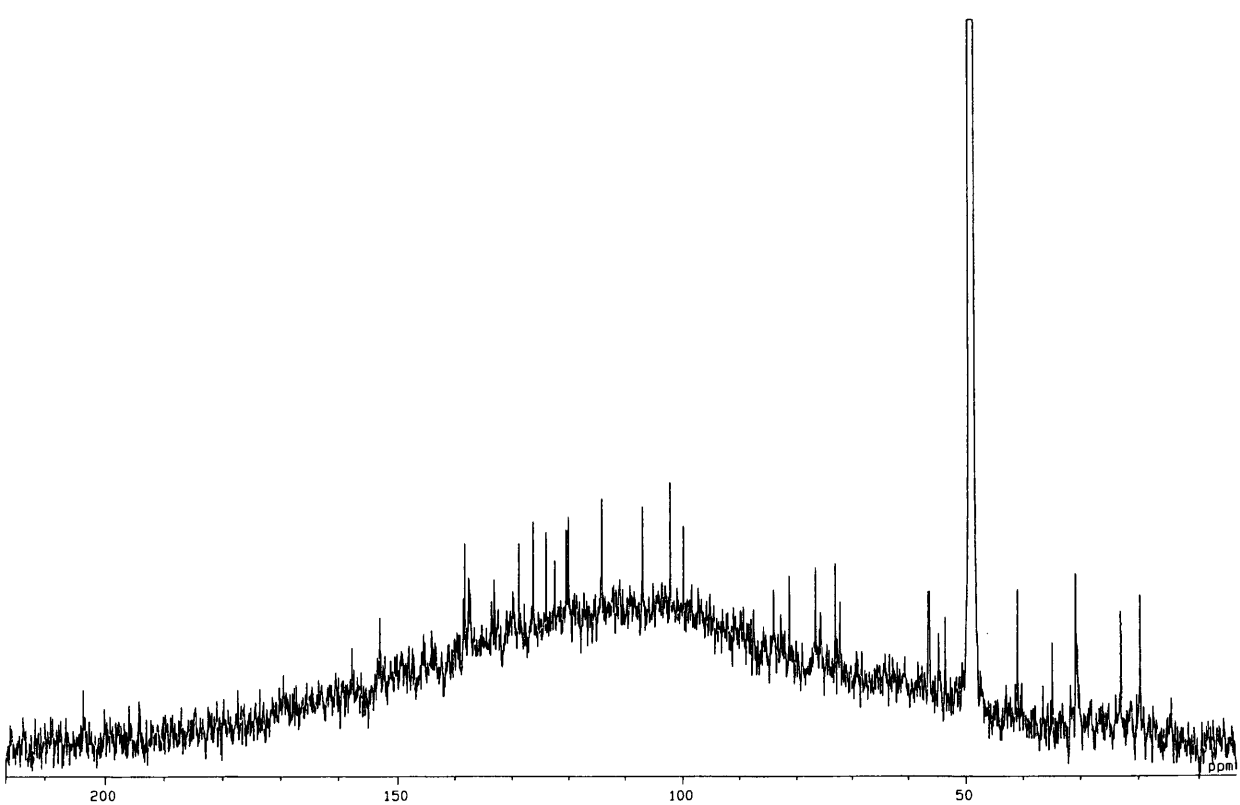

Fig. IV-24. ^{13}C NMR spectrum of shishijimicin B (4-2) in CD_3OD at 300 K.

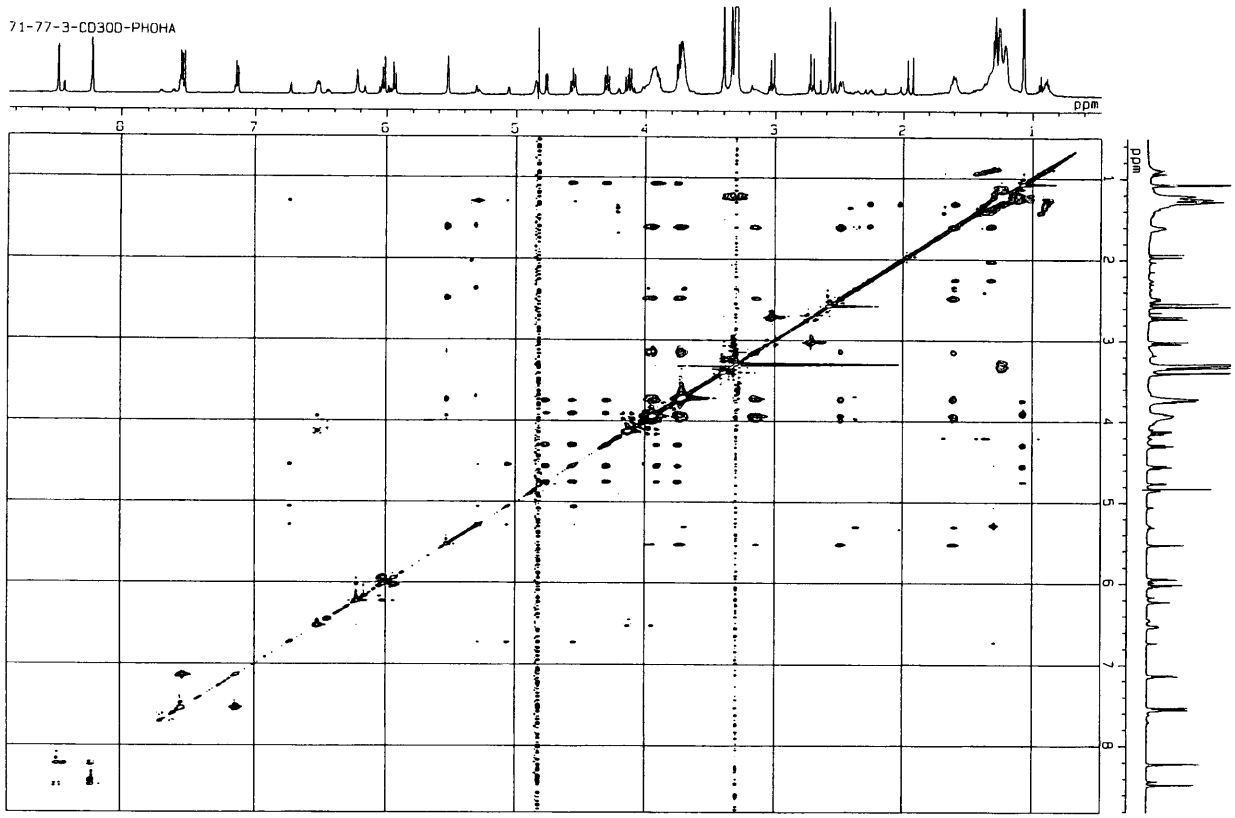

Fig. IV-25. PSHOHAHA spectrum of shishijimicin B (4-2) in CD_3OD at 300 K.

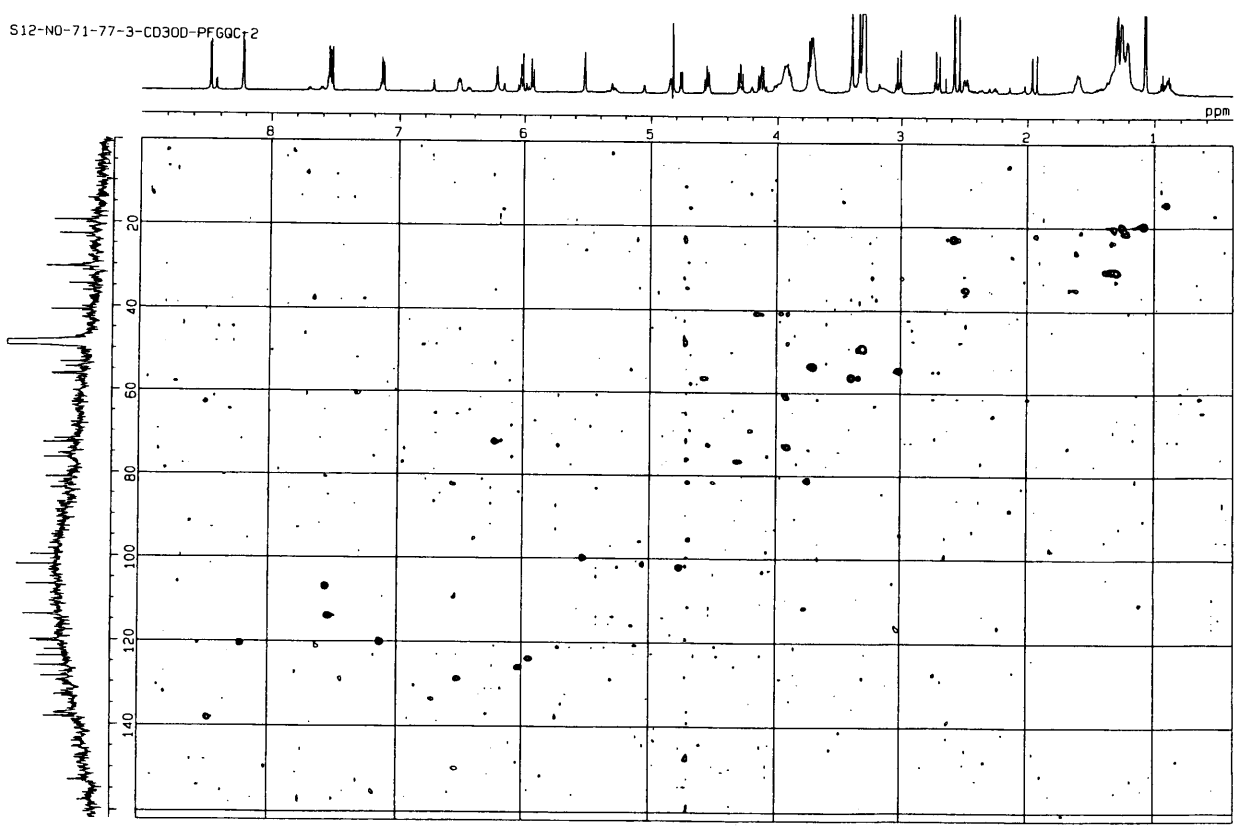

Fig. IV-26. PSFGHMQC spectrum of shishijimicin B (4-2) in CD_3OD at 300 K.

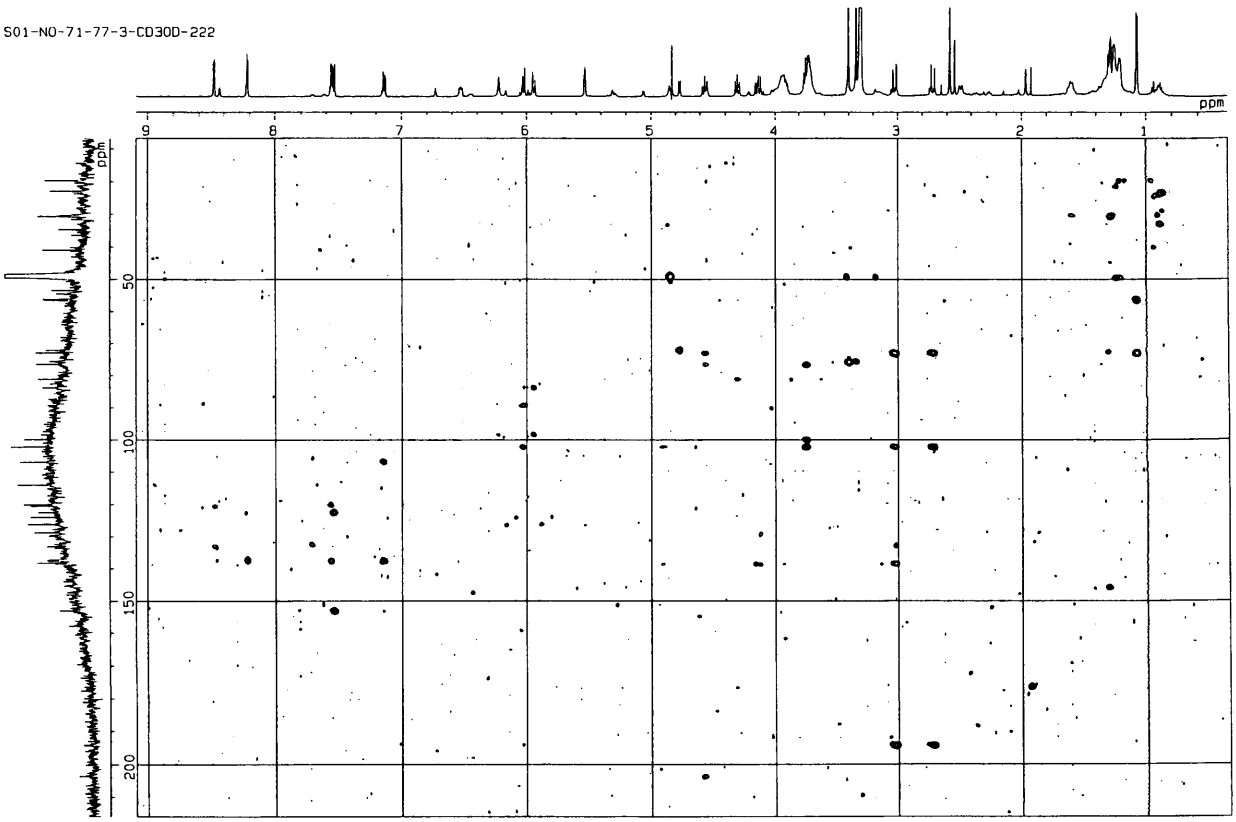

Fig. IV-27. FGHMBC spectrum of shishijimicin B (4-2) in CD_3OD at 300 K.

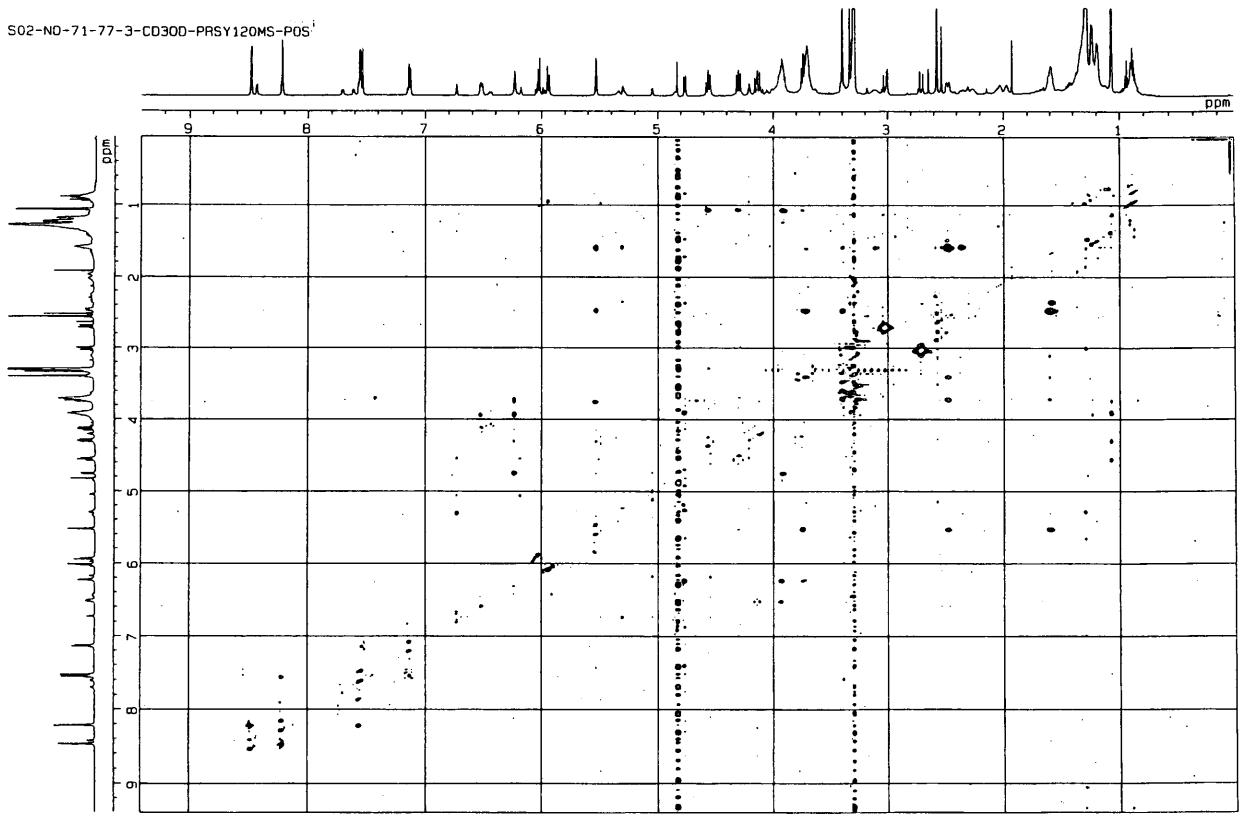

Fig. IV-28. PSROESY spectrum of shishijimicin B (4-2) in CD_3OD at 300 K.

Mixing time: 140 ms.

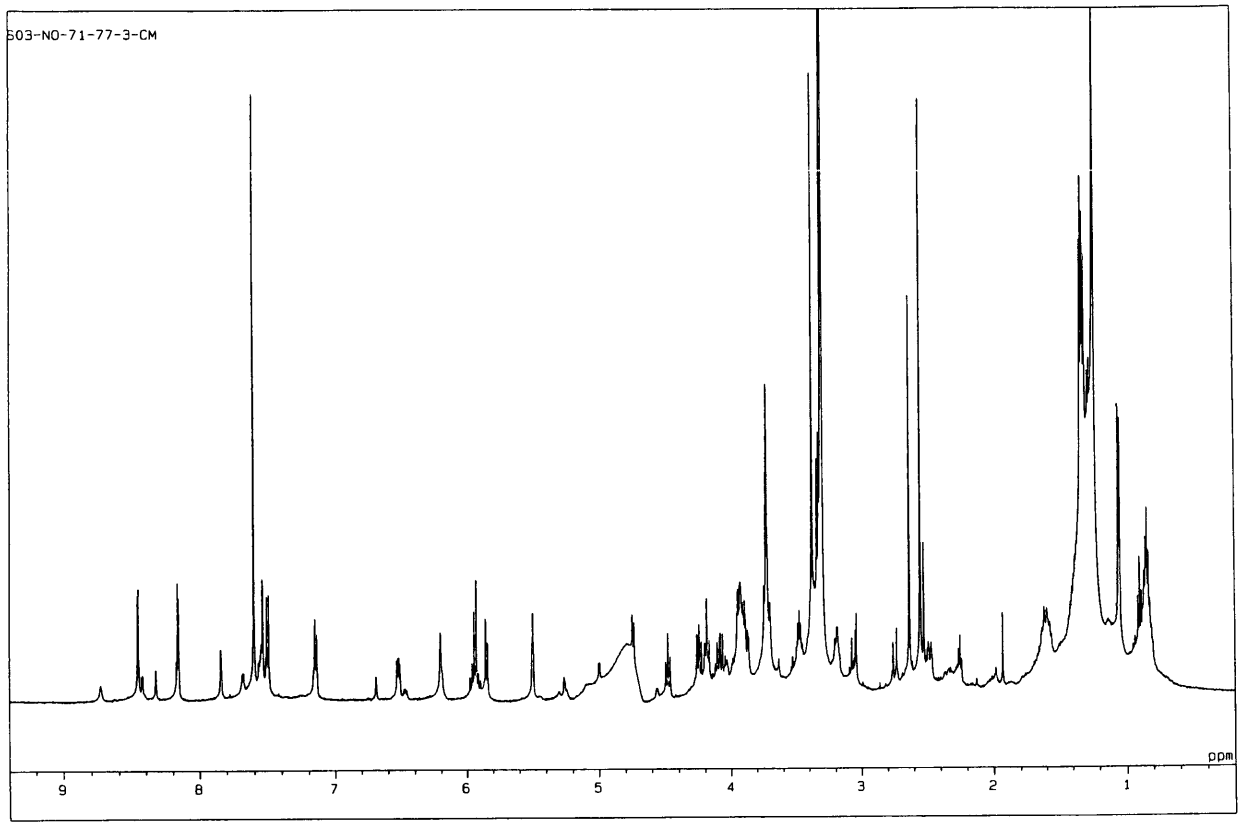

Fig. IV-29. ^{1}H NMR spectrum of shishijimicin B (4-2) in CD_3OD:$CDCl_3$:pyridine-d_5 (100:100:0.1) at 300 K.

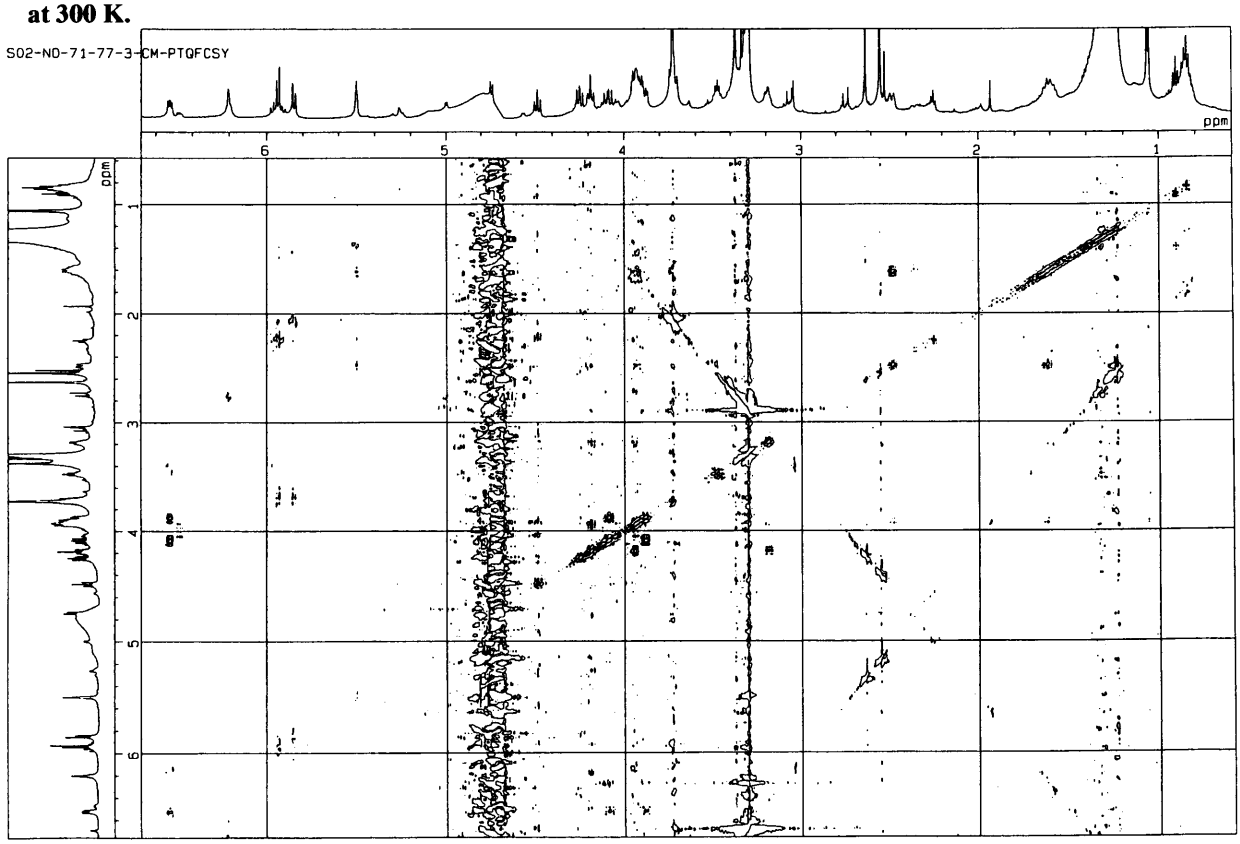

Fig. IV-30. PSTQFCOSY spectrum of shishijimicin B (4-2) in CD_3OD:$CDCl_3$:pyridine-d_5 (100:100:0.1) at 300 K.

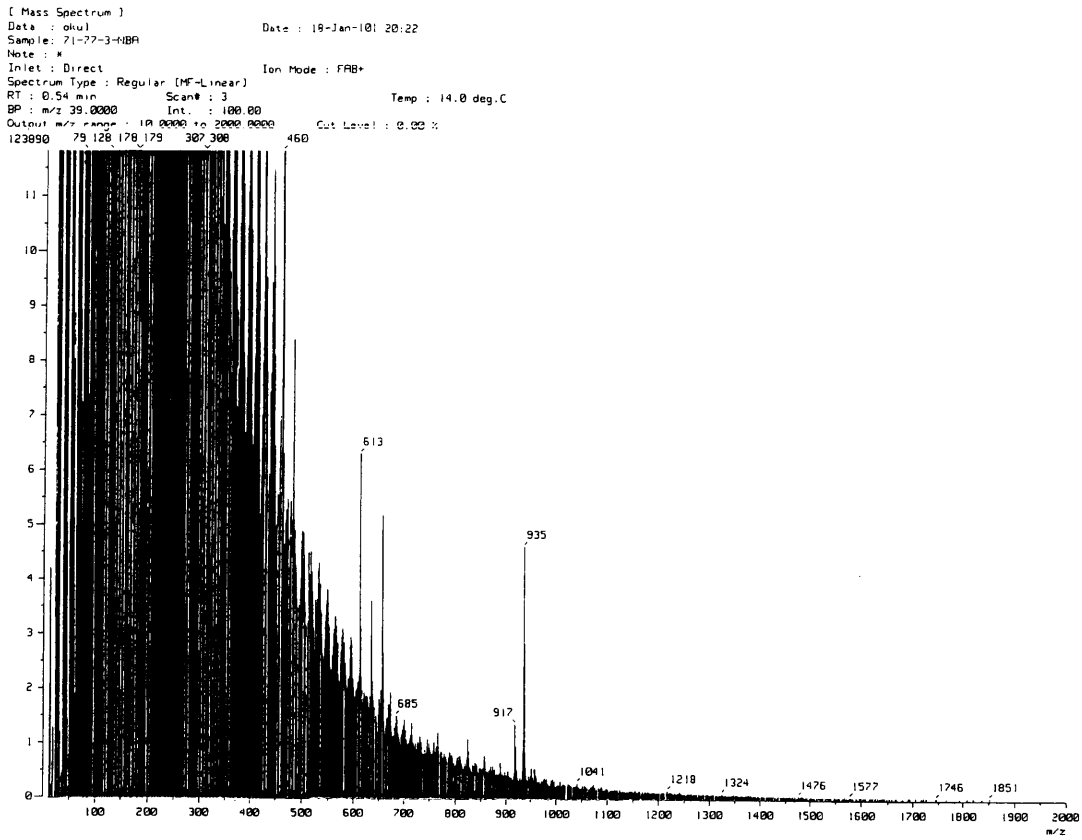

Fig. IV-31. LRFABMS spectrum (NBA matrix) of shishijimicin B (4-2).

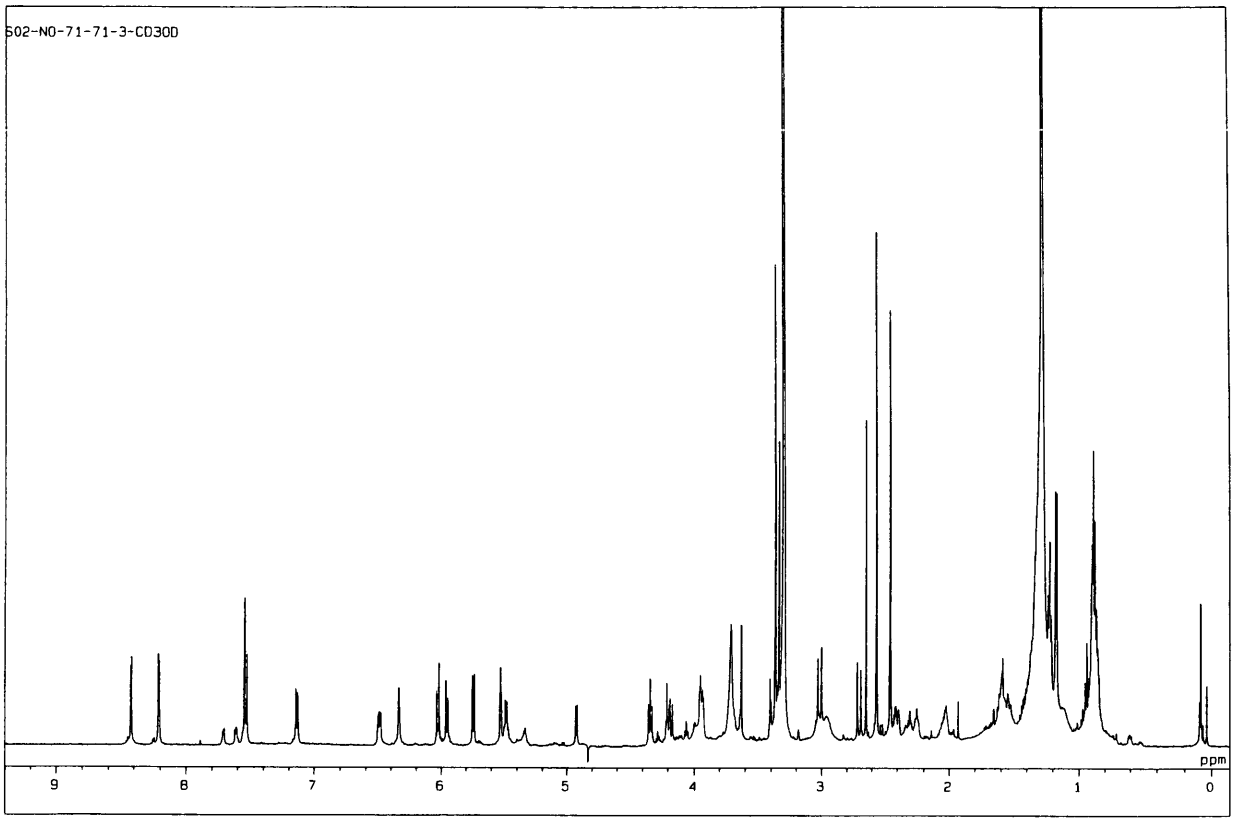

Fig. IV-32. ^{1}H NMR spectrum of shishijimicin C (4-3) in CD_3OD at 300 K.

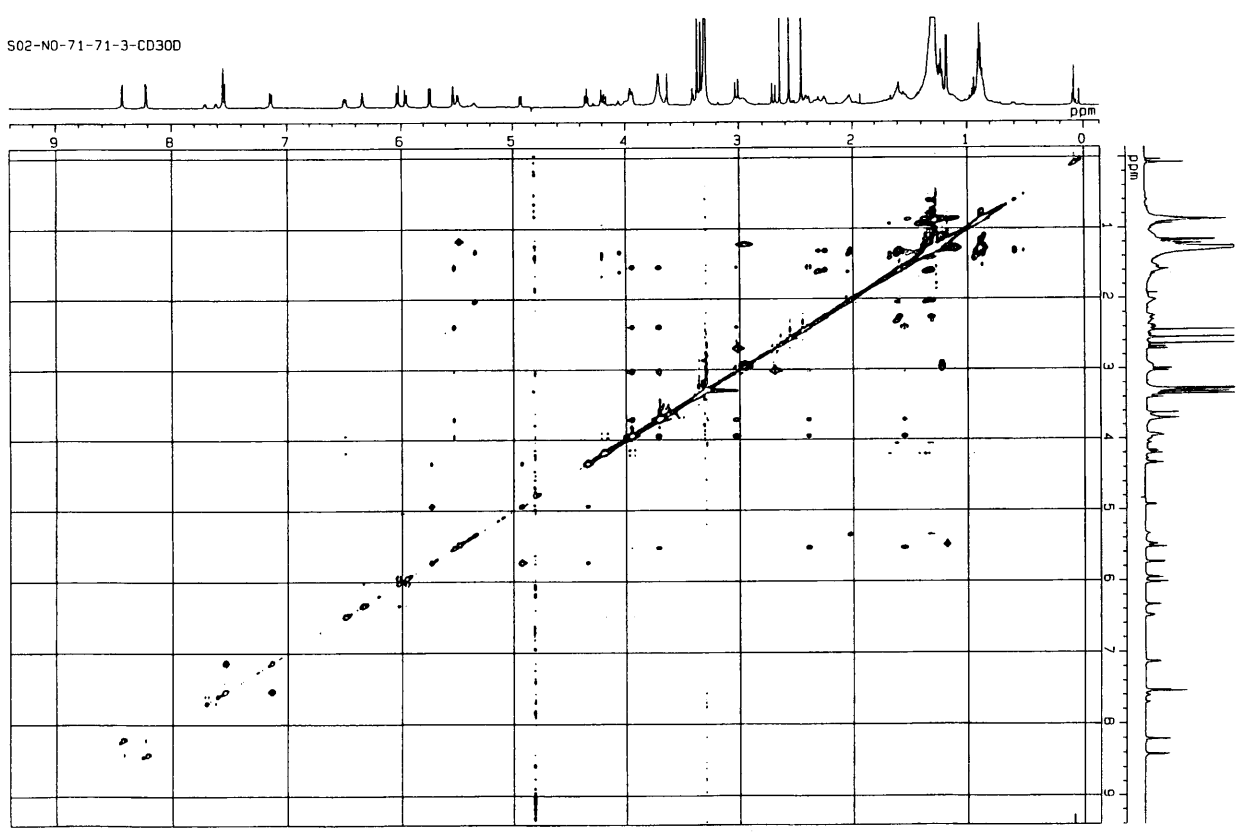

Fig. IV-33. PSHOHAHA spectrum of shishijimicin C (4-3) in CD_3OD at 300 K.

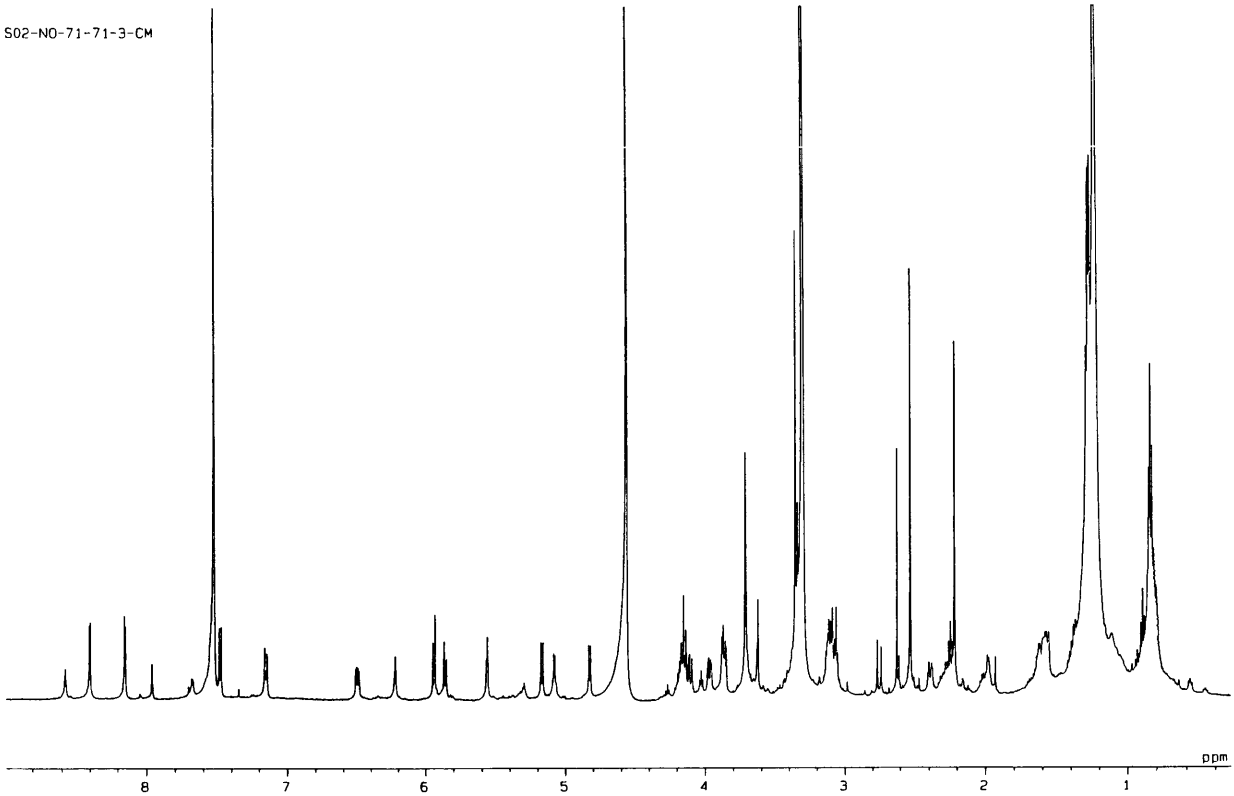

Fig. IV-34. ^{1}H NMR spectrum of shishijimicin C (4-3) in CD_3OD at CD_3OD-$CDCl_3$-pyridine-d_5 (100:100:0.1) at 300 K.

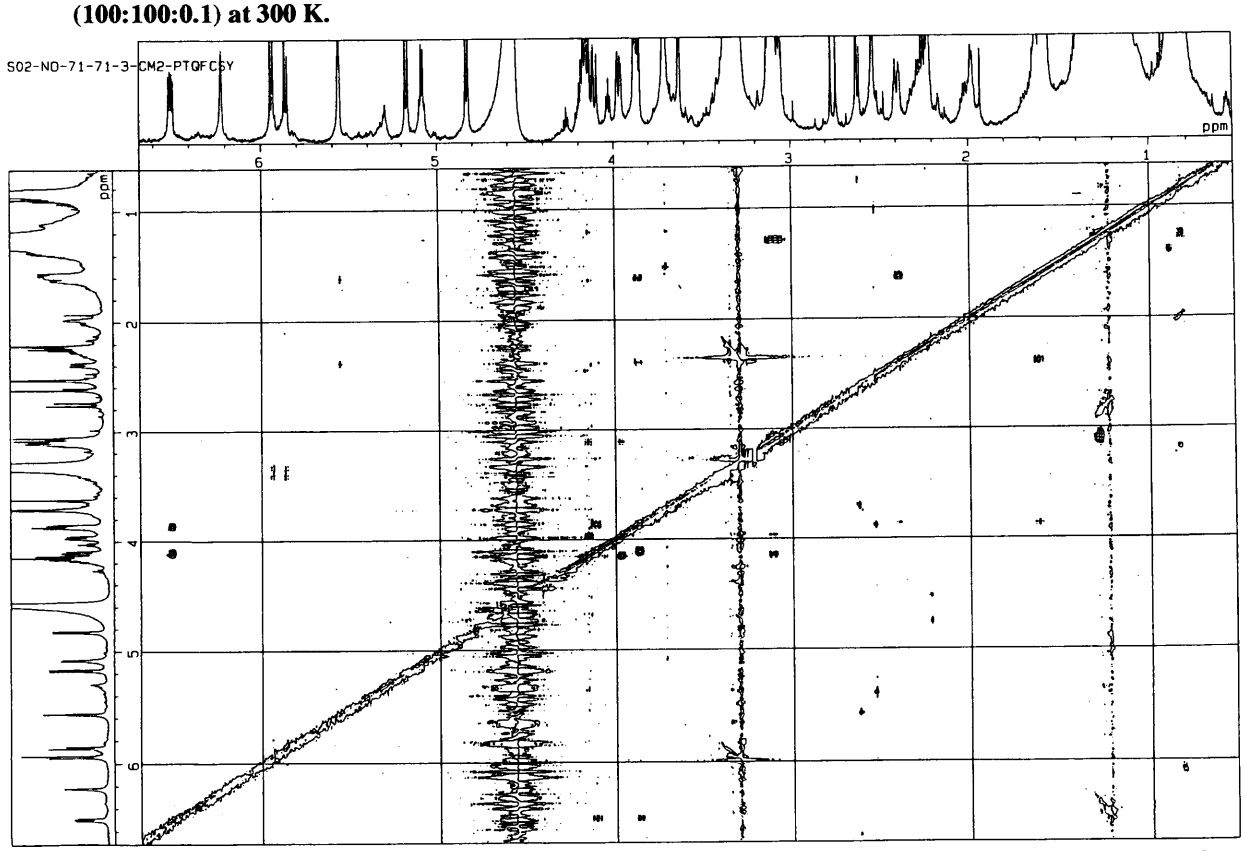

Fig. IV-35. PSTQFCOSY spectrum of shishijimicin C (4-3) in CD_3OD-$CDCl_3$-pyridine-d_5 (100:100:0.1) at 300 K.

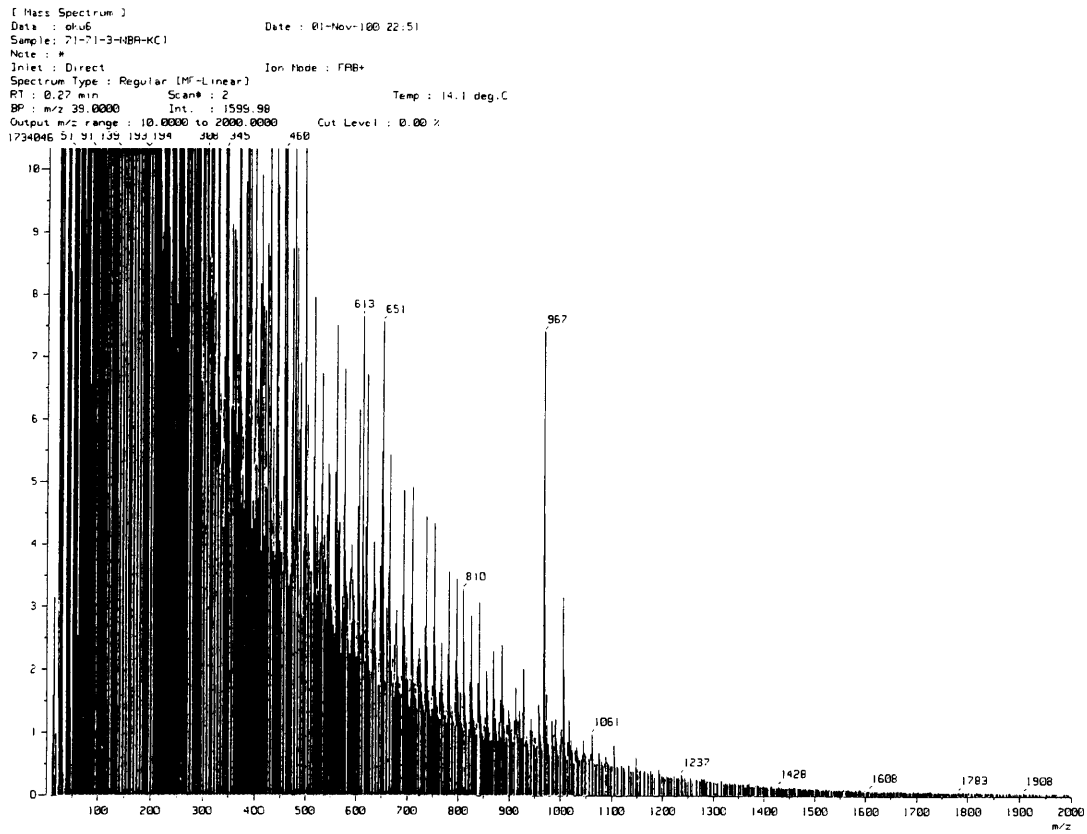

Fig. IV-36. LRFABMS spectrum (NBA matrix) of shishijimicin C (4-3).

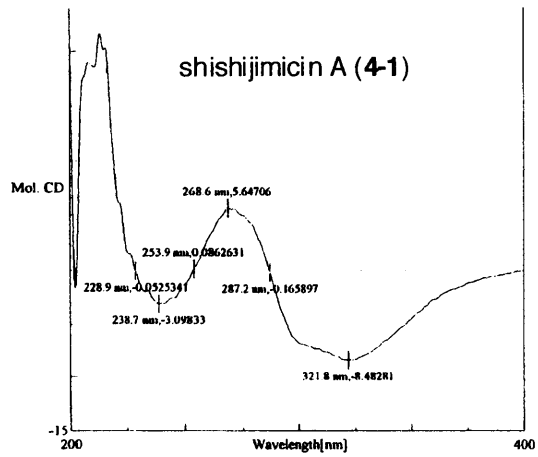

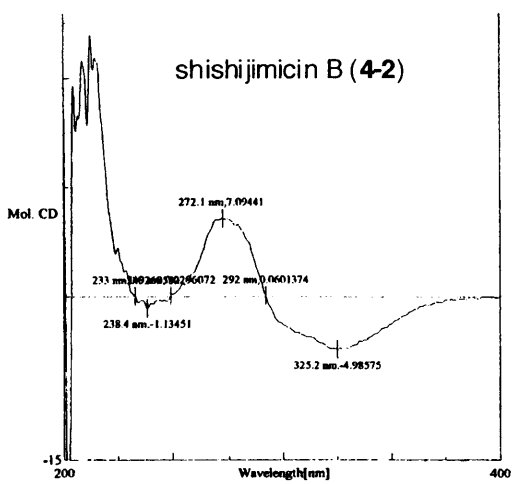

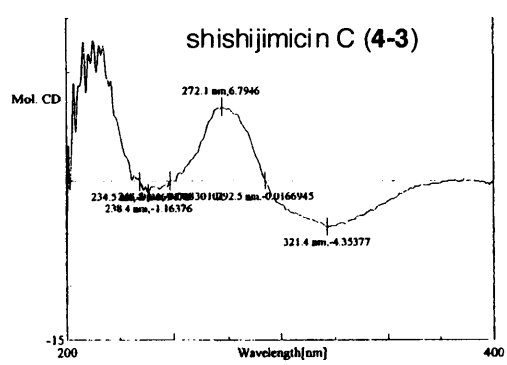

Fig. IV-39. CD spectra of shishijimicins A-C (4-1~4-3) in MeOH.

CHAPTER V

RENIERAMYCIN J, DIMERIC TETRAHYDROISOQUINOLINE ALKALOID THAT INDUCE MORPHOLOGY CHARACTERISTIC OF RNA/PROTEIN SYNTHESIS INHIBITORS FROM AN UNIDENTIFIED PURPLE-BLUE SPONGE

1. Introduction

In the screening of the samples that had been collected in the Satsunan Archipelago during the cruise on R/V Toyoshio-maru, June 2000, the organic extract of a purple-blue sponge, coded S00-151 (**Fig. V-1**), showed promising activity in the cell-morpholoIgy based assay. The cells exposed to 1 μg/mL of the extract shrank their nucleoli, in some cases they completely disappeared, and the outline of the cells became unclear, looked as if they fused to be polyploidal cells (**Fig. V-2**) within 24 hours. Similar changes are often observed when the cells are treated with inhibitors of macromolecule (RNA or protein) syntheses (see CHAPTER I). The extract also showed potent antibacterial activity, suggesting that the active substance should inhibit RNA or protein synthesis of mammalian cells and bacteria. Isolation and structure elucidation of the active principle(s) have been attempted.

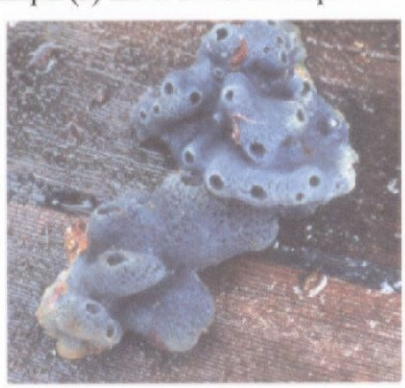

Fig. V-1. The unidentified purple-blue sponge S01-051.

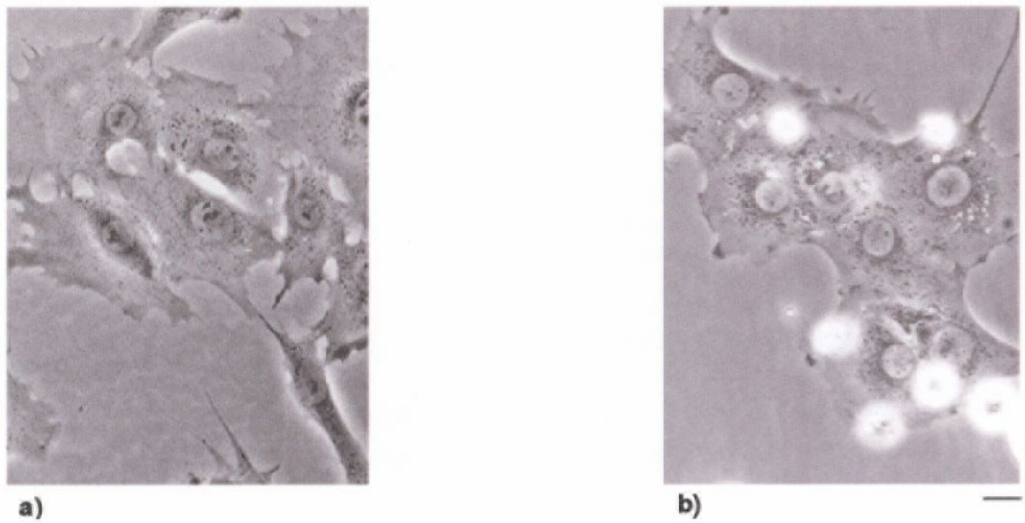

Fig. V-2. Morphological change of 3Y1 cells caused by the organic extract of the purple-blue sponge S00-151. a) Untreated cells. b) Cells treated with 1μg/mL of the extract for 24 hours. Bar represents 20 μm.

2. Results and Discussion

2-1. Isolation

In a prelimminary experiment, the active fractions in the cell-morphology based assay were always associated with antimicrobial activity against *E. coli*. Therefore, each fractionation step was guided by bioautography against *E. coli* followed by cytotoxicity tests using 3Y1 cells to confirm the validity of the choice. The activity was lost when the crude extract was treated with aqueous MeOH containing 5% ammonia so that use of basic solvents was avoided.

The ethanolic extract of the frozen sample (800 g) was partitioned between 60% MeOH and dichloromethane, and the dichloromethane layer was further partitioned between 90% MeOH and *n*-hexane. The 90% MeOH layer was then partitioned into EtOAc/*n*-heptane/MeOH/H_2O (7:4:4:3). The activity was found in both phases; the lower phase was gel-filtered on Sephadex LH-20 and separated successively by ODS-HPLC and phenylhexyl-HPLC using aqueous MeCN containing 0.2 M NaCl to afford renieramycin J (**5-1:** 2.0×10^{-3}%, wet wt) as a brown solid. The isolation procedure is shown in **Scheme. V-1**.

S01-051
(Kuchinoerabujima Island, 800 g)

1) extracted with EtOH (12 L)
2) partitioned between **DCM** / 60% MeOH
3) partitioned between**90% MeOH** / *n*-hexane
4) EA/*n*-hepane/MeOH/H_2O (7:4:4:3)
lower / upper
5) Sephadex LH-20 (MeOH)
6) ODS-HPLC (38% MeCN-0.2M NaCl)
7) Phenylhexyl-HPLC (38% MeCN-0.2M NaCl)

Renieramycin J (5-1)
(16.2 mg; 2.0×10^{-3}%, wet wt)

Scheme V-1. Isolation Scheme of Renieramycin J (5-1).

2-2. Structure Elucidation

Renieramycin J (**5-1**) was susceptible to air-oxidation; even a fresh preparation from HPLC contained an oxidation product (**5-2**) as a minor component. Oxidation also proceeded in the NMR tube, in which the content of **5-2** increased from 20% to 30% in 24 hours. (**Fig. V-9**).

2-2-1. Planar Structure (Fig. V-3)

Although the ^{1}H NMR spectrum (**Fig. V-8**) of renieramycin J (**5-1**) showed well-dispersed signals in CD_3OD, signal assignment was not easy, especially the region of δ 4.25-4.35 because of overlapping of the oxidation product. ^{13}C NMR and HMQC data (**Figs. V-10 and V-14**) showed the presence of characteristic units of reniearmycin-type alkaloids[112-116]; the *N*-methyl group, 2-methoxy-3-methyl-1,4-benzoquinone (ring A), and angelate ester. However, HMQC crosspeaks of δ 2.14/9.48 and 3.69/60.89 indicated the presence of 2-methoxy-3-methylhydroquinone (ring E), instead of two quinonoid structure as the case of other renieramycins, which was supported by a UV maximum at 273 nm (ε 12000). Analysis of the COSY spectrum (**Fig. V-12**) revealed three spin systems, H1-H22, $H_2$4-H3-H11, and H13-H21 together with a characteristic homoallylic coupling between H1 and H4 (~2.3 Hz) and a W-coupling between H11

and H13 (1.8-2.8 Hz), which was constructed into rings B and C based on HMBC data (**Fig. V-15**). The angelate moiety could be linked to C22 by an HMBC cross peak from $H_2$22 to ester carbonyl C24 (δ 168.57), whereas the benzoquinone unit was placed adjacent to ring B by HMBC correlations from H_{eq}4 (δ 3.03) to quinone carbonyl C5 (δ 186.96) as well as 6-Me (δ 1.85) to C5. HMBC correlations from oxymethine proton H14 (δ 4.79) to C21, C15 (δ 148.08), C16 (δ 120.70), C19 (δ 113.17), and C20 (δ 118.73) as well as H11 to C18 (δ 142.05) and C19 constructed the tetrahydropyridine unit (ring D) and placed the hydroquinone unit as shown. It should be mentioned that the chemical shift values of carbinolamine methine (δ 4.58/90.24) was downfield-shifted from typical values for hemiaminals (δ_H: ~4.4, δ_C: ~83, see **Fig. V-3**, inset), thus indicating that renieramycin J (**5-1**) formed a methyl-d_3 aminal by replacing hydroxyl group on C21 with deuteromethoxyl during measurements of the NMR spectra in CD_3OD. This was also verified by the spectra measured in MeCN-d_3 (*vide infra*). Key HMBC correlations are summarized in **Fig.V-3**.

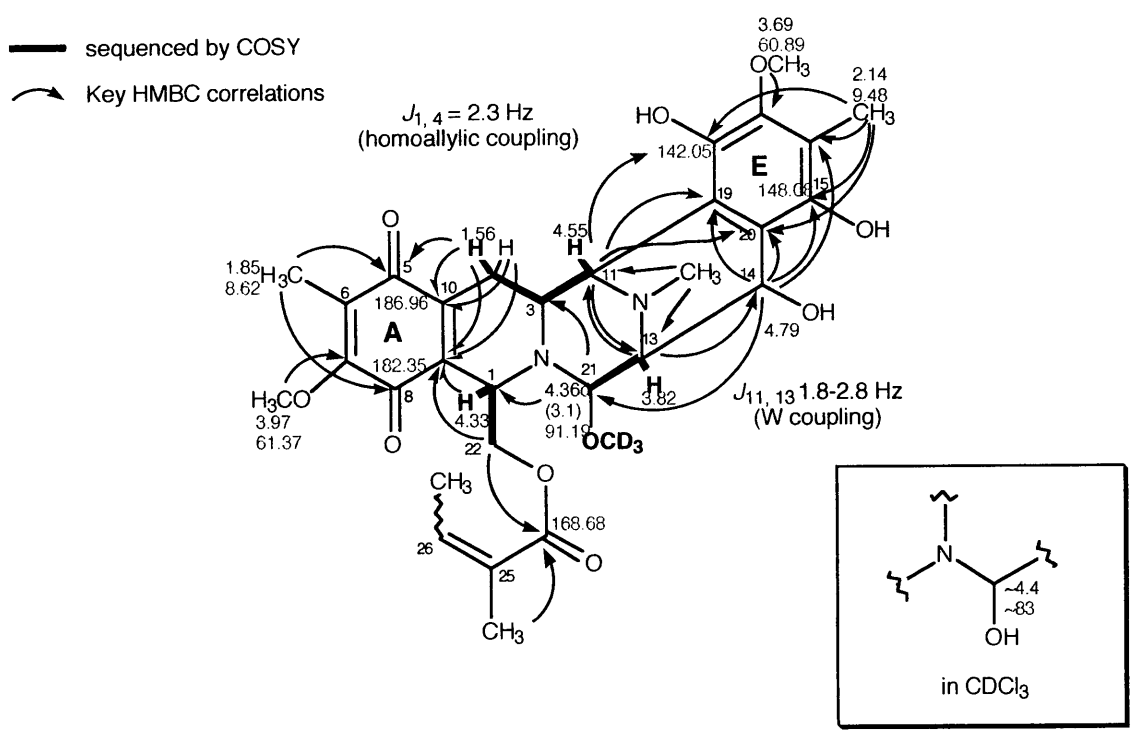

Fig. V-3. Key HMBC correlations of renieramycin J (5-1) (mixing time = 60 ms). The nset shows typical δ values for hemiaminal methines.

The FAB mass spectrum of renieramycin J (**5-1**) showed an intensive ion peak at *m/z* 569.2502 ([M+2H-OH]$^+$, calcd for $C_{30}H_{37}N_2O_9$, **Fig. V-11**), which was smaller by 32 mass units than the value for the methyl-d_3-aminal structure established from NMR data. This difference was rationalized by formation of an iminium ion during FAB ionization after elimination of the methoxyl-d_3 group with concomintant reduction of the quinone (ring A) to a hydroquinone[117] (**Scheme V-2**).

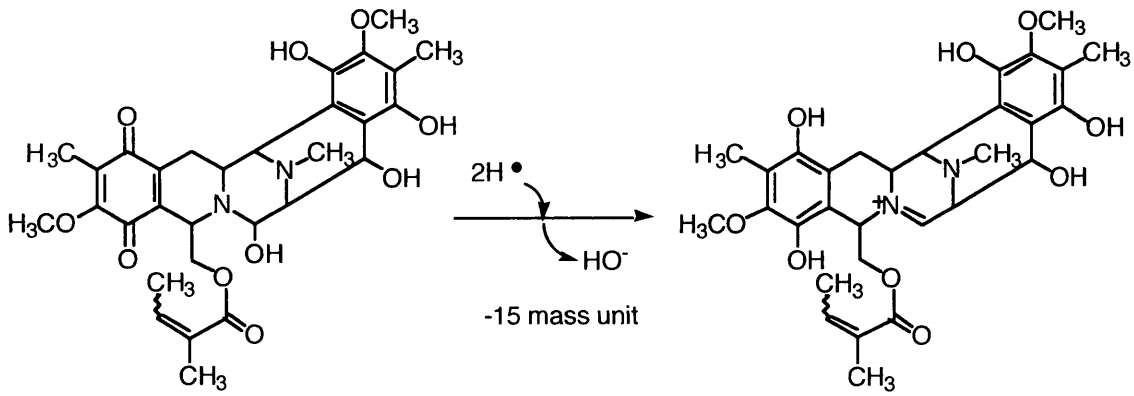

Renieramycin J (5-1)

Structure established from NMR data
Exact Mass: 584

HRFABMS data:
m/z 569.2502 [M+2H-CD_3O]$^+$

Scheme. V-2. FAB Ionization Process of Renieramycin J (5-1).

The minor component, oxidized renieramycin J (**5-2**) exhibited a pseudo-molecular ion peak at *m/z* 569 as the original compound **5-1**. The ^{1}H NMR spectrum of **5-2** was almost identical with that of **5-1** except for the downfield-shift of 17-OMe (δ 3.69 → 3.97) and upfield-shift of 16-Me (δ 2.14 → 1.91), indicative of oxidation of hydroquinone to quinone in ring E. This assignment was confirmed by interpretation of the HMBC spectrum and chemical conversion of renieramycin J by air oxidation (see below). NMR data for renieramycin J (**5-1**) and the oxidized derivative **5-2** are summarized in **Tables V-2** and **V-3**, respectively.

2-2-2. Relative Stereochemistry

The relative stereochemistry of renieramycin J (**5-1**) was deduced from the coupling constants and NOESY data (**Fig. V-16**) as shown in **Fig. V-4**. An NOE correlation between 25-Me and H26 confirmed the ester was angelate but not tiglate. The stereochemistry of the 3,9-diaza-bicyclo[3.3.1]nonane (ring CD) portion was determined as shown based on the *trans*-diaxial relationship of $H_{ax}4$ and H3 (J=11.2 Hz) and NOE correlations between H3 and H11 which in turn was correlated with $H_{eq}4$, but not with $H_{ax}4$. The β-orientations of both H14 and H21 were determined by a correlation between them.

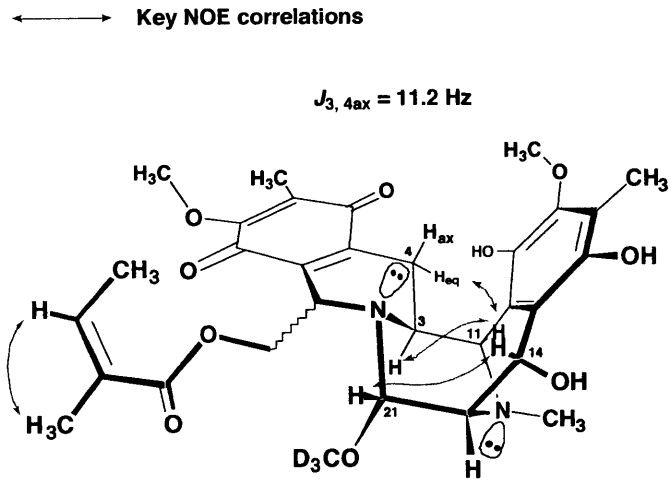

Fig. V-4. Key NOE correlations for renieramycin J (5-1) in CD_3OD.

The configuration of C1 was at first misassigned as *R** because of the absence of 1,3-diaxial NOESY correlation between H1 and H3 as well as the presence of a strong NOE between H1 and H21. However, all of the related compounds so far isolated have (*S**)-configuration at C1, which led to reexamination of this chiral center.

The crystal structures of saframycin C[118] (**Fig. V-5**) and brominated safracin A[119] show that the pyruvylamide or alanylamide unit linked to C22 is axially oriented, rather than being in an equatorial position. This conformation fixes H1 in a pseudo-equatorial position and prevents it to show an NOE between H-3. The same conformation seems to be the case of renieramycin J (**5-1**); H1 should be actually *cis* to H3.

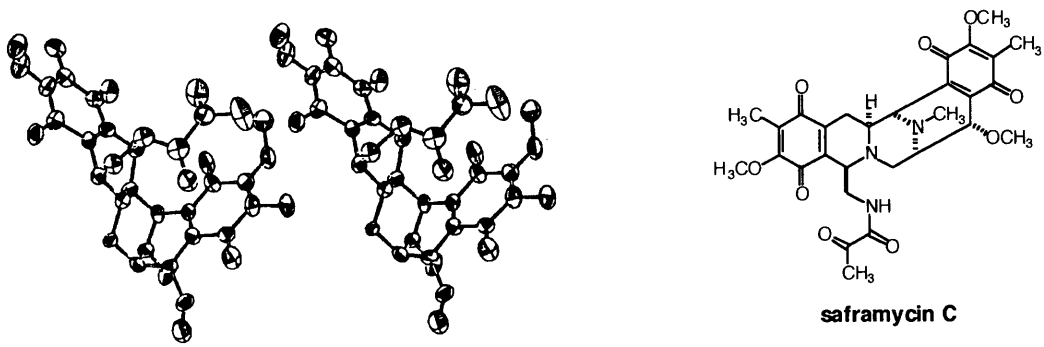

Fig. V-5. Stereoprojection of saframycin C.[118]

To substantiate this idea, renieramycin J (**5-1**) was converted to 21-methoxy derivative by evaporating in MeOH. Although unstable in CD_3CN-d_3, all of the ^1H signals were assignable (**Table V-4**) and a NOESY crosspeak (**Fig. V-17**) from the 21-methoxy methyl (δ 3.46s/57.0) to H1 (δ 4.29) was observed (**Fig. V-6**), thus concluding that renieramycin J (**5-1**) has a (1*S*)-configuration.

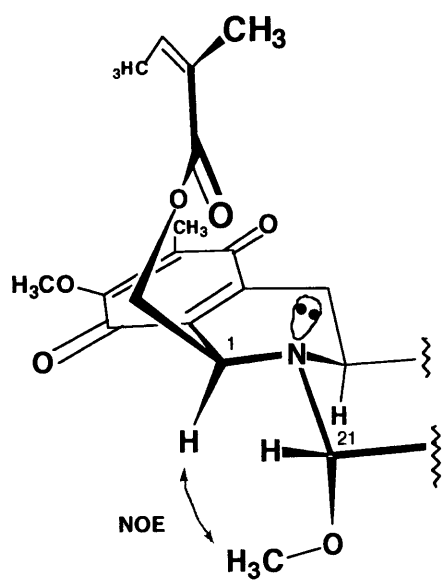

Fig V-6. The diagnostic NOE correlation for the configuration of C1 observed in CD_3CN.

2-2-3. Absolute Stereochemistry

The absolute stereostructure of renieramycin J (**5-1**) was determined by the modified Mosher method.[120] To avoid undesirable esterification at the phenolic hydroxyl groups, renieramycin J (**5-1**) was first air-oxidized to the bisquinone by stirring in the 50% MeCN phosphate buffer (50 mM) at pH 8.3,[121] and then reacted with (+)- or (-)-MTPACl in pyridine. The Δδ values around C14 denoted (*S*)-configuration, thus stereochemistry of renieramycin J (**5-1**) was (*1S, 3R, 11S, 13S, 14S*).

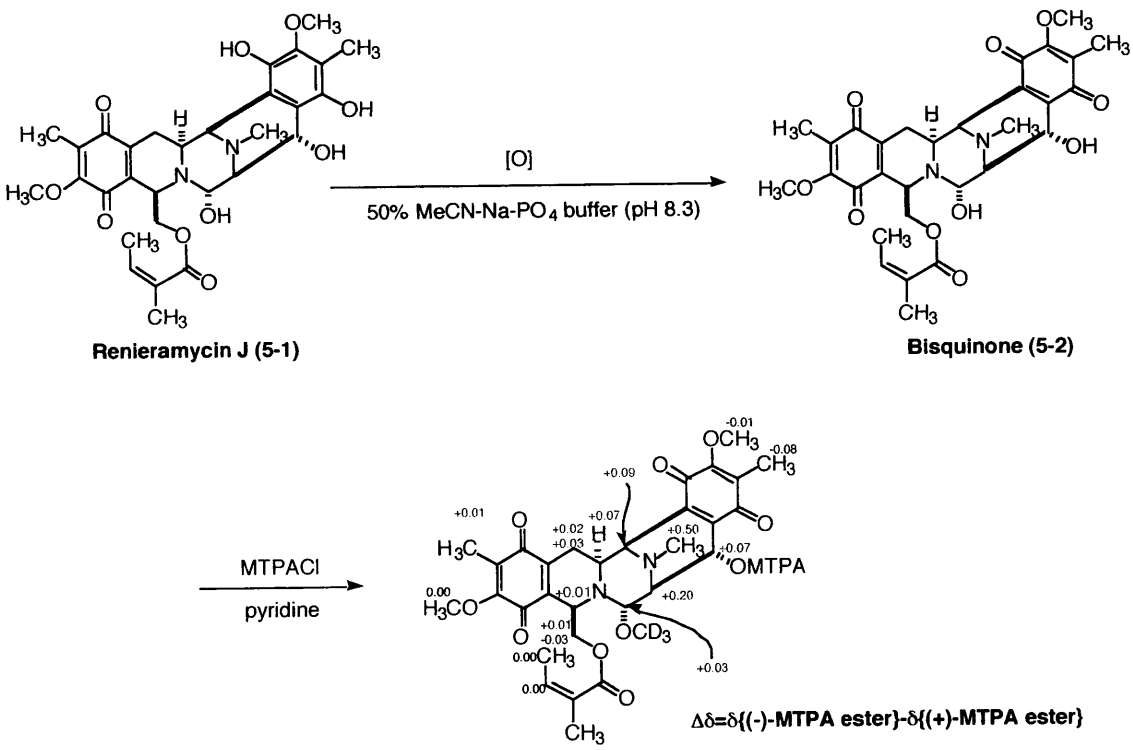

Scheme V-3. Preparation of MTPA Esters of Bisquinone (5-2)

2-3. Biological Activity

Renieramycin J (**5-1**) induced shrinkage of nucleoli in 3Y1 cells within 6 hours at a concentration of 86 nM. Inhibition of filopodia development was also observed. Boundaries between the cells became obscure after 12 hours (**Fig. V-7 b)**). Then the number of the living cells was gradually decreased and all cells died within 5 days.

Such course of events is typically seen when the cells are treated with an inhibitor of RNA synthesis (actinomycin D) or protein synthesis (cycloheximide). However, at a higher concentration different effects were observed: when exposed to 1.7 μM of the compound, cells retracted themselves and became round in 6 hours (**Fig. V-7 c)**), and 90% of them died within 24 hours.

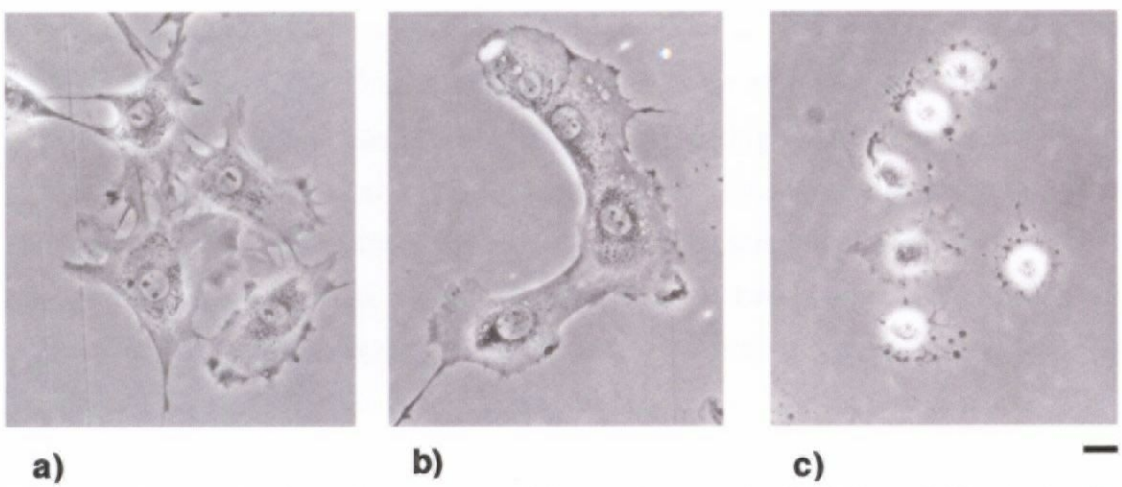

Fig. V–7. Morphological change caused by renieramycin J (5-1). a) Control cells. b) Cells treated with 86 nM of renieramycin J for 12 hours. c) Cells treated with 1.7 μM of renieramycin J (5-1) for 6 hours. Bar represents 20 μm.

The cytotoxicity of renieramycin J (**5-1**) against 3Y1, HeLa, and P388 cells was evaluated as IC_{50} 5.3 nM, 12.3 nM, and 0.53 nM, respectively (**Table V-1**), showing comparable potency to related ecteinascidin 743 (**5-3;** IC_{50} 0.2 ng/mL against P388).[122] It is noteworthy that renieramycin J (**5-1**) has 10-20 times selectivity toward P388 cells over other two cell lines.

Table V-1. Cytotoxicity of Renieramycin J (V-1) against Three Cell Lines (IC_{50}: nM)

	3Y1	HeLa	P388
Renieramycin J	5.3	12.3	0.53
Adriamycin[a]	8.1	10.2	11.6

[a]Positive cytotoxicity control

Renieramycin J (**5-1**) is an additional member of dimeric tetrahydroisoquinoline

alkaloids which have been reported both from terrestrial bacteria and marine organisms: saframycins[118,124-130] from *Streptomyces luvendulae*, safracins A and B[119,131] from *Pseudomonas fluorescens*, saframycins Mx1 and Mx[121,132] from a myxobacterium *Myxococcus xanthus*, renieramycins,[112-116] crybrostatin 4[133] from marine sponges, and jorumycin[134] from a nudibranch. There are also trimeric counterparts ecteinascidins[122,135,136] from the tunicate *Ecteinascidia turbinata.* Like other carbinolamine-containing antitumor antibiotics such as anthramycin (**5-4**)[137,138] and naphtyridinomycin (**5-5**),[139] ecteinascidins[140] and some members of saframycins[141,142] have been shown to bind covalently to DNA by replacing their carbinolamine OH (or CN in the case of saframycin A (**5-6**)) with 2-NH_2 of guanine in the minor groove of the duplex. The reason why DNA alkylation leads to the scission of DNA double strands has not long been answered. However, most recently two groups have put forward a new theory that ecteinascidin 743 interacts with the transcription-coupled NER (nucleotide excision repair) machinery to induce lethal DNA strand breaks.[143,144] It seems probable that reineramycin J (**5-1**) may share the same mechanism to exert its bioactivity.

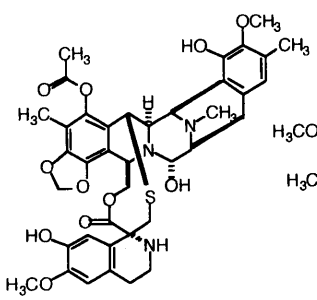

5-3

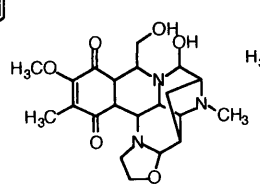

5-4

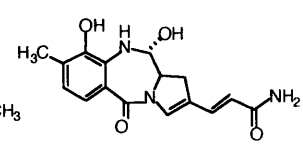

5-5

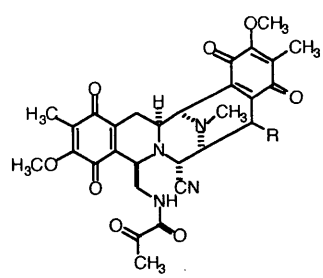

5-6

The implications obtained from the observation of the morphology of 3Y1 cells that renieramycin J (**5-1**) inhibits synthesis of RNA or protein is consistent with the report that saframycin A inhibited RNA synthesis *in vivo* and *in vitro*.[145]

3. Experimental Section

3-1. General Methods

Spectroscopic and chromatographic instruments were the same as described in

CHAPTER III.

3-2. Animal Material

The purple-blue unidentified sponge was collected off Kuchinoerabu-jima (30°28.31' N, 130°11.73' E, from -5 to -16 m) and Iwo-jima (30°48.35' N, 130°19.07' E, -22 m) islands, southern Japan, in July 2001. The animals were immediately preserved at –20°C until extraction.

3-3. Isolation

The frozen sponge (800 g) was crushed in EtOH (2.4 L) with about a half volume of Celite by a Waring blender and then filtered by a Buchner funnel. The residue was extracted four more times. The filtrates were combined and concentrated to a water suspension, to which MeOH was added to 60% MeOH solution (400 mL) and extracted with dichloromethane (400 mL × 3). 60% MeOH layer was discarded. The dichloromethane layer was then dissolved in 90% MeOH (400 mL) and defatted with *n*-hexane (400 mL × 3). The extract was dissolved in the lower layer (360 mL) of a solvent system EtOAc/*n*-heptane/MeOH/water (7:4:4:3, total 1440 mL) and then washed for three times with the upper layer (210 mL × 3) to give 1227.7 mg of the crude active fraction. The fraction was gel-filtered on Sephadex LH-20 (ϕ 5.1 × 90 cm, mobile phase: MeOH) and combined active fractions were purified by ODS-HPLC on Cosmosil ARII column (ϕ 2 × 25 cm, mobile phase: 38% aqueous MeCN-0.2 M NaCl, UV detection: 210 nm) to give 40.7 mg of crude renieramycin J. Purification on phenylhexyl-HPLC on Phenomenex PHENYL-HEXYL (ϕ 1 × 25 cm, mobile phase: 38% aqueous MeCN-0.2 M NaCl, UV detection: 210 nm) gave 16.3 mg (2.0×10^{-3} %, wet wt) of pure renieramycin J (**5-1**) as a severely tailing peak.

Renieramycin J (5-1): a brown solid; $[\alpha]_D^{21}$ 1.2° (c0.02, MeOH); UV (MeOH) λ_{max} 203 (ε 39000), 273 (12000) nm; HRFABMS (glycerol) m/z 569.2502 $(M+2H-OH)^+$ (calcd for $C_{30}H_{37}N_2O_9$, Δ+0.3 mmu); ^1H and ^{13}C NMR data, see **Tables V-2** and **V-4**.

3-4. Preparation of the Bisquinone 5-2

Oxidation of renieramycin J (**5-1**) to the bisquinone **5-2** was carried out by the method of Trowitzsch-Kienast et al.[121,146] with slight modification. 1.7 mg portion of renieramycin J (**5-1**) was dissolved in MeCN (2.5 mL) and the same volume of 50 mM Na-PO_4 buffer adjusted to pH 7.5 was added to the solution (final pH 8.3). After stirring for 3 hours in an open atmosphere, the solution was titrated with 100 mM NaH_2PO_4 to acidify pH below 7 and evaporated to dryness. The reaction mixture was desalted on ODS packed in a Pasteur pipet to give a crude bisquinone (**5-2;** 1.7 mg).

Bisquinone 5-2: a brown solid; UV (MeOH) λ_{max} 203 (ε 27000), 269 (15000) nm; FABMS (glycerol) m/z 569 $(M+4H-OH)^+$; ^1H and ^{13}C NMR data, see **Table V-3**.

3-5. Preparation of MTPA esters of Bisquinone 5-2

The crude bisquinone was divided into two Reacti-Vials.® To each vial were added 5 drops of dry pyridine and 10 μL of (+)- or (-)-MTPACl and the vials were vortexed for 10 seconds. After removing pyridine under vacuum, the reaction mixtures were separated by ODS-HPLC with a linear gradient of aqueous MeCN containing 0.05% TFA (40% → 80% MeCN over 60 min) to furnish 0.2 mg of MTPA esters and the unreacted bisquinone **5-2** (0.2 mg).

(-)-MTPA Ester of 5-2; ^1H NMR (CD_3OD) δ 6.59 (1H, qq, *J* = 1.5, 7.3Hz, H-26), 5.67 (1H, s, H-14), 4.49 (1H, d, *J* = 2.7 Hz, H-21), 4.41 (1H, ddd, *J* = 2.2, 2.7, 3.5 Hz, H-1), 4.31 (1H, dd, *J* = 2.7, 11.5 Hz, H-22), 4.19 (1H, dd, *J* = 3.5, 11.5 Hz, H-22), 4.06 (1H, dd, *J* = 1.2, 3.1 Hz, H-11), 3.98 (3H, s, Me-7), 3.97 (3H, s, Me-17), 3.32 (overlapped to the solvent peak, H-13), 3.31 (overlapped to the solvent peak, H-3), 2.73 (1H, dd, *J* = 2.7, 16.9 Hz, H-4), 2.38 (3H, s, NMe-12), 1.87 (3H, s, Me-6), 1.82 (3H, s, Me-16), 1.77 (3H, dd, *J* = 1.5, 7.3 Hz, Me-26), 1.60 (3H, dq, *J* = 1.5, 1.5 Hz, Me-25), 1.20 (1H, ddd, *J* = 2.0, 12.0, 16.0 Hz, H-4).

(+)-MTPA Ester of 5-2; ^1H NMR (CD_3OD) δ 6.59 (1H, qq, *J* = 1.5, 7.3Hz, H-26), 5.60 (1H, s, H-14), 4.46 (1H, d, *J* = 2.3 Hz, H-21), 4.40 (1H, ddd, *J* = 2.3, 2.7, 3.5 Hz,

H-1), 4.34 (1H, dd, J = 2.5, 11.4 Hz, H-22), 4.18 (1H, dd, J = 3.1, 11.2 Hz, H-22), 3.98 (3H, s, Me-7), 3.98 (3H, s, Me-17), 3.97 (overlapped, H-11), 3.24 (1H, ddd, J = 2.3, 3.1, 11.9 Hz, H-3), 3.12 (1H, brs, H-13), 2.70 (1H, dd, J = 2.3, 16.9 Hz, H-4), 1.90 (3H, s, Me-16), 1.88 (3H, s, NMe-12), 1.86 (3H, s, Me-6), 1.77 (3H, brd, J = 7.3 Hz, Me-26), 1.60 (3H, dq, J = 1.5, 1.5 Hz, Me-25), 1.18 (1H, ddd, J = 2.4, 11.8, 16.8 Hz, H-4).

3-6. Cell-morphology-based Assay

The assay was carried out by the procedure essentially the same as described in CHAPTER I.

3-7. Cytotoxicity Tests

Cytotoxicity of renieramycin J was evaluated by the method described in CHAPTER IV.

Table V-2. ^{1}H and ^{13}C NMR Data of Renieramycin J (5-1) in CD_3OD at 300 K

position	^{13}C	^{1}H, m, *J* (Hz)	HMBC	NOESY
1	54.37	4.33ddd 2.4, 2.4, 2.4	9	2
3	52.10	3.42ddd 2.7, 3.1, 11.2		4-eq, 11
4	25.67	1.56ddd 2.3, 11.1, 17.4 (ax)	3, 9, 10, 11	4-eq
		3.03dd 2.4, 17.4 (eq)	5, 9, 10	3, 4-ax, 11
5	186.96			
6	128.99			
6-Me	8.62	1.85s	5, 6, 7, 7-Me, 8	
7	157.51			
7-OMe	61.31	3.97s	7	
8	182.35			
9	138.14			
10	142.71			
11	58.39	4.55brd 2.8	13, 18 19, 20	3, 12-Me
12-Me	42.39	2.71s	11, 13	11, 13
13	63.91	3.82brd 1.8	11, 14, 21	12-Me, 14, 21
14	64.28	4.79s	15, 19, 20, 21	13, 21
15	148.08			
16	120.70			
16-Me	9.48	2.14s	15, 16, 17, 17-OMe, 18, 20	17-OMe
17	147.54			
17-OMe	60.88	3.69s	17	16-Me
18	142.05			
19	113.17			
20	118.73			
21	90.24	4.58d 2.4	1, 3,	1, 13, 14, 22
22	64.39	4.25br (2H)	9, 24	21
24	168.57			
25	128.23			
25-Me	20.41	1.30dq 1.5, 1.5	24, 25, 26	26
26	139.95	5.87qq 1.6, 7.2	24, 25-Me, 26-Me	25-Me, 26-Me
26-Me	15.17	1.65dq 7.3, 1.6	24, 25, 26	26

Table V-3. ^{1}H and ^{13}C NMR Data of Bisquinone 5-2 in CD_3OD at 300 K

position	^{13}C	^{1}H, m, J (Hz)	HMBC
1	54.10	4.34ddd 2.4, 2.4, 2.4	
3	51.00	3.24ddd 2.7, 3.1, 11.5	
4	26.78	1. 17ddd 2.4, 11.8, 16.6 (ax)	3, 10
		2.67dd 2.6, 16.9 (eq)	5, 9, 10
5	186.87		
6	128.99		
6-Me	8.62	1.85s	5, 6, 7, 7-Me, 8
7	157.47		
7-OMe	61.31	3.97s	7
8	182.39		
9	138.53		
10	142.54		
11	56.21	3.99dd 2.7, 3.4	3, 13, 18, 19, 20
12-Me	42.70	2.47s	11, 13
13	62.25	3.38dd 0.9, 2.8	11, 14, 21
14	61.82	4.31overlapped	15, 18, 19, 20, 21
15	188.06		
16	130.46		
16-Me	8.69	1.91s	15, 16, 17, 17-OMe, 18
17	156.71		
17-OMe	61.43	3.97s	17
18	184.52		
19	136.11		
20	142.84		
21	90.62	4.31overlapped	3
22	64.92	4.23dd 2.6, 11.4	1, 24
		4.29dd 2.7, 11.3	1, 24
24	168.47		
25	128.11		
25-Me	20.70	1.54dq 1.5, 1.5	22, 24, 25, 26
26	140.29	5.96qq 1.6, 7.2	25-Me
26-Me	15.85	1.72dq 7.3, 1.6	24, 25, 26

Table V-4. ^{1}H and ^{13}C NMR Data of Renieramycin J (5-1) in MeCN

position	^{13}C	^{1}H, m, J (Hz)	NOESY
1	53.5	4.29overlapped	21, 21-OMe
3	ND[a]	3.45overlapped	4-eq, 11
4	24.9	1.51overlapped (ax)	4-eq
		2.90dd 2.4, 17.4 (eq)	3, 4-ax
5	186.8		
6	129.1		
6-Me	8.9	1.82s	
7	157.0		
7-OMe	61.5	3.90s	
8	ND[a]		
9	137.7		
10	142.0		
11	57.5	4.44brs	3
12-Me	41.6	2.71br	
13	63.2	3.84br	21
14	64.9	4.68brs	21
15	147.9		
16	120.8		
16-Me	9.6	2.10s	17-OMe
17	146.8		
17-OMe	61.2	3.66s	16-Me
18	ND[a]		
19	ND[a]		
20	ND[a]		
21	89.3	4.58d 2.4	1, 13, 14, 21-OMe, 22
21-OMe	57.0	3.46s	1, 21
22	64.3	4.10dd 2.2, 11.4	21
		4.22dd 2.9, 10.4	21, 22
24	167.8		
25	127.9		
25-Me	20.2	1.27dq 1.5, 1.5	26
26	139.3	5.85qq 1.5, 7.2	25-Me, 26-Me
26-Me	15.6	1.65dq 7.3, 1.5	26
OH		6.62br, 7.50br	

[a] Not determined.

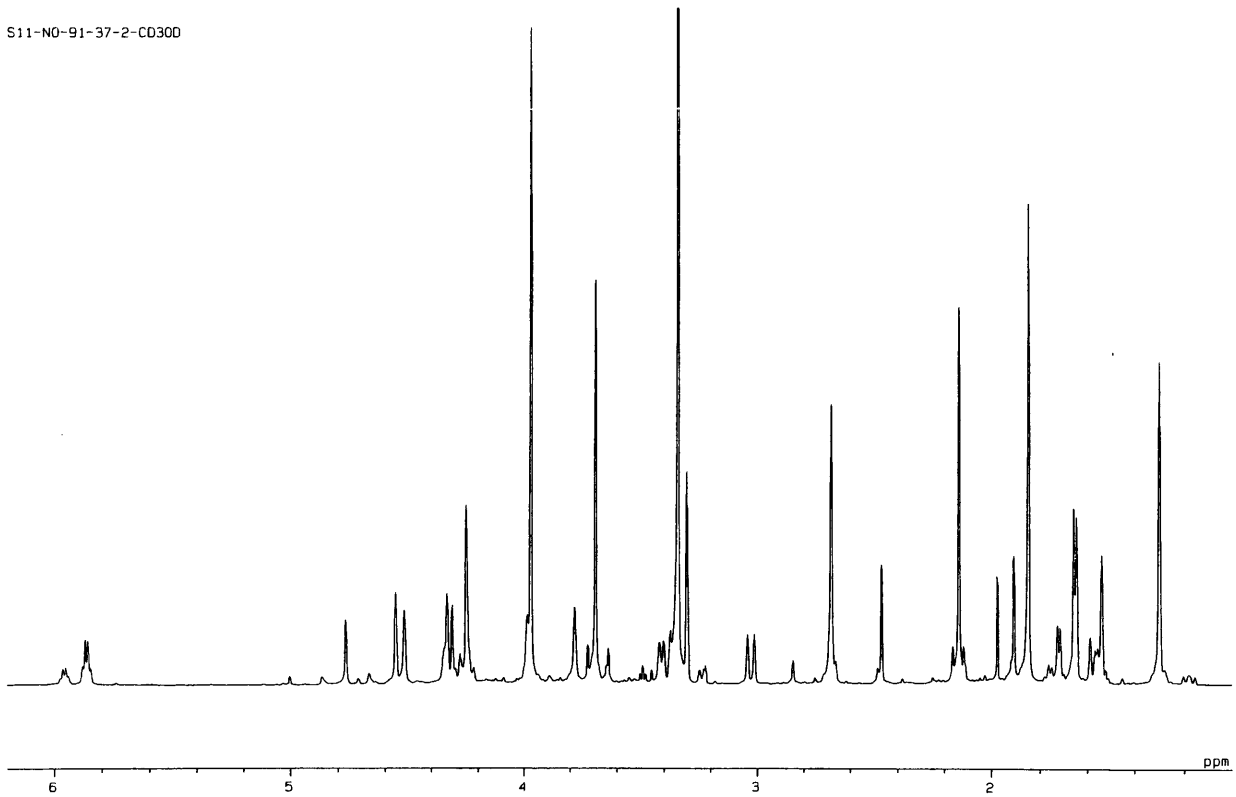

Fig. V-8. ^{1}H **NMR spectrum of renieramycin J (5-1) in CD_3OD at 300 K.**

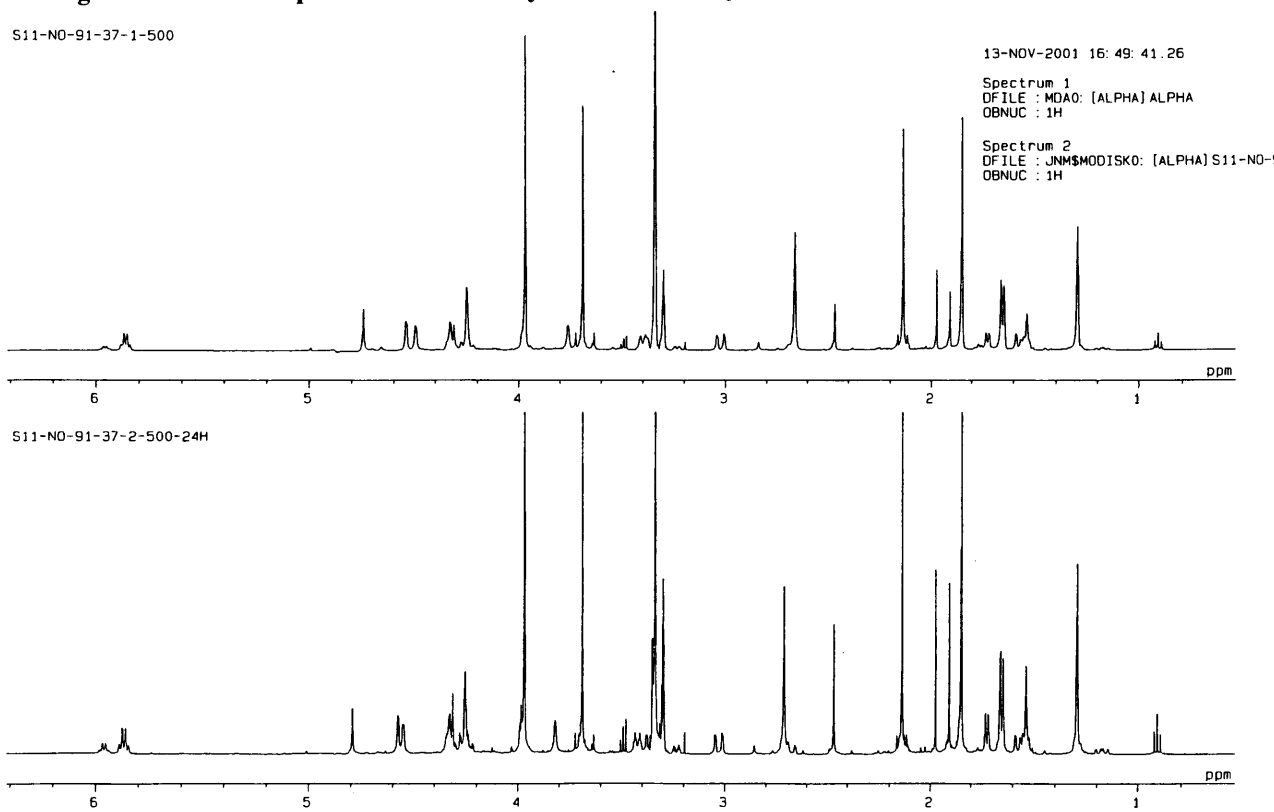

Fig. V-9. Time course change of renieramycin J (5-1) in CD_3OD at 300 K. Uppper: Time 0. Lower: Time 24 hour.

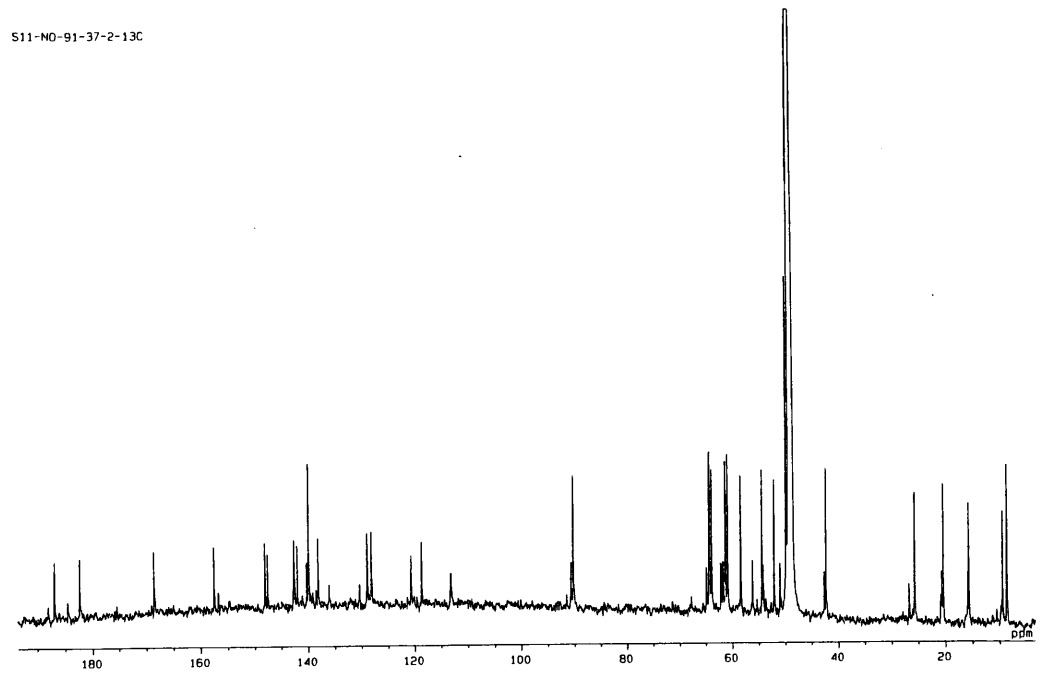

Fig. V-10. ^{13}C NMR spectrum of renieramycin J (5-1) in CD_3OD at 300 K.

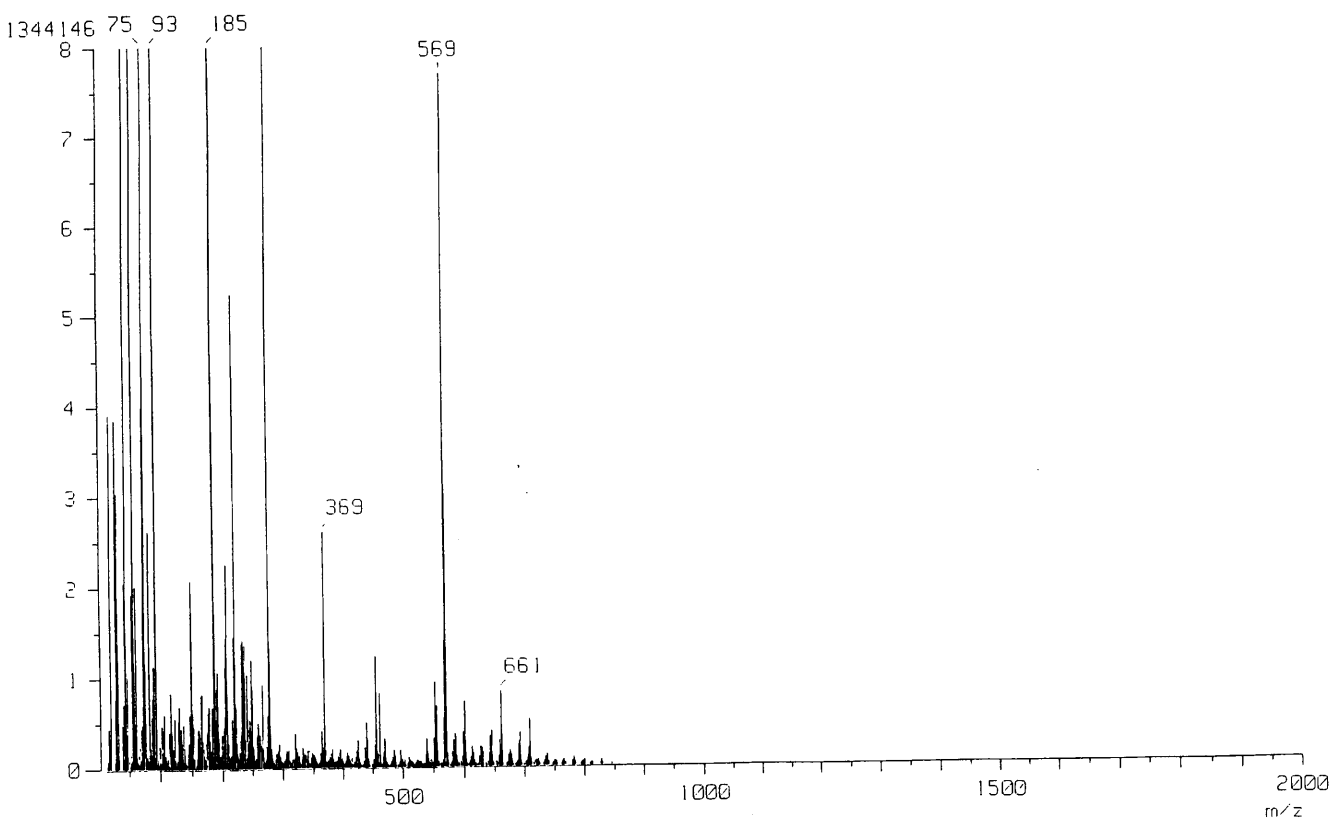

Fig. V-11. LRFABMS (glycerol matrix) spectrum of renieramycin J (5-1)

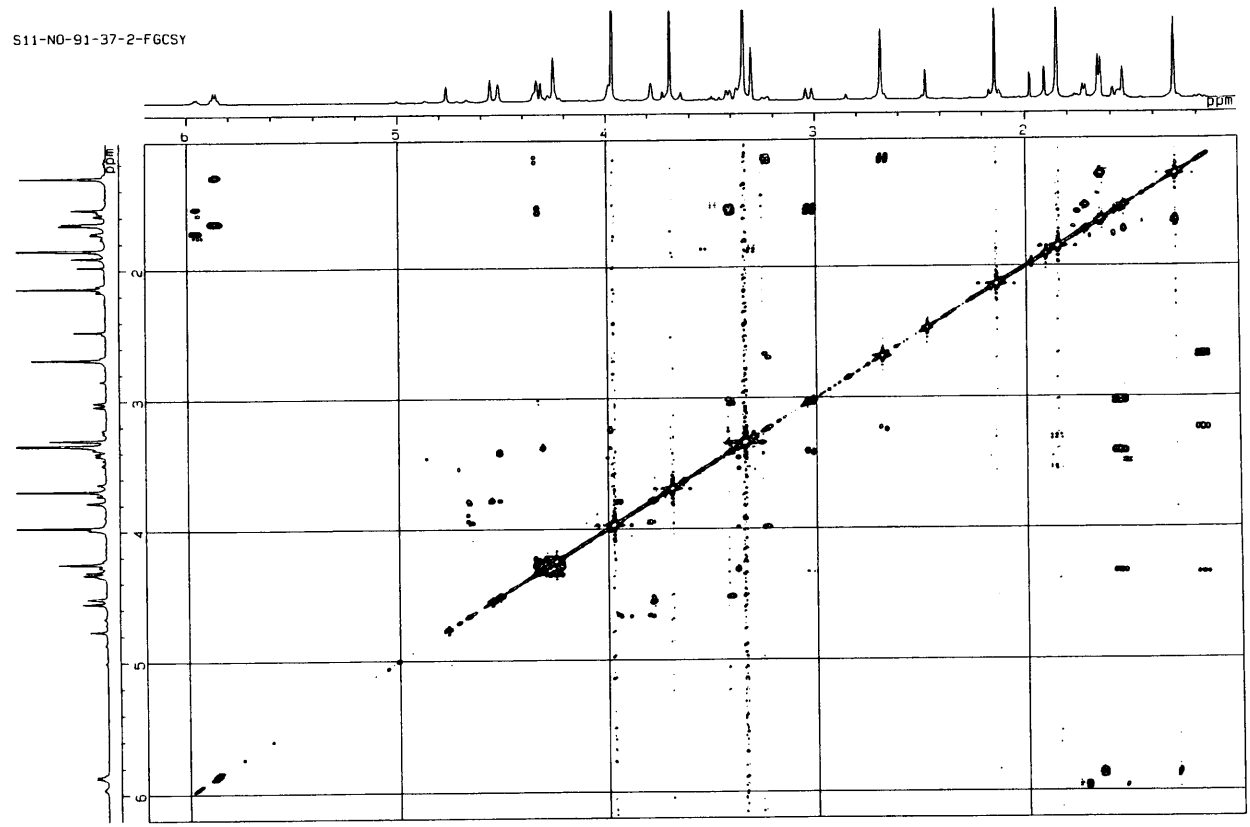

Fig. V-12. FGCOSY45 spectrum of renieramycin J (5-1) in CD_3OD at 300 K.

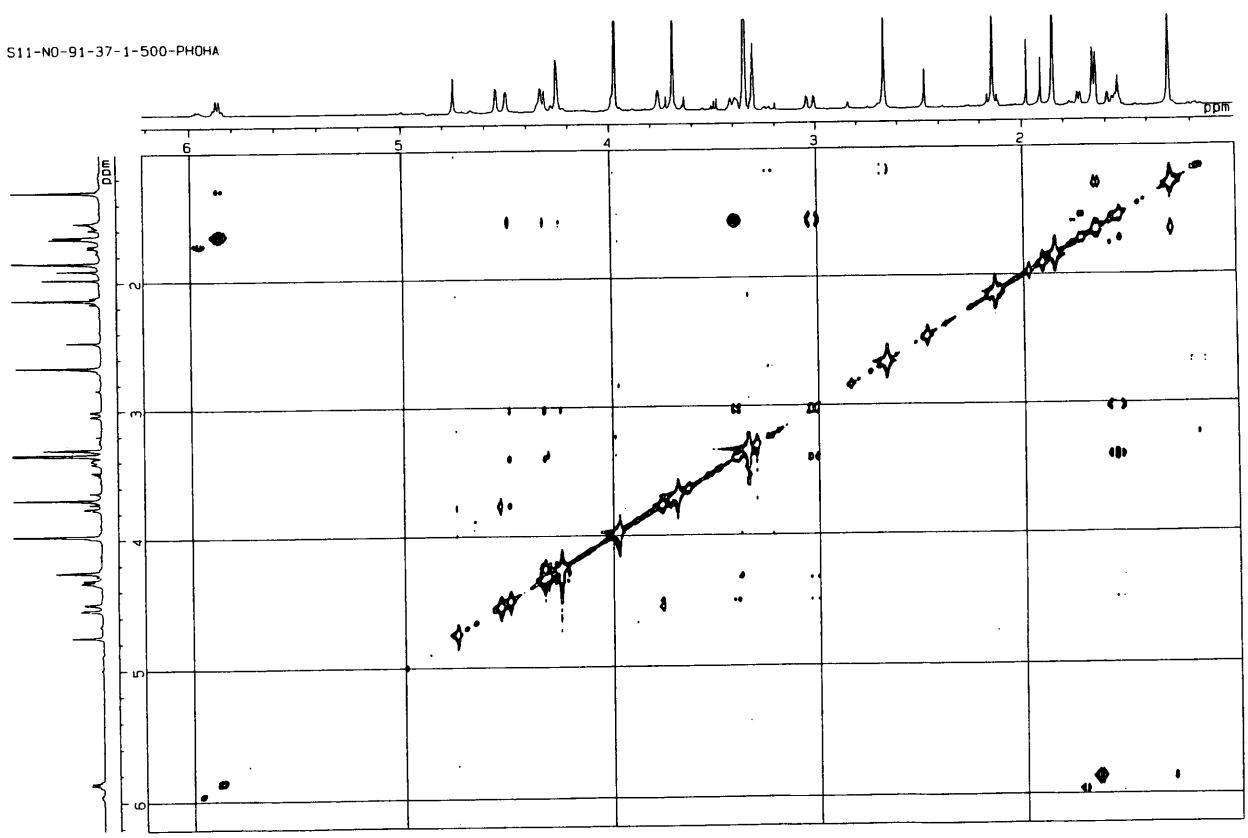

Fig. V-13. PSHOHAHA spectrum of renieramycin J (5-1) in CD_3OD at 300 K.

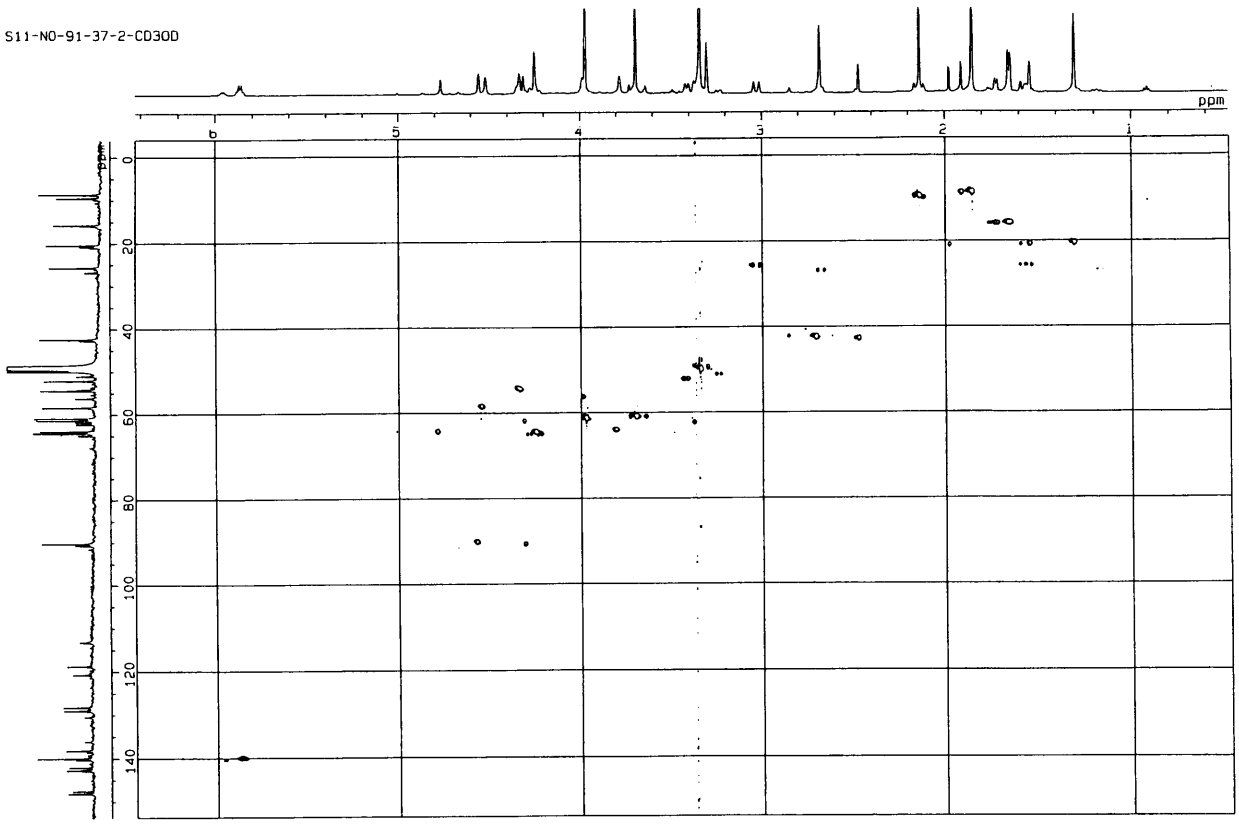

Fig. V-14. PSFGHMQC spectrum of renieramycin J (5-1) in CD_3OD at 300 K.

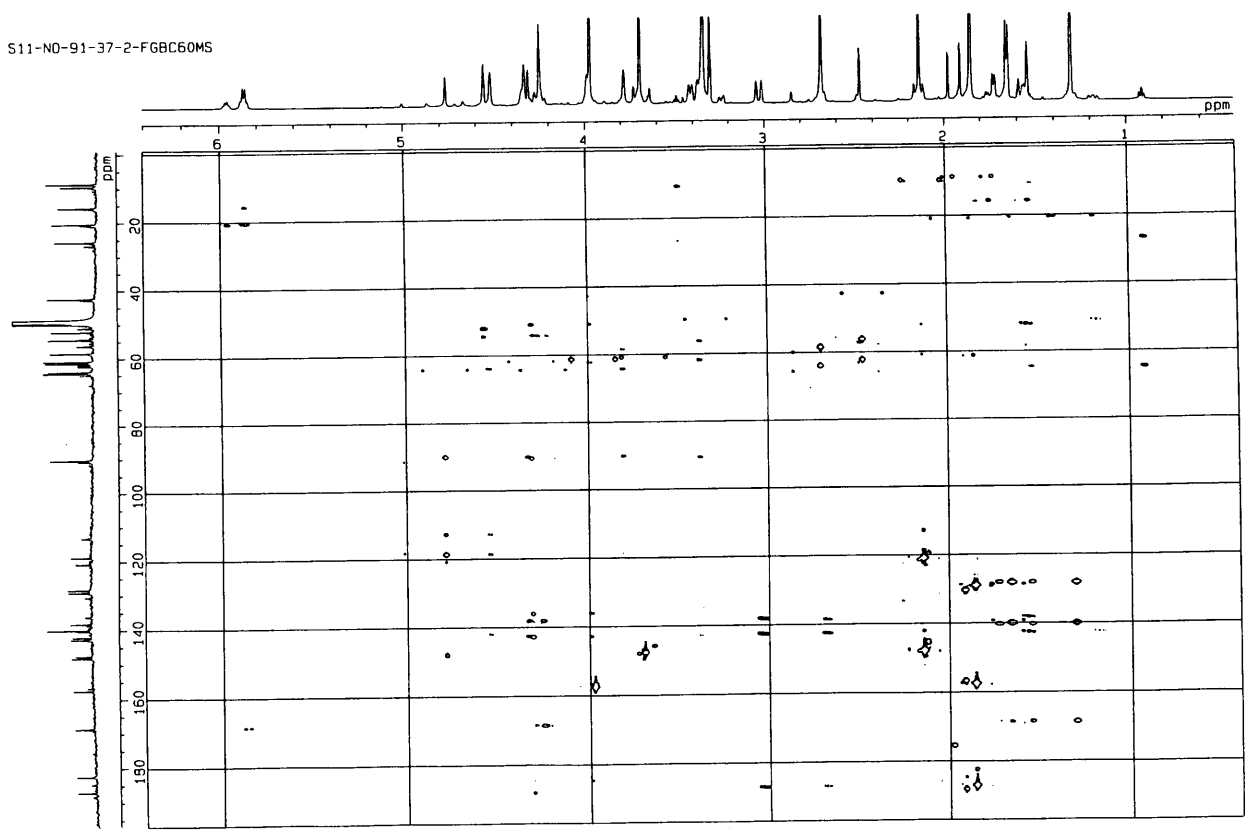

Fig. V-13. FGHMBC spectrum of renieramycin J (5-1) in CD_3OD at 300 K.

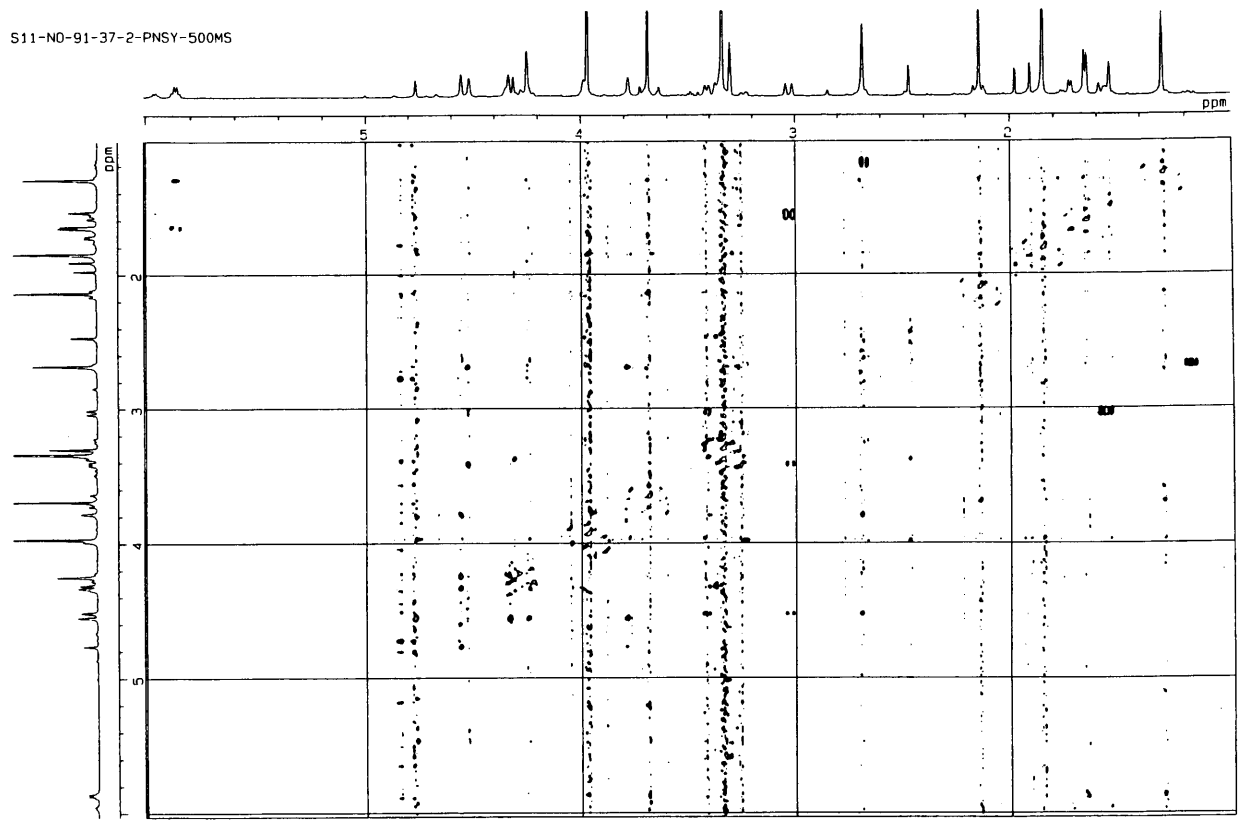

Fig. V-16. PSNOESY (mixing time: 500 ms) spectrum of renieramycin J (5-1) in CD_3OD at 300 K.

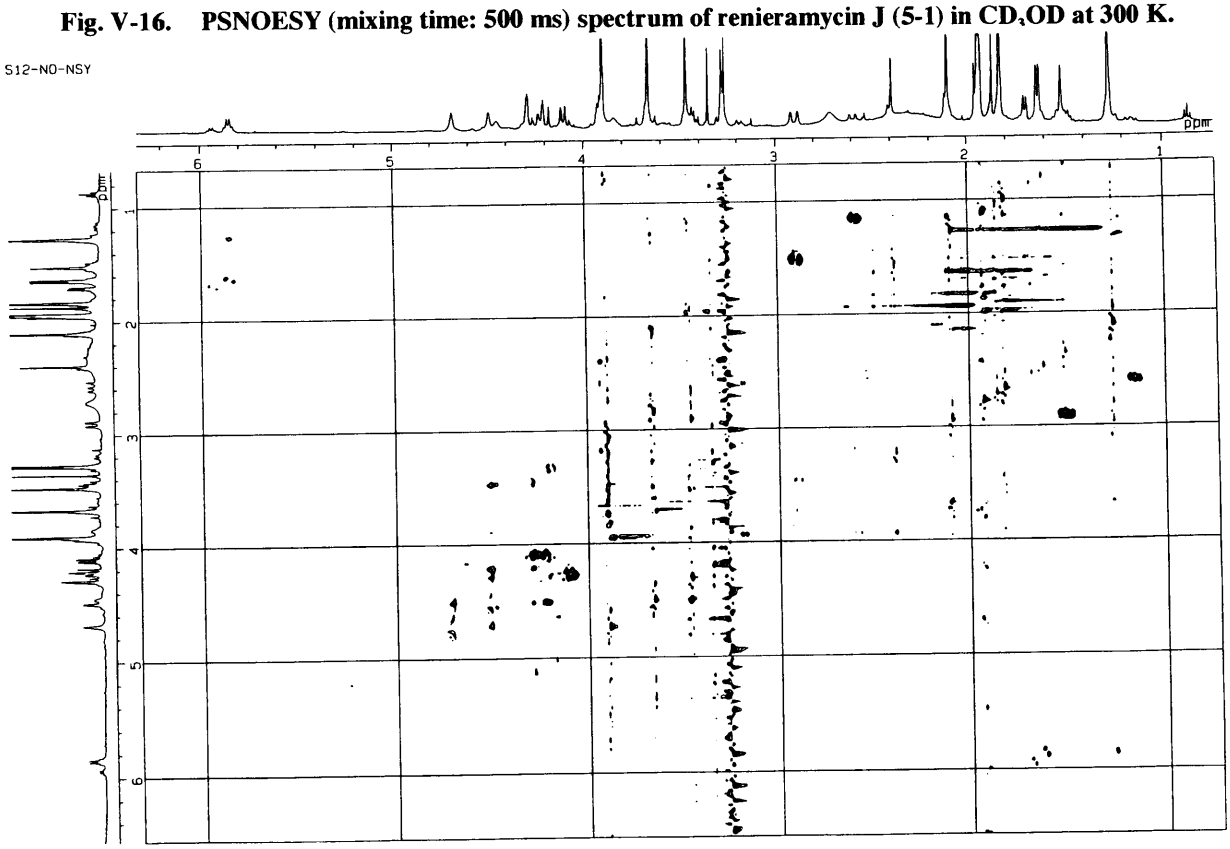

Fig. V-17. PSNOESY (mixing time: 500 ms) spectrum of renieramycin J (5-1) in MeCN-d_3 at 300 K.

CONCLUSIONS

The assay system based on the morphological changes of 3Y1 rat embryonic fibroblasts was developed to discover compounds that have biomedical and cell biological potential. By using this assay system, totally 11 including 7 new compounds were isolated from 2 species of sponges and one each of a zoanthid and a tunicate, all of which were collected in southwest islands of Japan, demonstrating the practicability of this system.

Firstly, the morphological changes of 3Y1 cells caused by the known compounds, the molecular targets of which have been already established, were observed. Twelve out of 26 agents induced characteristic manners of morphological changes, showing the possibility to distinguish between different pharmacological activities. Then, the lipophilic and aqueous extracts of 437 specimens of marine invertebrates from four phyla including sponge, coelenterate, bryzoan, and tunicate were screened by this system (CHAPTER I).

Several specimens showing promising activity were picked and subjected to further chemical investigation.

Three new isomalabaricane triterpenes, 29-hydroxystelliferin D (**2-2**), 3-*epi*-29-hydroxystelliferin E (**2-3**), and 3-*epi*-29-hydroxystelliferin A (**2-4**) were isolated together with known stelliferins A (**2-5**) and D (**2-6**) from the marine sponge *Stelletta globostellata* collected off Magejima Island. 3Y1 cells treated with 0.2 μM of stelliferins induced cyrindrical cell shape followed by death in five days (CHAPTER II).

Palytoxin (**3-1**) was identified as an extremely potent cell-bursting principle from the zoanthid *Palythoa* aff. *margaritae* collected off Nakanoshima Island. Palytoxin induced rapid swelling and successive rupture of the treated cells at 5 nM (CHAPTER III).

Three new enediyne glycosides, shishijimicins A-C (**4-1**~**4-3**) were isolated as the constituents that induce collapse of the nucleus from the ascidian *Didemnum proliferum* collected off Shishijima Island. 200 μM of shishijimicin B induced collapse of the nucleus within 24 hours. The IC_{50} values against 3Y1, HeLa, and P388 cells were as

low as the orders of picomolar.

Finally, renieramycin J (**5-1**), a new dimeric tetrahydroisoquinoline alkaloid, was isolated from an unidentified purple-blue sponge collected off Kuchinoerabujima and Iohjima Islands. Renieramycin J induced characteristic morphology that is similar to that induced by inhibitors of protein or RNA synthesis at a concentration of 86 nM. The cells exposed to a higher concentration (1.7 μM) of the compound exhibited a different manner of morphological change: they retracted themselves and became round in 6 hours. The cytotoxicity of renieramycin J against 3Y1, HeLa, and P388 cells was evaluated as IC_{50} 5.3 nM, 12.3 nM, and 0.53 nM, respectively, showing 10-20 times selectivity toward P388 cells.

REFERENCES AND NOTES

1. Osada, H.; Magae, J.; Watanabe, C.; Isono, K. *J. Antibiot.* **1988,** *41,* 925-931.
2. Ubukata, M.; Cheng, X.-C.; Isono, K. *J. Chem. Soc. Chem. Commun.* **1990,** 244.
3. Magae, J.; Watanabe, C.; Osada, H.; Cheng, X.-C.; Isono, K. *J. Antibiot.* **1988,** *41,* 932-937.
4. Magae, J.; Osada, H.; Fujiki, H.; Saido, T. C.; Suzuki, K.: Nagai, K.; Yamasaki, M.; Isono, K. *Proc. Jpn. Acad. Ser. B-Phys. Biol. Sci.* **1990.** *66,* 209-212.
5. Hori, M.; Magae, J.; Han, Y. G.; Hartshorne, D. J.; Karaki, H. *FEBS Lett.* **1991,** *285,* 145-148.
6. Osada, H.; Takahashi, H.; Tsunoda, K.; Kusakabe, H.; Isono, K. *J. Antibiot.* **1990,** *43,* 163-167.
7. Takahashi, H.; Osada, H.; Uramoto, M.; Isono, K. *J. Antibiot.* **1990,** *43,* 168-173.
8. Osada, H.; Satake, M.; Koshino, H.; Onose, R. *J. Antibiot.* **1990,** *43,* 278-279.
9. Osada, H.; Koshino, H.; Kudo, T.; Onose, R.; Isono, K. *J. Antibiot.* **1992,** *45,* 189-194.
10. Koshino, H.; Osada, H.; Isono, K. *J. Antibiot.* **1992,** *45,* 195-198.
11. Koshino, H.; Osada, H.; Amano, S.; Onose, R.; Isono, K. *J. Antibiot.* **1992,** *45,* 1428-1432.
12. Hayakawa, Y.; Nakagawa, M.; Kawai, H.; Tanabe, K.; Nakayama, H.; Shimazu, A.; Seto, H.; Otake, N. *J. Antibiot.* **1983,** *36,* 934-937.
13. Hayakawa, Y.; Nakagawa, M.; Kawai, H.; Tanabe, K.; Nakayama, H.; Shimazu, A.; Seto, H.; Otake, N. *Agric. Biol. Chem.* **1985,** *49,* 2685-2691.
14. Sakai, T.; Shindo, K.; Odagawa, A.; Suzuki, A.; Kawai, H.; Kobayashi, K.; Hayakawa, Y.; Seto, H.; Otake, N. *J. Antibiot.* **1995,** *48,* 899-900.
15. Kamishohara, M.; Kawai, H.; Odagawa, A.; Isoe T.; Mochizuki, J.; Uchida, T.; Hayakawa, Y.; Seto, H.; Tsuruo, T.; Otake, N. *J. Antibiot.* **1993,** *46,* 1439-1446
16. Kamishohara, M.; Kawai, H.; Odagawa, A.; Isoe. T.; Mochizuki, J.; Uchida, T.; Hayakawa, Y.; Seto, H.; Tsuruo, T.; Otake, N. *J. Antibiot.* **1994,** *47,* 1305-1311.
17. Sakai, T.; Kawai, H.; Kamishohara, M.; Odagawa, A.; Suzuki, A.; Uchida, T.; Kawasaki, T.; Tsuruo, T. Otake, N. *J. Antibiot.* **1995,** *48,* 504-508.
18. Takama, H.; Tanaka, H.; Sudo, T .; Tamura, T.; Tanigawara, Y. *Cancer*

Chemother. Pharmacol. **2001,** *47,* 404-410.

19. Kamishohara, M.; Kenney, S.; Domergue, R.; Vistica, D. T.; Sausville, E. A. *Exp. Cell Res.* **2000,** *256,* 468-479.
20. Oka, H.; Asahi, K.; Morishima, H.; Sanada, M.; Shiratori, K.; Iimura, Y.; Sakurai, T.; Uzawa, J.; Iwadare, S.; Takahashi, N. *J. Antibiot.* **1985,** *38,* 1100-1102.
21. Kubohara, Y.; Okamoto, K.; Tanaka, Y.; Asahi, K.; Sakurai, A.; Takahashi, N. *FEBS Lett.* **1993,** *322,* 73-75.
22. Vantini, G.; Skaper, S. D. *Pharmacol. Res.* **1992,** *26,* 1-15.
23. Brade, Y. -A. *Neuron* **1989,** *2,* 1525-1534.
24. Omura S.; Matsuzaki, K.; Fujimoto, T.; Kosuge, K.; Furuta, T.; Fujita, S.; Nakagawa, A. *J. Antibiot.* **1991,** *44,* 117-118.
25. Omura, S.; Fujimoto, T.; Otoguro, K.; Matsuzaki, K.; Moriguchi, R.; Tanaka, H.; Sasaki, Y. *J. Antibiot.* **1991,** *44,* 113-116.
26. Fenteany, G.; Standaert, R. F.; Lane, W. S.; Choi, S.; Corey, E. J.; Schreiber, S. L. *Science,* **1995,** *268,* 726-731.
27. Hideaki, K.; Takahashi, I.; Okada, G.; Isono, K.; Osada, H. *J. Antibiot.* **1995,** *48,* 733-735.
28. Marumoto, S.; Kogen, H.; Naruto, S. *J. Org. Chem.* **1998,** *63,* 2068-2069.
29. Aoki, S.; Matsui, K.; Tanaka, K.; Satari, R.; Kobayashi, M. *Teterahedron* **2000,** *56,* 9945-9948.
30. Aoki, S.; Matsui, K.; Tanaka, K.; Hong, W.; Kobayashi, M. *Biochem. Biophys. Res. Commun.* **2001,** *289,* 558-563.
31. Adjei, A. A. *Curr. Pharm. Design* **2001,** *7,* 1581-1594.
32. Irby, R. B.; Yeatman, T. J. *Oncogene* **2000,** *19,* 5636-5642.
33. Heldin, C. H.; Westermark, B. *Physiol. Rev.* **1999,** *79,* 1283-1316.
34. Itazaki, H.; Nagashima, K.; Sugita, K.; Yoshida, H.; Kawamura, Y.; Yasuda, Y.; Matusmoto, K.; Ishii, K.; Uotani, N.; Nakai, H.; Terui, A.; Yoshimatsu, S.; Ikenishi, Y.; Nakagawa, Y. *J. Antibiot.* **1990,** *43,* 1524-1532.
35. Matsumoto, M.; Matsutani, S.; Sugita, K.; Yoshida, H.; Hayashi, F.; Terui, Y.; Nakai, H.; Uotani, N.; Kawamura, Y.; Matsumoto, K.; Shoji, J.; Yoshida, T. *J. Antibiot.* **1992,** *45,* 879-885.
36. Ueda, H.; Nakajima H.; Hori, Y.; Fujita, T.; Nishimura, M.; Goto, T.; Okuhara, M.

J. Antibiot. **1994,** *47,* 301-310.

37. Shigematsu, N.; Ueda, H.; Takase, S.; Tanaka, H. *J. Antibiot.* **1994,** *47,* 311-314.
38. Ueda, H.; Nakajima, H.; Hori, Y.; Goto, T.; Okuhara, M. *Biosci. Biotechnol. Biochem.* **1994,** *58,* 1579-1583.
39. Piekarz, R. L.; Robey, R.; Sandor, V.; Bakke, S.; Wilson, H . W.; Dahmoush, L.; Kingma, D. M.; Turner, M. L.; Altemus, R.; Bates, S. E. *Blood,* **2001,** *98,* 2865-2868.
40. Aoki, S.; Higuchi, K.; Kato, A.; Murakami, N.; Kobayashi, M. *Tetrahedron* **1999,** *55,* 14865-14870.
41. Kimura, G.; Itagaki, A.; Summers, A. *Int. J. Cancer* **1975,** *15,* 694-706.
42. Watabe, S.; Wada, S.; Saito, S.;Matsunaga, S.; Fusetani, N.; Ozaki, H; Karaki, H. *Cell Struc. Funct.* **1996,** *21,* 199-212.
43. Wada, S.; Matsunaga, S.; Saito, S.; Fusetani, N.; Watabe, S. *J. Biochem.* **1998,** *123,* 946-952.
44. Arai, T. *FEBS Lett.* **1983,** *155,* 273-276.
45. ter Haar E. *Expert Opin. Ther. Pat.* **1998,** *8,* 571-586.
46. Chartier, L.; Rankin, L. L.; Allen, R. E.; Kato, Y.; Fusetani, N.; Karaki, H.; Watabe, S.; Hartshorne, D. J. *Cell Motil. Cytoskel.* **1991,** *18,* 26-40.
47. Bowman, E.-J.; Siebers, A.; Altendorf, K. *Proc. Natl. Acad. Sci. USA,* **1988,** *85,* 7972-7976.
48. Matsunaga, S. Symposium Papers, 33th *Tennenbutsukagaku Danwakai,* Ishikawa; Organizing Committee of the symposium, 1998; p42-46.
49. Although *Stelletta globostellata* (often called *Rhabdastrella* or *Aurora globostellata*) and *Jaspis stellifera*, both of which contain isomalabaricane triterpenes, are closely related, they are apparently different. It is most likely that the latter sponge does not belong to the genus Jaspis (Rob W. M. van Soest, personal communication).
50. Ryu, G.; Matsunaga, S.; Fusetani, N. *J. Nat. Prod.* **1996,** *59,* 512-514.
51. Rao, Z.; Deng, S.; Wu, H.; Jiang, S. *J. Nat. Prod.* **1997,** *60,* 1163-1164.
52. Tsuda, M.; Ishibashi, M.; Agemi, K.; Sasaki, T.; Kobayashi, J. *Tetrahedron* **1991,** *47,* 2181-2194.
53. McCabe, T.; Clardy, J.; Minale, L.; Pizza, C.; Zollo, F; Riccio, R. *Tetrahedron*

Lett. **1982,** *23,* 3307-3310.

54. Otani, I.; Kusumi, T.; Kashman, Y.; Kakisawa, H. *J. Am. Chem. Soc.* **1991,** *113,* 4092-4096.
55. The crude MTPA esters gave only one spot on a TLC plate. After purification by HPLC they gave four spots on TLC, but exhibited a clean ^{1}H NMR spectrum.
56. Kobayashi, J.; Yuasa, K.; Kobayashi, T.; Sasaki, T.; Tsuda, M. *Tetrahedron,* **1996,** *52,* 5745-5750.
57. Only the 12α-alcohol was produced.
58. The NOESY cross peak between H9 and H12 unambiguously established that the 12OH group was α-oriented.
59. Sata, N. U.; Wada, S.; Matsunaga, S.; Watabe, S.; van Soest, R. W. M.; Fusetani, N. *J. Org. Chem.* **1999,** *64,* 2331-2339.
60. McKee, T. C.; Bokesch, H. R.; McCormick, J. L.; Rashid, M. A.; Spielvogel, D.; Gustafson, K. R.; Alavanja, M. M.; Cardellina II, J. H.; Boyd, M. R. *J. Nat. Prod.* **1997,** *60,* 431-438.
61. McCormick, J. L.; McKee, T. C.; Cardellina II, J. H.; Leid, M.; Boyd, M. R. *J. Nat. Prod.* **1996,** *59,* 1047-1050.
62. Fukuzawa, S.; Matsunaga, S.; Fusetani, N. *J. Org. Chem.* **1995,** *60,* 608-614.
63. Moore, R. E.; Scheuer, P. J. *Science* **1971,** *172,* 495-498.
64. Moore, R.E.; Bartolini, G.; Barchi, J.; Bothner-By, A. A.; Dadok, J.; Ford, J. *J. Am. Chem. Soc.* **1982,** *104,* 3776-3779.
65. Uemura, D. In *Bioorganic Marine Chemistry*; Scheuer, P. J., Ed.; Springer-Verlag: Berlin Heidelberg 1991; Volume 4, pp 2-31.
66. Uemura. D.; Hirata, Y.; Iwashita, T.; Naoki, H. *Tetrahedron* **1985,** *41,* 1007-1017.
67. Quinn, R. J.; Kashiwagi, M.; Moore, R. E.; Norton, T. R. *J. Pharm. Sci.* **1974,** *63,* 257-260.
68. Attaway, D. H.; Ciereszko, L. S. *Proc. Int. Symp. Coral Reefs,* **1974,** *2nd,* 497-504.
69. Beress, L.; Zwick, J.; Kolkenbrock, H. J.; Kaul, P. N.; Wassermann, O. *Toxicon* **1983,** *21,* 285-290.
70. Moore, R. E.; Bartolini, G. *J. Am. Chem. Soc.* **1981,** *103,* 2491-2494.
71. Moore, R. E.; Woolard, F. X.; Bartolini, G. *J. Am. Chem. Soc.* **1980,** *102,* 7370-

7372.

72. Maeda, M.; Kodama, R.; Tanaka, T.; Yoshizumi, H.; Nomoto, K.; Takemoto, T.; Fujita, M. 1985. Structure of insecticides isolated from the red algae Chondria armata. Symposium Papers, 27th Symposium on the Chemistry of Natural Products, Hiroshima; Organizing Committee of the symposium' Hiroshima, 1985; p616-623.
73. Mahnir, V. N.; Kozlovskaya, E. P.; Kalinovsky, A. I. *Toxicon* **1992,** *30,* 1449-1456.
74. Usami, M.; Satake, M.; Ishida, S.; Inoue, A.; Kan, Y.; Yasumoto, T. *J. Am. Chem. Soc.* **1995,** *117,* 5389-5390.
75. Ukena, T.; Satake, M.; Usami, M.; Oshima, Y.; Naoki, H.; Fujita, T.; Kan, Y.; Yasumoto, T. *Biosci. Biotech.; Biochem.* **2001,** *65,* 2585-2588.
76. Yasumoto, T.; Yasumura, D.; Ohizumi, Y.; Takahashi, M.; Alcala, A. C.; Alcala, L. C. *Agric. Biol. Chem.* **1986,** *50,* 163-167.
77. Alcala, A. C.; Alcala, L. C.; Garth, J. S.; Yasumura, D.; Yasumoto, T. *Toxicon* **1988,** *26,* 105-107.
78. Onuma, Y.; Satake, M.; Ukena, T.; Roux, J.; Chanteau, S.; Rasolofonirina, N.; Ratsimaloto, M.; Naoki, H.; Yasumoto, T. *Toxicon* **1999,** *37,* 55-65.
79. Muramatsu, I.; Nishio, M.; Kigoshi, S.; Uemura, D. *Br. J. Pharmacol.* **1988,** *93,* 811-816.
80. Rouzaire Dubois, B.; Dubois, J. M. *Toxicon,* **1990,** *28,* 1147-1158.
81. Albert, B. *Molecular Biology of the Cell 3rd Edition;* Garland Publishing: New York, 1994; p 515-516.
82. McDonald, L. A.; Capson, T. L.; Krishnamurthy, G.; Ding, W.-D.; Ellestad, G. A.; Bernan, V. S.; Maiese, W. M.; Lassota, P.; Discafani, C.; Kramer, R. A.; Ireland, C. M. *J. Am. Chem. Soc.* **1996,** *118,* 10898-10899.
83. Frederich, M.; Tits, M.; Hayette, M.-P.; Brandt, V.; Penelle, J.; DeMol, P.; Llabres, G.; Angenot, L. *J. Nat. Prod.* **1999,** *62,* 619-621.
84. Ito, A.; Lee, Y.-H.; Chai, H.-B.; Gupta, M. P.; Farnsworth, N. R.; Cordell, G. A.; Pezzuto, J. M.; Kinghorn, A. D. *J. Nat. Prod.* **1999,** 1346-1348.
85. Lee, M. D.; Dunne, T. S.; Chang, C. C.; Siegel, M. M.; Morton, G. O.; Ellestad, G. A.; McGahren, W. J.; Borders, D. B. *J. Am. Chem. Soc.* **1992,** *114,* 985-997.

86. Lindquist, N.; Fenical, W. *Tetrahedron Lett.* **1990,** *31,* 2389-2392.

87. Beutler, J. A.; Clark, P.; Alvarado, A. B.; Golik, J. *J. Nat. Prod.* **1994,** *57,* 629-633.

88. Lee, M. D.; Dunne, T. S.; Siegel, M. M.; Chang, C. C.; Morton, G. O.; Borders, D. B. *J. Am. Chem. Soc.* **1987,** *109,* 3464-3466.

89. Lee, M. D.; Dunne, T. S.; Chang, C. C.; Ellestad, G. A.; Siegel, M. M.; Morton, G. O.; McGahren, W. J.; Borders, D. B. *J. Am. Chem. Soc.* **1987,** *109,* 3466-3468.

90. Golik, J.; Clardy, J.; Dubay, G.; Groenewold, G.; Kawaguchi, H.; Konishi, M.; Krishnan, B.; Ohkuma, H.; Saitoh, K.; Doyle, T. W. *J. Am. Chem. Soc.* **1987,** *109,* 3461-3462.

91. Golik, J.; Dubay, G.; Groenewold, G.; Kawaguchi, H.; Konishi, M.; Krishnan, B.; Ohkuma, H.; Saitoh, K.; Doyle, T. W. *J. Am. Chem. Soc.* **1987,** *109,* 3462-3464.

92. Konishi, M.; Ohkuma, H.; Matsumoto, K.; Tsuno, T.; Kamei, H.; Miyaki, T.; Oki, T.; Kawaguchi, H.; VanDuyne, G. D.; Clardy, J. *J. Antibiot.* **1989,** *42,* 1449-1452.

93. Konishi, M.; Ohkuma, H.; Tsuno, T.; Oki, T. *J. Am. Chem. Soc.* **1990,** *112.* 3715-3716.

94. Ando, T.; Ishii, M.; Kajiura, T.; Kameyama, T.; Miwa, K.; Sugiura, Y. *Tetrahedron Let.* **1998,** *39,* 6495-6498.

95. Edo, K.; Mizugaki, M.; Koide, Y.; Seto, H.; Furihata, K.; Otake, N.; Kshida, N. *Tetrahedron Lett.* **1985,** *26,* 331-334.

96. Myers, A.; Proteau, P. J.; Handel, T. M.: *J. Am. Chem. Soc.* **1988,** *110,* 7212-7214.

97. Leet, J. E.; Schroeder, K. R.; Hofstead, S. J.; Golik, J.; Colson, K. L.; Huang, S.; Klohr, S. E.; Doyle, T. W.; Matson, J. A. *J. Am. Chem. Soc.* **1992,** *114,* 7946-7948.

98. Kawata, S.; Ashizawa, S.; Hirama. M. *J. Am. Chem. Soc.* **1997,** *199,* 12012-12013.

99. Schroeder, D. R.; Colson, K. L.; Klohr, S. E.; Zein, N.; Langley, D. R.; Lee, M. S.; Matson, J. A.; Doyle, T. W. *J. Am. Chem. Soc.* **1994,** *116,* 9351-9352.

100. Sievers, E. L.; Larson, R. A.; Stadtmauer, E. A.; Estey, E.; Lowenberg, B.; Dombret, H.; Karanes, C.; Theobald, M.; Bennett, J. M.; Sherman, M. L.; Berger, M. S.; Elen, C. B.; Loken, M. R.; Van Dongen, J. J. M.; Bemstein, I. D.; Appelbaum, F. R.; Boogaerts, M.; Erba, H.; Huijgens, P.; Spielberger, R.; Tarantolo, S.; Castaigne, S.; Mignot, A.; Gramatski, M.; Harousseau, J.-L.;

Mineur, P.; Roy, D.; Tallman, M.; Voliotis, D.; Ehninger, G.; Goldstone, A.; Juliusson, G.; List, A.; Aglietta, M.; Burnett, A.; Cambier, M.; Cassileth, P.; Fernandez, M.-N.; Fiere, D.; Gobbi, M.; Heil, G.; Hess, U.; Horst, A.; Karp, J.; Minden, M.; Paul, C.; Rai, K.; Schenkein, D.; Schuster, M.; Sierra, J.; Stenke, L.; Wahlin, A.; Wemli, M. *J. Clin. Oncol.* **2001,** *19,* 3244-3254.

101. Gillespie, A. M.; Broadhead, T. J.; Chan, S. Y.; Owen, J.; Farnsworth, A.; Sopwith, M.; Coleman, R. E. *Ann. Oncol.* **2000,** *11,* 735-741.
102. Thorson, J. S.; Sievers, E. L.; Ahlet, J.; Shepard, E.; Witwam, R. E.; Onwueme, K. C.; Ruppen, M. *Curr. Pharm. Design* **2000,** *6,* 1841-1879.
103. Nicolaou, K. C.; Dai, W. –M. *Angew. Chem. Int. Ed. Engl.* **1991,** *30,* 1387-1416.
104. Smith, A. L.; Nicolaou, K. C. *J. Med. Chem.* **1996,** *39,* 2103-2117.
105. Jones, R. R.; Bergman, R. G. *J. Am. Chem. Soc.* **1972,** *94,* 660-661.
106. Bergman, R. G. *Acc. Chem. Res.* **1973,** *6,* 25-31.
107. Lockhart, P. B.; Comita, R. G.; Bergman, R. G. *J. Am. Chem. Soc.* **1981,** *103,* 4082-4090.
108. Lockhart, T. P.; Bergman, R. G. *ibid.* **1981,** *103,* 4091-4096.
109. Zein, N.; Sinha, A, M.; McGahren, W. J.; Ellestad, G. A. *Science* **1988,** *240,* 1198-1201.
110. Walker, S.; Landovitz, R.; Ding, W. D.; Ellestad, G. A.: Kahn, D. *Proc. Natl. Acad. Sci. USA* **1992,** *89,* 4608-4612.
111. Kumar, R. A.; Ikemoto, N.; Patel, D. J. *J. Mol. Biol.* **1997,** *265,* 187-201.
112. Frincke, J. M.; Faulkner, D. J. *J. Am. Chem. Soc.* **1982,** *104,* 265-269.
113. He, H.-Y.; Faulkner, D. J. *J. Org. Chem.* **1989,** *54,* 5822-5824.
114. Davidson, B. S.; *Tetrahedron Lett.* **1992,** *33,* 3721-3724.
115. Parameswaran, P. S.; Nalik, C. G.; Kamat, S. Y. *Ind. J. Chem.* **1998,** *38B,* 1258-1263.
116. Saito, N.; Sakai, H.; Suwanborirux, K.; Pummangura, S.; Kubo, A. *Heterocycles* **2001,** *55,* 21-28.
117. Das, B. C.; Lounasmaa, M.; Tendille, C.; Lederer, E. *Biochem. Biophys. Res. Comm.* **1965,** *21,* 318-322.
118. Arai, T.; Takahashi, K.; Kubo, A.; Nakahara, S.; Sato, S.; Aiba, K.; Tamura, C. *Tetrahedron Lett.* **1979,** *20,* 2355-2358.

119. Ueda, I.; Kawano, S. *Acta Cryst.* **1984,** *C40,* 1578-1580.

120. Ohtani, I.; Kusumi, T.; Kashman, Y.; Kakisawa, H. *J. Am. Chem. Soc.* **1991,** *113,* 4092-4096.

121. Trowitzsch-Kienast, W.; Irschik, H.; Reichenbach, H.; Wray, V.; Hofle, G. *Liebig Ann. Chem.* **1988,** 475-481.

122. Sakai, R.; Jares-Erijman, E. A.; Manzanares, I.; Silva Elipe, M. V.; Rinehart, K. L. *J. Am. Chem. Soc.* **1996,** *118,* 9017-9023.

123. Arai, T.; Takahashi, K.; Kubo, A.; *J. Antibiot.* **1977,** *30,* 1015-1018.

124. Arai, T.; Takahashi, K.; Nakahara, S.; Kubo, A. *Experientia,* **1980,** *36,* 1025-1027.

125. Mikami, Y.; Yokoyama, K.; Tabeta, H.; Nakagaki, K.; Arai, T. *J. Pharm. Dyn.* **1981,** *4,* 282-286.

126. Yazawa, K.; Takahashi, K.; Mikami, Y.; Arai, T.; Saito, N.; Kubo, A. *J. Antibiot.* **1986,** *39,* 1639-1650.

127. Kubo, A.; Saito, N.; Kitahara, Y.; Takahashi, K.; Yazawa, K.; Arai, T. *Chem. Pharm. Bull.* **1987,** *35,* 440-442.

128. Mikami, Y.; Takahashi, K.; Yazawa, K.; Hour-Young, C.; Arai, T. *J. Antibiot. q***1988,** *41,* 734-740.

129. Saito, N.; Kameyama, N.; Kubo, A. *Tetrahedron,* **2000,** *56,* 9937-9944.

130. Ozturk, T. In *The Alkaloid*; Cordell, G. A., Ed.; Academic: New York, 2000; Vol. 3, 119-238.

131. Ikeda, Y.; Matsuki, H.; Ogawa, T.; Munakata, T. *J. Antibiot.* **1983,** *36,* 1284-1289.

132. Irschik, H.; Trowitzsch-Kienast, W.; Gerth, K.; Hofle, G.; Reichenbach, H. *J. Antibiot.* **1988,** *41,* 993-998.

133. Pettit, G.; Knight, J. C.; Collins, J. C.; Herald, D. L.; Pettit, R. K.; Boyd, M. R.; Young, V. G. *J. Nat. Prod.* **2000,** *63,* 793-798.

134. Fontana, A.; Cavaliere, P.; Wahidulla, S.; Nalik, C. G.; Cimino, G. *Tetrahedron* **2000,** *56,* 7305-7308.

135. Rinehart, K. L.; Holt, T. G.; Fregeau, N. L.; Stroh, J. G.; Keifer, P. A.; Sun, F.; Li, L. H.; Martin D. G. *J. Org. Chem.* **1990,** *55,* 4512-4515.

136. Sakai, R.; Rinehart, K. L.; Guan, Y.; Wang, A. H.-J. *Proc. Natl. Acad. Sci. USA,* **1992,** *89,* 11456-11460.

137. Hurley, L. H.; Gairola, C.; Zmijewski, M. *Biochim. Biophys. Acta* **1977,** *475,* 521-

535.

138. Lown, J. W.; Joshua, A. V. *Biochem. Pharm.* **1979,** *28,* 2017-2026.

139. Zmijewski, M. J.; Miller-Hatch, K.; Mikolajczak, M. *Chem. -Biol. Intera.* **1985,** *52,* 361-375.

140. Seaman, F. C.; Hurley, L. H. *J. Am. Chem. Soc.* **1998,** *120,* 13028-13041.

141. Lown, J. W.; Joshua, A. V.; Lee, J. S. *Biochemstry* **1982,** *21,* 419-428.

142. Rao, K. E.; Lown, J. W. *Biochemistry* **1992,** *31,* 12076-12082.

143. Damia, G.; Silvestri, S.; Carrassa, L.; Filiberti, L.; Faircloth, G.; Foiani, M.; D'Incalci, M. *Int. J. Cancer* **2001,** *92,* 583-588.

144. Takebayashi, Y.; Pourquier, P.; Zimonjic D. B.; Nakayama, K.; Emmert, S.; Ueda, T.; Urasaki, Y.; Kanzaki, A.; Akiyama S.; Popescu, N.; Kraemer, K. H.; Pommier Y. *Nature Medicine* **2001,** *7,* 961-966.

145. Ishiguro, K.; Sakiyama, S.; Takahashi, K.; Arai, T. *Biochemistry,* **1978,** *17,* 2545-2550.

146. James, T. H.; Snell, J. M.; Weissberger *J. Am. Chem. Soc.* **1938,** *60,* 2084-2093.